Winter 12-2013

Random search models of foraging behavior: theory, simulation, and observation.

Ben C. Nolting
University of Nebraska-Lincoln, bcn13@case.edu

RANDOM SEARCH MODELS OF FORAGING BEHAVIOR: THEORY, SIMULATION, AND OBSERVATION

by

Ben C Nolting

A DISSERTATION

Presented to the Faculty of

The Graduate College at the University of Nebraska

In Partial Fulfilment of Requirements

For the Degree of Doctor of Philosophy

Major: Mathematics

Under the Supervision of Professors J. David Logan & Chad E. Brassil

Lincoln, Nebraska

December, 2013

RANDOM SEARCH MODELS OF FORAGING BEHAVIOR: THEORY, SIMULATION, AND OBSERVATION

Ben C Nolting, Ph.D.

University of Nebraska, 2013

Advisers: J. David Logan & Chad E. Brassil

Many organisms, from bacteria to primates, use stochastic movement patterns to find food. These movement patterns, known as search strategies, have recently become a focus of ecologists interested in identifying universal properties of optimal foraging behavior. In this dissertation, I describe three contributions to this field. First, I propose a way to extend Charnov's Marginal Value Theorem to the spatially explicit framework of stochastic search strategies. Next, I describe simulations that compare the efficiencies of sensory and memory-based composite search strategies, which involve switching between different behavioral modes. Finally, I explain a new behavioral analysis protocol for identifying the factors that influence pollinator foraging. The utility of this protocol is demonstrated using data gathered on sweat bees (*Agapostemon*) in Western Nebraska.

DEDICATION

To Mom and Dad

ACKNOWLEDGMENTS

To all those whose kindness and assistance have made this work possible, I offer the Tlingit term of gratitude: Gunalchéesh!

Thank you to my mom and dad, to whom this work is dedicated. I love them dearly.

I am very grateful to all of the professors who have guided me during my development as a scientist and mathematician. I was privileged to be advised by Chad Brassil and David Logan. Chad's brilliance in science, passion for teaching, and generosity in personal relationships are all traits I hope to emulate. His patience, encouragement, and unflinching optimism sustained me through the many challenges I encountered during graduate school. David inspired me to pursue a career in mathematical biology. Our many long discussions about mathematics are some of my fondest memories.

My other committee members, Richard Rebarber, Glenn Ledder, and Sabrina Russo, were hugely influential in my graduate education. Richard provided excellent advice on everything from mathematics to music. Glenn's creative insights about mathematical models always amazed me. Sabrina showed me that ecology is every bit as fascinating, challenging, and enjoyable as math.

I am grateful to the faculty and staff of the Department of Mathematics and the School of Biological Sciences at the University of Nebraska. Quite simply, they are wonderful people.

Large parts of this dissertation stem from collaboration with Travis Hinkelman, who I have worked closely with for years. Travis is an extremely gifted scientist and an awesome friend. Sara Reynolds was my academic sibling. Together, we navigated the challenges of cross-disciplinary work. Her ideas and advice have been immensely helpful.

During my graduate school career, I developed strong friendships with many fellow students. In the math department, these include: Nathan Corwin, Kathryn Haymaker, Zach Roth, Courtney Gibbons, Mike Janssen, Lauren Sipe, Amanda Croll, Laura Janssen, and many others. In the biology department, these include: RaeAnn Powers, Natalie West, Kathy Roccaforte, Dan Gates, Joseph Phillips, Jean Philippe Gibert, and many others. I am very grateful to all of them.

Thank you to Higgs and Emerson. Thank you to the Wahl family for including me in their lives.

Finally, thank you to all of the students that I taught at the University of Nebraska. You made teaching an absolute joy, and I am grateful for the opportunity to be part of your education.

Chapter two of this dissertation is collaborative work with Travis Hinkelman, Chad Brassil, and Brigitte Tenhumberg. We are grateful to the Holland Computing Center at the University of Nebraska, and to the NSF, which supported our work.

Chapter three of this dissertation is collaborative work with Kathy Roccaforte, Chad Brassil, Sabrina Russo, Dan Gates, Jocelyn Olney, Anthony Duren, Jillian Schneider, and Megan Friessen. Jocelyn, Anthony, Jillian, and Megan were participants in the Research for Undergraduates in Theoretical Ecology program at the University of Nebraska. They did the fieldwork in western Nebraska under Dan's guidance.

Contents

List of Figures

List of Tables

Preface

For many organisms, ranging from bacteria to primates, foraging for food is critical for survival. Understanding how organisms forage has long been a central goal of behavioral ecology. By studying the factors that influence foraging behavior, we can gain insights into the interactions between organisms and their environments, and make predictions about how organisms will react to changing environmental conditions.

Frequently, a foraging organism does not know where food resources are located, and hence must rely on search strategies to find them. Empirical observations indicate that a variety of species use random movement patterns to locate resources. These stochastic search strategies include movement patterns like Brownian motion, Lévy walks and straight-line (ballistic) motion. The effectiveness of different stochastic movement patterns in locating resources largely depends on the spatial distribution of resources. Therefore, a forager's evolutionary fitness rests heavily on the interaction between its movement strategy and the type of landscape it is exploring.

In this dissertation, I use mathematical models of organism movement to analyze foraging behavior. A key theme throughout the dissertation is how the stochastic processes of organism movement and resource distribution combine to influence foraging success. Three main research projects compose this dissertation. Chapter one describes a new approach to modeling optimal search strategies for foraging organisms.

Chapter two is an investigation of the efficiencies of different potential search modulation mechanisms. Chapter three presents a new framework for analyzing pollinator foraging behavior. Each of these chapters emphasizes a different quantitative approach: chapter one focuses on analytic mathematical methods, chapter two focuses on simulation, and chapter three focuses on statistical analysis and field methods.

Chapter 1 Overview

Optimal foraging theory is devoted to the study of how organisms should exploit food resources to maximize efficiency. Traditionally, this field has been dominated by spatially implicit patch-use models that emphasize the role of different patch-leaving criteria on foraging efficiency. Random search models, in which resources are represented as points on a landscape and a forager moves according to a stochastic process, are a departure from the traditional approach. In this chapter, I seek to connect patch-use models with random search models.

Many animals have been observed to execute composite stochastic movement patterns, consisting of intensive and extensive search modes. The decisions that a forager in a random search models makes about search mode are analogous to the decisions that a forager in a patch-use model makes about patch departure. In both cases, the criteria the forager uses is crucial in determining its foraging efficiency.

In my models, foragers move via Brownian motion in intensive mode and ballistic (i.e., straight-line) motion in extensive mode. The locations of resources are specified by particular spatial point processes. I consider two types of mode-switching criteria: giving-up time, and optimal zone. A giving-up time forager uses the time elapsed since its last resource encounter to determine when to switch modes. An optimal zone forager determines the regions of a landscape that warrant intensive search.

I analyze both of these strategies using mean first passage times. I consider both one and two-dimensional cases, and show how the models can accommodate any spatial distribution of resources. I consider a few examples, and suggest ways that this modeling framework can provide a bridge between random search and patch-use models. In particular, I explain how the optimal zone composite search model represents a spatially explicit analog of Charnov's marginal value theorem.

Chapter 2 Overview

Empirical observations indicate that a variety of organisms use composite random search strategies to find resources. In many cases, there is evidence that non-proximate sensory cues are used to identify areas that warrant intensive search. These cues are not precise enough to allow a forager to directly orient itself to a resource, but can be used as a criterion to determine the appropriate search mode. Together with Travis Hinkelman, Chad Brassil, and Brigitte Tenhumberg, I developed a model of composite search based on non-proximate sensory cues. With simulations, we compared the search efficiencies of composite foragers that use resource encounters as their mode-switching criterion with those that use non-proximate sensory cues. Non-proximate sensory foragers had higher search efficiencies across a range of different resource distributions, and were more robust to changes in resource distribution. Our results suggest that current assumptions about the role of resource encounters in models of optimal composite search should be re-examined.

Chapter 3 Overview

Pollinator behavior is key to determining the gene flow between flowers. In extreme cases, pollinator behavior can contribute to hybridization or speciation. Bias (the preference of one species of flower over another) and constancy (the preference to visit flowers of the same species sequentially) are two phenomena that are of particular interest to ecologists. Unfortunately, it is difficult to assess these phenomena in field observations, because the spatial arrangement of flowers confounds the results. Together with a research team including Kathy Roccaforte, Chad Brassil, Sabrina Russo, and Dan Gates, I developed a maximum likelihood framework that incorporates a variety of factors, including bias, constancy, and flower locations. This framework is novel in its ability to detect bias and constancy in field settings. We demonstrate the framework using data gathered on sweat bee behavior in western Nebraska.

Chapter 1

Optimal Composite Search Strategies

1.1 Introduction

Mathematical models of optimal foraging provide predictions about the most efficient way for animals to acquire food resources. These predictions can serve as null-models to compare against empirical observations. There are two general modeling approaches in optimal foraging theory: classic patch-use models, and random search models [8]. The former, perhaps best exemplified by Charnov's marginal value theorem [22], describe how foragers should exploit discrete, well-defined resource patches. These classic models emphasize how foragers determine when to leave patches; the details of how foragers find the patches are frequently neglected. In contrast, random search models represent resources as points, and describe the movement patterns that foragers should execute to find these points.

In recent years, researchers have called on their colleagues to unify these traditionally disparate modeling approaches [8, 10] under the heading "stochastic optimal foraging theory". Contributions to the synthesis these modeling approaches date back to at least 2008, when Plank and James [89] suggested a rough analogy between a

random search model and Charnov's marginal value theorem. In this chapter, I explore the connections between random search models and the marginal value theorem more deeply. I consider how optimally foraging organisms should use different criteria to switch between distinct stochastic search patterns.

1.1.1 Classic patch-use models

Before turning to random search models, it is worth reviewing the patch-use models that have traditionally underpinned optimal foraging theory. Identifying the key features of these patch-use models will provide a foundation for the random search models that follow. Charnov's marginal value theorem [22] is one of the cornerstones of classic optimal foraging theory. In Charnov's model, there are an infinite number of resource patches, divided into a finite number of types. A patch's type determines how its resource level changes in response to harvesting. The expected travel time between patches is fixed, patches are never revisited, and the probability of visiting a particular patch type is equal to the fraction of patches that are that type. When in a patch, a forager continuously depletes the resources there, causing its resource intake rate to diminish. To optimize it's overall resource intake rate, a forager in Charnov's model should behave according to the marginal value theorem: it should leave a patch when its resource intake rate in that patch equals its expected resource intake rate, averaged over the entire habitat.

A serious problem with Charnov's model was identified soon after its publication: the behavior of the model's optimal forager is completely determined before it even begins foraging [85]. The model represents foraging as a deterministic process, so the optimal behavior is predetermined by simultaneously solving a set of equations; hence the forager's behavior is not influenced by its experiences. In the real world, foraging is

not a continuous, deterministic process; instead, it is better characterized by discrete, stochastic resource encounters [85]. In this situation, a forager's instantaneous intake rate does not provide perfect knowledge of a patch's quality. Instead, a forager must infer the quality of a patch from the discrete encounters.

Two basic criteria have been proposed for how foragers should evaluate patch quality: giving-up density (GUD) and giving-up time (GUT). A GUD forager stays in a patch until the density of resources in the patch reaches a specified level. This is a relatively easy criterion to apply when resource intake is a continuous process, as it is in Charnov's model. When resources encounters are discrete, stochastic events, it seems reasonable to define resource density as the number of remaining resources in a patch divided by the patch's area. There is a problem with this definition, though: if the forager knows the number of resources that remain in a patch, then why does the forager not move to those resources and consume them?

Unlike the GUD criterion, the GUT criterion can logically apply to discrete, stochastic resource encounters. The GUT criterion was elaborated [45, 46, 47, 44, 86] to allow a forager to use more information than just the elapsed time since its last resource encounter. In its most complex incarnations, these models use dynamic programming to find the optimal decision at every possible state of the system. These models are too specific to provide attractive null models for foraging theory. The beauty of Charnov's marginal value theorem is that it provided simple patch residence times that could be compared with empirical data. Dynamic programming optimal decision models predict a series of conditional decisions; testing these is extremely difficult [110].

The problems that Charnov's model has with stochasticity have been widely discussed [85, 78, 59, 83] but a direct solution to the problem—namely, a spatially explicit representation of resource encounters—has received less attention than it de-

serves. Charnov's model, and its patch-use model descendants, provide only spatially implicit representations of the within-patch interactions between the forager and resources. This leads to ambiguities about the relationships between the number of resources a forager has consumed, the amount of time it has spent in a patch, and the future expected profitability of a patch.

The lack of spatially explicit representation is a criticism that applies to classic patch-use models, not only at the intra-patch level, but also at the inter-patch level. A fully spatially explicit model would take into account both the location of resources within patches and the location of patches on the landscape. Furthermore, the very assumption that patches are even well-defined entities is a limitation. In many natural environments, patches lack clearly demarcated boundaries.

Arditi and Dracogona [4] addressed these issues, by creating a fully spatially explicit model that allows resources to take on arbitrary spatial distributions. Resources in Arditi and Dracogna's model can be points scattered across the plane, patches of any shape, or a combination of these forms. Unlike most patch-use models, this model is fully spatially explicit. Unfortunately, the behavior it predicts is unrealistic. When resources are distributed as points, the model essentially predicts that an optimal forager should solve the traveling salesman problem, a huge computational task that is NP-hard. When resources occupy continuous regions, the trajectory of the optimal forager is calculated using the calculus of variations. Although Arditi and Dracogna's model identifies the true optimal behavior for a forager, its predictions are too precise to be a useful null model. When an optimal model predicts a specific trajectory through space, it is unrealistic to assume that empirical observations will exactly match that trajectory, and it is difficult to assess how close observed movements are to the optimal path. If, for example, an observed forager makes a slightly non-optimal choice early in its trajectory, the rest of its movement path might differ

widely from the optimal model. Furthermore, the movements of animals typically observed in natural systems display much more complexity than the perfect lines and curves of an optimal deterministic model. These factors limit the utility of Arditi and Dracogna's model.

1.1.2 Random Search Models

Random search models provide an alternative approach to modeling foraging behavior. Unlike patch-use models, random search models provide a spatially explicit representation of animal movement. In a random search model, resources are represented as points. A forager has a small fixed perceptual radius, within which it can detect resources. It does not have prior knowledge of the location of resources, and must move through space until a resource falls within its perceptual radius. The movement pattern executed by a forager is called its search strategy, and is a stochastic process.

The use of stochastic processes as models of animal movement has a long history [117, 108, 27]. Stochastic movement models are often preferred over deterministic ones on the grounds of pragmatism and realism. An ideal model would include the full set of deterministic rules that dictate an animal's behavior. Such a model would describe, with complete certainty, how the animal responds to any given set of environmental conditions. This type of deterministic model is unattainable—even if the complete set of rules that govern an animal's behavior is known, tracking all of the relevant environmental variables would be impossibly complex. By treating unknown factors probabilistically, stochastic models provide a tractable alternative [113].

Ballistic motion is the simplest of all random search strategies. A forager using this strategy travels in a straight line in a randomly selected direction until it encounters a resource. After consuming a resource, a forager randomly selects a new direction,

and again heads in a straight line until it encounters another resource.

Random walks are among the most frequently invoked random search strategies. In these models, a forager selects a step—a line segment—by selecting a distance and direction according to specified probability distributions. The forager moves along the step until it reaches the end, or until it encounters a resource, in which case it truncates the step. At the end of a step, it selects a new step. When the distribution of directions is uniform and the step lengths are fixed, the resulting stochastic process is called a simple random walk. A biased random walk is a random walk with a direction distribution concentrated along a specific direction. These are useful in modeling animal movement affected by phenomena like prevailing winds or ocean currents. A correlated random walk is a random walk in which the direction distribution for steps depends on the direction of the previous step. These are useful in modeling animal movement that has an element of directional persistence.

Brownian motion is a stochastic process that, on a heuristic level, can be thought of as the limit of a simple random walk, as the step sizes approach zero. The resulting trajectories are continuous, but nowhere differentiable. Brownian motion is characterized by a diffusivity parameter D, which determines the rate of change of the mean square displacement. It is among the most commonly invoked stochastic models of animal movement.

When the step lengths of a random walk are drawn from a probability distribution with finite variance, the random walk converges to Brownian motion at sufficiently long time scales. In other words, a zoomed out version of such a random walk would be indistinguishable from Brownian motion. Brownian motion, and random walks that converge to Brownian motion, are called diffusive. If a particle moves according to one of these stochastic processes, its displacement from its initial position scales in proportion to $t^{1/2}$. If a particle's displacement from its initial position scales

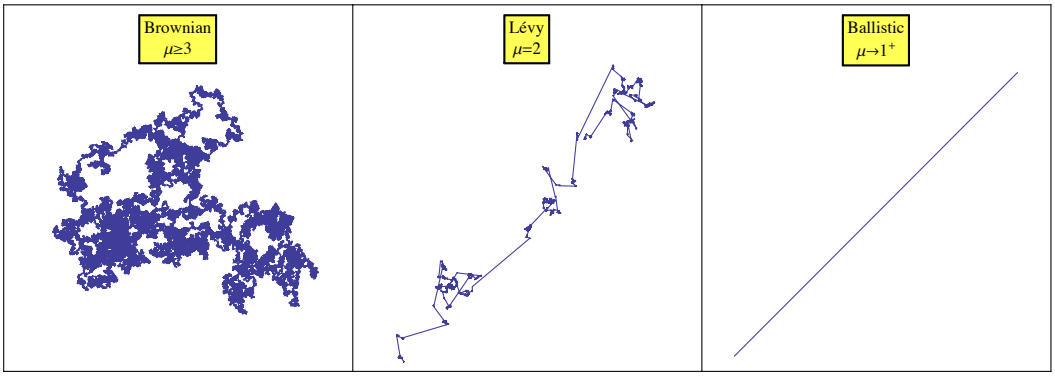

Figure 1.1: Power-law random walks

slower than $t^{1/2}$ (i.e., if it scales as t^{α}, $\alpha < 1/2$), its motion is sub-diffusive. If a particle's displacement from its initial condition scale faster than $t^{1/2}$ (i.e., if it scales as t^{α}, $\alpha > 1/2$), its motion is super-diffusive. Ballistic motion is an example of super-diffusive motion.

Lévy walks are super-diffusive random walks that have received much attention in modeling animal movement [117, 116, 95, 99]. In these random walks, step lengths are selected from power-law distributions. That is, $p(l) \sim l^{-\mu}$, where μ is a parameter between 1 and 3. For $\mu = 1$, the probability distribution ceases to be a distribution at all, resulting in ballistic motion. For $\mu > 3$, the variance of the probability distribution is finite, and the resulting random walk converges to Brownian motion at sufficiently long times. Hence power-law walks with $\mu > 3$ are referred to as Brownian walks. Lévy walks occupy a region between ballistic and Brownian motion. Some authors reserve the term Lévy walks for the case $\mu = 2$, but here a more broad definition of the term is used. Trajectories of Lévy walks are "scale-free", that is, they are self-similar fractals. This implies that a searcher employing a Lévy strategy does not have to adjust the scale of its behavior to the environment under consideration. Hence Lévy walks provide flexible and parsimonious descriptions of animal movement. Ballistic, Lvy, and Brownian walks are shown in figure 1.1.

In recent years, considerable discussion has been sparked by the claim that Lévy walks are a ubiquitous foraging strategy [14, 63, 106, 27]. The empirical evidence for animals moving via Lévy walks is controversial. Some researchers think that the appearance of Lévy walks is a statistical artifact [37, 6]. Others maintain that Lévy walks provide accurate descriptions of the data, but arise from other stochastic processes [89, 99, 95]. Still others hold that Lévy walks constitute an evolved strategy [9, 7].

This latter viewpoint is largely motivated by claims that Lévy walks (in particular, Lévy walks with parameter μ=2) constitute a theoretically optimal search strategy. These claims were initially based on mean-field analysis of "non-destructive" searching [116]. "Non-destructive" searching refers to situations where resources do not disappear after a forager encounters them. These claims were further supported by more rigorous mathematical analysis done for the one-dimensional case [93]. Two-dimensional simulations sometimes show that these conclusions hold [93] and sometimes do not [63].

The theoretical work on the optimality of Lévy walk searches has been hugely influential, but several important points of uncertainty remain. Initial claims that simulations and analysis of non-destructive foraging on uniformly distributed resources can serve as a stand-in for destructive foraging on clustered resources have been shown to be false [98]. Thus, it is important to conduct separate simulations and analysis for the destructive case. The generalizability of mathematically rigorous one-dimensional models to higher dimensions has not yet been firmly established.

Finally, and perhaps most importantly, the set of candidate strategies for "optimal search strategy" has been widely debated. The initial studies that identified Lévy walks with parameter $\mu = 2$ as optimal came from examining Brownian motion, ballistic motion, and the set of Lévy walks that occupy the spectrum in between those

two extremes. More complicated strategies that consist of combinations of random walks, and strategies that involve memory or sensory information were not included. In some ways, the restriction to the ballistic-Lévy-Brownian family of strategies makes sense, because these strategies occupy the simplest descriptions of movement. All of these strategies are non-oriented, and require no memory or sensory ability (outside of the perceptual radius) for the forager. On the other hand, there are other relatively simple models that agree with empirical data and are theoretically more efficient than Lévy walks. Key among these is the composite search strategy.

1.1.3 Composite search

Foragers should seek to match their search effort to the relative profitability of different parts of their habitats. In the context of random search, this can be accomplished by dividing search into intensive and extensive search modes, the former to be employed in resource rich areas and the latter in resource poor areas. In intensive mode, a forager searches an area thoroughly by taking short step lengths with frequent reorientations. In extensive search mode, a forager moves efficiently across resource poor areas by making long straight-line steps with few interruptions. This combination of search modes is known as a composite search strategy [89]. The ecological literature generally refers to composite searches as area-restricted search [120] or area-concentrated search [13].

There are numerous examples of animals that utilize composite search strategies. These include slime moulds [68], beetles [39], honeybees [114], fish [54], birds [84], ungulates [114], turtles [114] and weasels [49]. Sometimes organisms use resource encounters to determine when to engage in intensive and extensive search modes; examples include Ladybird beetle (*Coccinella septempunctata*) larvae feeding on aphids

[21] and houseflies (*Musca domestica*) feeding on sucrose drops [11]. In other situations, sensory cues determine when to switch search mode. Parasitoids like *Nermeritis canecens* [118], *Venturia canescens* [11], and *Cardiochiles nigriceps* [109] use chemical cues to determine when to search intensively for hosts. When deciding when to leave a foraging site, wolf spiders rely more heavily on visual and vibratory cues than elapsed time since their last prey encounter [87]. Procellariiform seabirds use chemicals like dimethyl sulfide to identify where to engage in intensive search [82]. Further examples of animals that use sensory cues to determine search mode include ciliates like *Paramecium* and *Tetrahymena* [72, 71, 51], bacteria, like *Escherichia coli* and *Salmonella typhimurium* [1, 35, 80], cod larvae [34], and fruit flies [29].

Several methods for modeling composite random search have been investigated: composite correlated random walks, intermittent search, and non-correlated composite walks. In composite correlated random walks, both the distribution of turn angles and the distribution of step lengths depend on whether the forager is in intensive or extensive mode [88]. Correlated random walks are not as parsimonious a description as non-oriented random walks, because there are parameters associated with the orientation distribution in each mode. Furthermore, there is a fundamental relationship between correlated random walks and Lévy walks [99]. The sharp corners present in random walk models of animal movement are often modeling or observational artifacts. The true motion of an animal tends to be a continuously differentiable curve, which is best modeled by a Langevian equation. The resulting trajectories are compatible with both correlated random walks and non-oriented walks from the Brownian-Lévy-ballistic spectrum, depending on the sampling resolution used for discretization. In light of this underlying compatibility, we restrict the analysis in this chapter to non-oriented random searches.

Intermittent random searches are related to composite searches [15, 16]. Like com-

posite searches, intermittent searches involve intensive and extensive search modes. In intermittent searches, foragers can only detect resources in intensive mode. Foragers switch from one search phase to the other with fixed rates per unit time. Hence the time spent in a given search mode follows an exponential distribution. This differs from the composite searches that I will focus on, which allow foragers to discover resources in extensive search, and which use different criteria for mode-switching.

Plank and James [89] proposed a model for composite search that involves Brownian motion in the intensive mode and ballistic motion in the extensive mode (figure 1.2). This basic model was later generalized by Reynolds [101], and further in chapter 2 of this work, to allow for Lévy walks in each search mode. Simulation work described in chapter 2 indicates that Brownian/ballistic composite search outperforms composite searches based on less extreme dichotomies, so we focus on these here. Nonetheless, analytic exploration of the efficiency of composite searches using Lévy search modes remains an open area.

Plank and James used their model of composite search to show that claims about the optimality of Lévy searches with $\mu = 2$ were misleading. They broadened the field of candidate strategies beyond the Brownian/Lévy/ballistic spectrum to include composite search strategies, and showed that composite search strategies faired better than their non-composite competitors. Furthermore, they showed that composite search strategies can produce trajectories that look much like Lévy walks; hence empirical observations that are consistent with Lévy walks could also be consistent with composite search strategies.

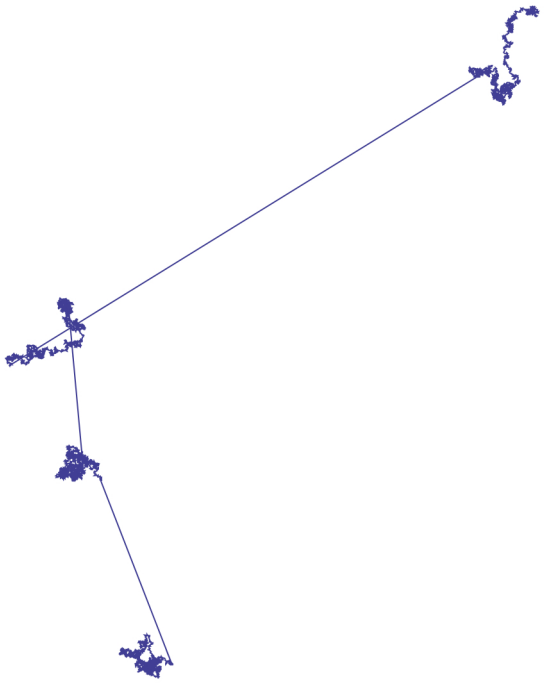

Figure 1.2: Sample trajectory, with alternating periods of Brownian and ballistic motion

1.1.4 The Patch-use/ composite search connection

The patch-use models and random search models described above represent two different paradigms for describing foraging. Patch-use models tend to be spatially implicit and emphasize how foragers decide when to leave a patch. Random search models are spatially explicit, and emphasize the role of movement in encountering resources. Bridging the gap between these two approaches promises to yield interesting insights into animal behavior [8]. Composite search models, like that of Plank and James, represent a step toward this unification.

In composite search models, intensive search and extensive search can be seen as analogous to the within-patch foraging and between patch travel in patch-use models. In Plank and James' composite search model, a forager switches from extensive to

intensive mode if it encounters a resource. If a fixed giving-up time elapses without a subsequent resource encounter, the forager switches from intensive mode to extensive mode. The giving-up time mode-switching criterion is a familiar part of the patch-use literature. Plank and James claim that their composite search model is a generalization of the Marginal Value Theorem, however this is not quite the case. In the patch-use context, GUT-based foraging does not exactly correspond to MVT optimal foraging. A GUT-forager has a memory, something that a patch-use MVT forager lacks. Furthermore, a MVT has complete knowledge of the landscape, which a GUT-based forager does not. Nonetheless, Plank and James' insight about finding a MVT-like model for random search is intriguing, and I pursue that question further in this work.

I begin by analyzing optimal giving-up times for a composite random searcher. My work expands on that of Plank and James in several ways. First, I consider the case of destructive foraging, while Plank and James considered only non-destructive foraging. Second, I consider how search efficiency depends on the spatial distribution of resources. This involves explicitly accounting for the types of point processes that generate resource distributions, and specifically on the auto-correlation of resource locations. This departs from the uniform approximations taken by Plank and James. Third, I use Fourier series to find implicit solutions for optimal giving-up times based on specific resource configurations. Fourth, I extending the the analysis beyond a single spatial dimension.

After considering composite foragers that use giving-up time as their mode-switching criterion, I propose a composite random search model that is a better analogy to the MVT searcher of patch-use theory. To do this, I develop a framework that determines the optimal zones on a landscape for intensive and extensive search. I consider this in both one and two dimensions, and discuss why it is the most appropriate spatially

explicit interpretation of the marginal-value theorem. Finally, I discuss the ecological implication of my results, and future directions for work.

1.1.5 Mathematical connections

In the following, I model foraging for resources in terms of first passage times. Basically, this modeling framework views a forager as a particle that moves through a landscape until it runs into, and is absorbed by a resource. The efficiency of the forager is then inversely proportional to the first passage time of the process. This modeling framework follows in the direction of a variety of previous researchers [93, 89, 10, 76, 77, 67].

Several related mathematical concepts are worth noting. The narrow escape problem concerns the time it takes for a particle to exit a domain, when most of the domain is reflecting but some is absorbing escape [107]. This problem is especially of interest to cellular biologists, but the underlying mathematics is similar to the first passage foraging problems we study.

In statistical physics, the trapping problem is basically a rephrasing of the first passage time problem. This problem has applications in chemical kinetics, and tends to be addressed with the tools of large deviation theory [18, 74].

Finally, one can model foraging by drawing a disk around a forager representing its perceptual radius, and monitoring how the area traced by the disk changes as the forager moves. When the disk moves via Brownian motion, the geometrical object traced is called the Wiener sausage. The name is a pun, derived because mathematicians know Brownian motion as a Wiener process, and in three dimensions, the geometrical object looks somewhat like a sausage. For a measure-theoretic view of the Wiener sausage, see [69] and [33].

1.2 Model Description and Analysis: Optimal GUT forager

In section 1.21, I describe a model for an optimal GUT composite forager in one-dimension. I explain how the foraging efficiency depends on the spatial distribution of resources. In section 1.22, I consider how this model could be extended to two-dimensional landscapes.

1.2.1 GUT forager: one-dimensional case

Consider a forager in one dimension that uses giving-up time as its criterion for switching from intensive to extensive search mode. The forager moves in extensive search mode until it encounters (and immediately consumes) a resource. A resource encounter triggers the forager to enter intensive search mode. The forager remains in intensive mode until a specified amount of time, called its giving-up time, τ, elapses without encountering another resource. If this happens, the forager reverts to extensive search mode. In my model, I assume that intensive search is Brownian motion and extensive search is ballistic motion. I also assume that, in both search modes, the forager travels with velocity one, so that measures of distance and time are equivalent.

Suppose that the forager has just encountered and consumed a resource. Without loss of generality, suppose that this resource is at the origin. The distances to the resources that are closest to the forager on its right and left are random variables, which we label as Y_L and Y_R, respectively. Later in this chapter, I examine how optimal foraging strategies depend on the distribution of these random variables. For now, let these random variables take on fixed values, $Y_L = y_L$ and $Y_R = y_R$. The position of the forager is given by a stochastic process $X(t)$. For times before τ, this

process obeys the stochastic differential equation:

$$dX(t) = \sqrt{2D}\, dW(t), \quad X(0) = 0$$

Here $W(t)$ is a standard Wiener process, and D is a constant that determines the diffusivity of the Brownian motion. To be specific, $E\left(X\left(t\right)^2\right) = 2Dt$. If X reaches one of the endpoints of the interval $[-y_L, y_R]$, it terminates. If X remains in the interval until time τ, then it switches to ballistic motion, at which point is described by:

$$X(t) = \chi(t - \tau) + X(\tau)$$

Here χ is a random variable that takes on value 1 with probability 1/2 and -1 with probability 1/2.

Let $u(x, t)$ be the probability density function for the location of the forager while it is engaged in intensive search. The first stochastic differential equation above can be translated into the related Fokker-Planck equation governing its probability density function:

$$u_t(x, t) = D\, u_{xx}(x, t), \quad -y_L < x < y_R;\ 0 < t < \tau$$

$$u(-y_L, t) = u(y_R, t) = 0,\ 0 < t < \tau$$

$$u(x, 0) = \delta(x),\ -y_L < x < y_R$$

Note that the endpoints of the interval, $-y_L$ and y_R, are absorbing boundaries. The Dirac function initial condition represents the fact that the forager is located at

the origin at time zero with probability one. The above equation can be solved via separation of variables and a Fourier series expansion to yield:

$$u(x,t) = \sum_{k=1}^{\infty} \frac{2}{y_L + y_R} \sin\left(\frac{k\pi y_L}{y_L + y_R}\right) \sin\left(\frac{k\pi}{y_L + y_R}(x + y_L)\right) e^{-\frac{Dk^2\pi^2 t}{(y_L+y_R)^2}}$$

The probability that the forager has not encountered a resource by time t, where $t < \tau$, is found by integrating $u(x,t)$ over the interval $(-y_L, y_R)$, which yields:

$$P_{in}(t) = \int_{-y_L}^{y_R} u(x,t)\, dx = \sum_{k=1}^{\infty} \frac{2(1-(-1)^k)}{k\pi} \sin\left(\frac{k\pi y_L}{y_L + y_R}\right) e^{-\frac{D\pi^2 k^2 t}{(y_L+y_R)^2}}$$

Let the time that elapses before the forager encounters a resource be represented by the random variable T. Let $F(t) = Prob\,(T \leq \mathrm{t})$ be the cumulative density function for T, and let $f(t) = F'(t)$ be the associated probability density function. Note that, if $T < \tau$, then the forager has only engaged in intensive search, and the probability that it has encountered a resource is $F(t) = Prob\,(T \leq \mathrm{t}) = 1 - P_{in}(t)$. If $T > \tau$, then the forager has spent time τ engaged in unsuccessful intensive search, and then switched to extensive search. If the forager is at position x when it makes the switch to extensive search, then it moves to the left with probability $\frac{1}{2}$ and travels a distance $|x + y_L|$, or to the right with probability $\frac{1}{2}$ and travels a distance $|y_R - x|$. Thus the expected time that a forager spends in extensive mode before encountering a resource is $\frac{1}{2}\,|x + y_L| + \frac{1}{2}\,|y_R - x| = \frac{1}{2}\,(y_R + y_L)$.

Let $E(T; y_L, y_R)$ be the expected value of T, conditional on $Y_L = y_L$ and $Y_R = y_R$. We can compute this as:

$$
\begin{aligned}
E(T; y_L.y_R) &= \int_0^\infty t\, f(t)\, dt = \int_0^\tau t\, f(t)\, dt + \left(\tau + \frac{1}{2}\,(y_L + y_R)\right) P_{in}(\tau) \\
&= \tau\, F(\tau) - \int_0^\tau F(t)\, dt + \left(\tau + \frac{1}{2}\,(y_L + y_R)\right) P_{in}(\tau) \\
&= \tau\, \left(1 - P_{in}(\tau)\right) - \int_0^\tau \left(1 - P_{in}(t)\right)\, dt + \left(\tau + \frac{1}{2}\,(y_L + y_R)\right) P_{in}(\tau) \\
&= \int_0^\tau P_{in}(t)\, dt + \frac{1}{2}\,(y_L + y_R)\, P_{in}(\tau)
\end{aligned}
$$

The integral in this expression can be evaluated term-by-term using the series expression for $P_{in}(t)$, yielding:

$$
\begin{aligned}
E(T; y_L, y_R) &= \sum_{k=1}^{\infty} \frac{2(-1 + (-1)^k)}{D\, k^3 \pi^3}\, (y_L + y_R)^2 \sin\left(\frac{k\pi y_L}{y_L + y_R}\right) \left(e^{-\frac{Dk^2\pi^2\tau}{(y_L+y_R)^2}} - 1\right) \\
&+ \frac{1}{2}\,(y_L + y_R) \sum_{k=1}^{\infty} \frac{2(1 - (-1)^k)}{k\pi} \sin\left(\frac{k\pi y_L}{y_L + y_R}\right) e^{-\frac{D\,\pi^2 k^2 \tau}{(y_L+y_R)^2}} \\
&= \sum_{k=1}^{\infty} \frac{1}{D\, k^3\, \pi^3}\, (y_L + y_R)\left(1 - (-1)^k\right) e^{-\frac{Dk^2\pi^2\tau}{(y_L+y_R)^2}} \sin\left(\frac{k\pi y_L}{y_L + y_R}\right) \\
&\qquad \left(D\, k^2\pi^2 + 2\left(e^{\frac{Dk^2\pi^2\tau}{(y_L+y_R)^2}} - 1\right)(y_L + y_R)\right)
\end{aligned}
$$

For a fixed y_L and y_R, we can determine the optimal giving-up time, τ^*. In figure 1.3, we see that this time exists at approximately $\tau^* = 3$. For some combinations of y_L and y_R, composite search is not optimal, and it is better to engage in exclusively Brownian or exclusively ballistic search. Figure 1.4 shows an example in which purely ballistic motion is optimal; that is, $\tau^* = 0$. The mean first passage time monotonically increases with giving-up time. It eventually asymptotes at the mean first passage time for a pure diffusion. In the case of the parameters in figure 1.5, this is at 234.75. Figure 1.5 shows an example in which purely Brownian motion is optimal; that is,

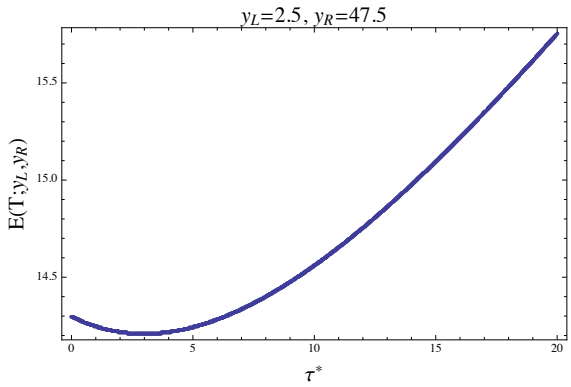

Figure 1.3: An example of the relationship between giving-up-time τ and mean first passage time $E\left(T; y_L, y_R\right)$. $D = 1$.

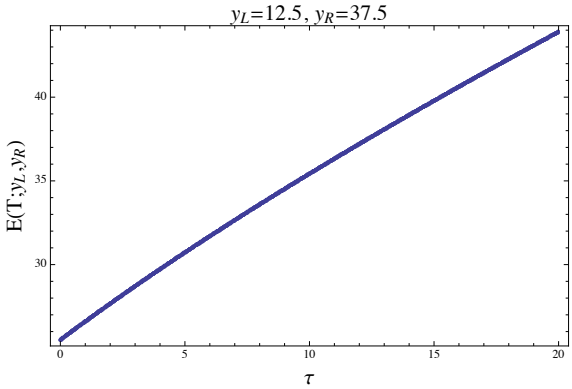

Figure 1.4: An example of the relationship between giving-up-time τ and mean first passage time $E\left(T; y_L, y_R\right)$. $D = 1$.

$\tau^* = \infty$. In this case, the mean first passage time approaches the diffusion time, 1.125 as $\tau \to \infty$, and this time is less than the purely ballistic time of 1.5.

Figure 1.6 shows the mean first passage time plots for a variety of different y_L, y_R parameter combinations. The plots in each row have the same inter-resource distance (i.e., $y_L + y_R$).

For a fixed length between resources of $y_L + y_R = 25$, we can examine the mean first passage time as a function of y_L and τ. The resulting surface is displayed in figure 1.7. Taking a cross-section with y_L fixed yields the type of plots in figures

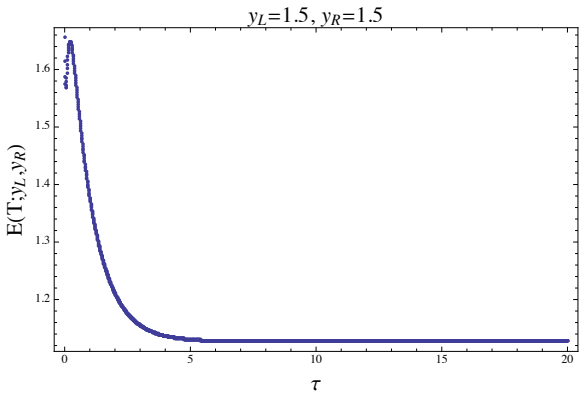

Figure 1.5: An example of the relationship between giving-up-time τ and mean first passage time $E\left(T; y_L, y_R\right)$. $D = 1$.

1.3-1.6.

It is difficult to analytically derive precise ranges of y_L and y_R such that favor pure Brownian, composite, and pure ballistic, respectively. Numerical exploration reveals some patterns in the regions of (y_L, y_R) parameter space that favor each strategy. These are shown in figure 1.8, in which purple corresponds to a purely ballistic strategy, lavender to a composite strategy, and white to a purely Brownian strategy. Several patterns are apparent. First, composite search is optimal when the forager starts near to one resource and far from the other ($y_L \ll y_R$ or vice versa). Second, when the distance between resources becomes very large ($y_L + y_R > 20$), virtually no initial conditions favor composite search.

One might logically ask: why is a pure Brownian strategy ever optimal? The answer lies in the difference between physical Brownian motion, which is comprised of microscopic steps taken at finite velocity, and the Wiener process, which is the mathematical representation of Brownian motion. The latter is an abstraction. The probability density for the displacement of a Wiener process exhibits a strange phenomenon: even at very small times, the density is non-zero very far from the initial condition. This physically unrealistic phenomenon means that the model's utility

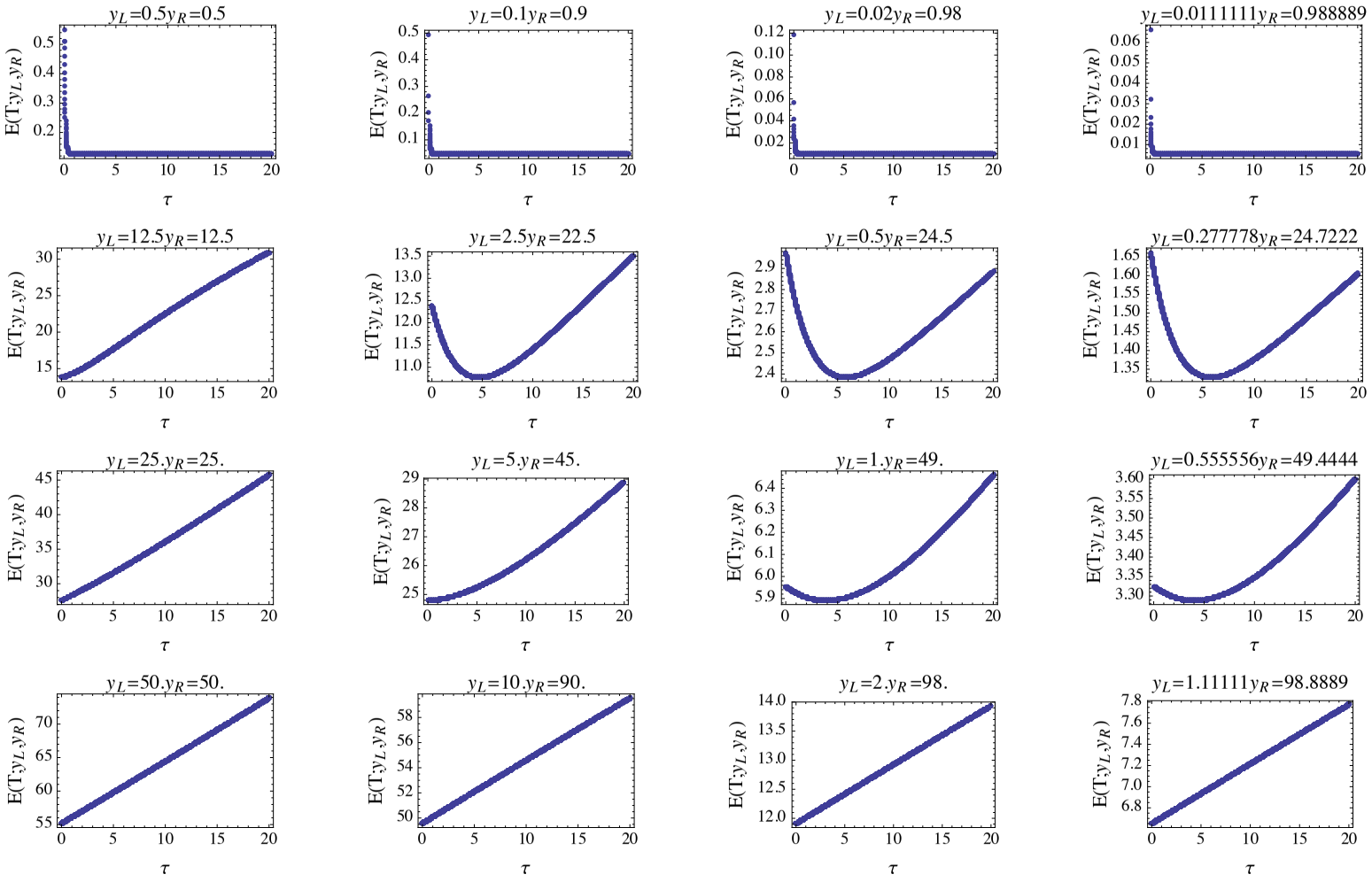

Figure 1.6: Relationships between giving-up-time τ and mean first passage time relationship between giving-up-time τ and mean first passage time $E\left(T; y_L, y_R\right)$ for a variety of values of y_L and y_R. $D = 1$.

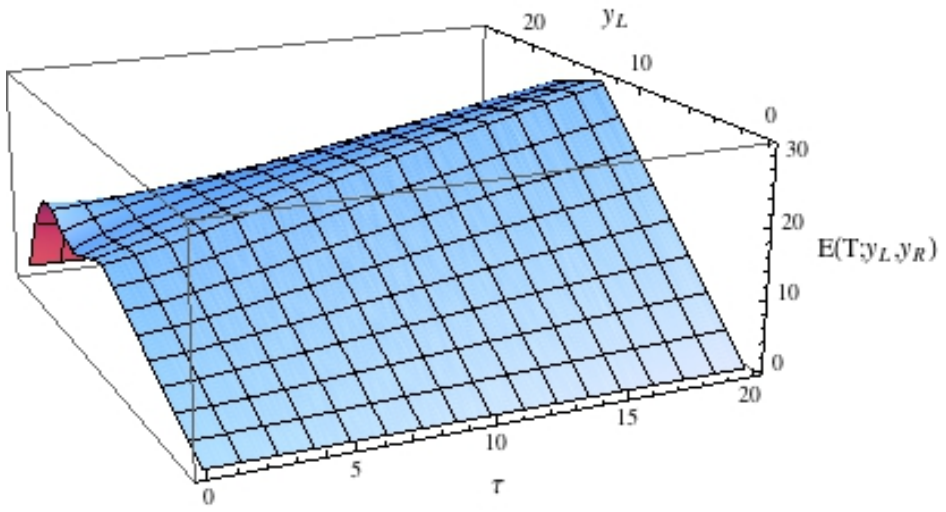

Figure 1.7: Relationships between giving-up-time τ and mean first passage time relationship between giving-up-time τ and mean first passage time $E(T; y_L, y_R)$ for a variety of values of y_L. Total interval length is 25. $D = 1$.

breaks down at very small time scales. This short time-scale regime is evident when mean first passage time decreases monotonically with GUT.

As an aside, one can directly compare the mean first passage times under pure Brownian and pure ballistic motion. Let $E(T; y_L, y_R, \tau)$ be the mean first passage time with giving-up time τ.

$$E(T : y_L, y_R, 0) = \frac{1}{2}(y_L + y_R)$$

and

$$\lim_{\tau \to \infty} E(T; y_L, y_R, \tau) = \frac{1}{2} y_L y_R,$$

so, in order for pure Brownian motion to be superior, it is required that $y_R < 1$ or $y_L > \frac{y_R}{y_R - 1}$. Note that these criteria just imply that a pure Brownian strategy is superior to a pure ballistic strategy; they do not rule out that a composite strategy is superior to both.

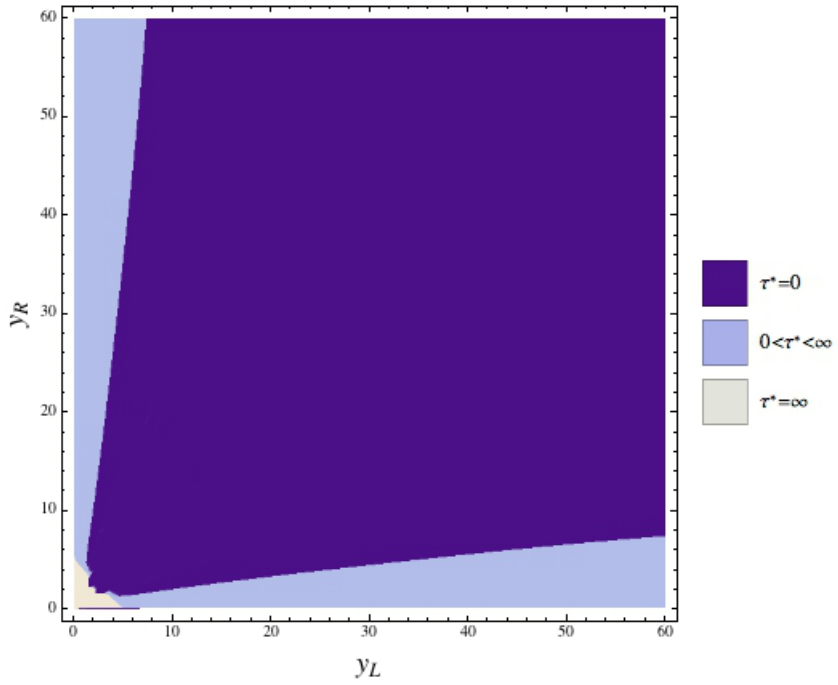

Figure 1.8: Horizontal coordinate is y_L, vertical coordinate is y_R. $D = 1$. Purple shading indicates regions where purely ballistic motion is optimal. Only regions with $y_L + y_R < 100$ are plotted.

So far, the model I've described has assumed that y_L and y_R are fixed. Consider now the case where Y_L and Y_R are random variables. In order to conduct this analysis, I first review some terminology from spatial point processes on the real line. Much of this information is distilled from helpful references like [57] and [30].

A spatial point process on $\mathbb{R}^n$ is defined as follows. First, let C be the set of all counting measures on $\mathbb{R}^n$. For a compact set $B \subset \mathbb{R}^n$, let

$$\Delta_{B,k} = \{N \in C | N(B) = k\},$$

and let Λ be the σ-field generated by the collection of all of these subsets. A spatial point process is a measurable function $N : \Omega \to C$, where (Ω, A, P) is some probability space. Thus, each point process maps an event ω to a counting measure N_ω on $\mathbb{R}^n$. If

$B \subset \mathbb{R}^n$ is compact, then $N(B)$ is a random variable representing the number of points of the process in B. The finite-dimensional distribution of a point process N are the joint probability distributions of the random variables $(N(B_1), N(B_2), ..., N(B_k))$ for any non-negative integer k, where the B_i are compact subsets of $\mathbb{R}^2$. The collection of finite-dimensional distributions for N are sufficient to completely specify N; i.e., if two point processes have the same finite-dimensional distributions, then they are identical. N is stationary if any translation of N has the same distribution as N. N is isotropic if its distribution is invariant under rotation.

The intensity of a point process N is defined as $\nu(B) = E(N(B))$, for a compact set $B \subseteq \mathbb{R}^n$. If there is a function β on $\mathbb{R}^n$ that satisfies $\nu(B) = \int_B \beta(s)\, ds$, then β is called the intensity function of N.

The second factorial moment measure of the point process is defined for compact sets $A, B \subseteq \mathbb{R}^n$ as:

$$\alpha^2(A \times B) = E(N(A)N(B)) - E(N(A))\, E(N(B))$$

If there is a function ϱ on $\mathbb{R}^n \times \mathbb{R}^n$ that satisfies $\alpha^2(C) = \int_c \varrho(x, y)\, dx\, dy$ for all compact $C \subseteq \mathbb{R}^n \times \mathbb{R}^n$, then ϱ is called the pair density function for N.

The pair-correlation function for N is defined as:

$$\rho(x, y) = \frac{\varrho(x, y)}{\beta(x)\beta(y)},\ x, y \in \mathbb{R}^n$$

When N is stationary and isotropic, as in is the cases I consider in this chapter, the pair-correlation function can be written as a function of the distance between two points: $\rho(r) = \rho(|x - y|) = \rho(x - y, 0)$.

The Palm-intensity function of N is defined as $h(r) = \beta\rho(r)$. It is this function

h that I will primarily be concerned with in this chapter. $h(r)$ gives the density of points at radius r from the origin, conditional on the origin being a point in the process.

The nearest-neighbor distribution function is given by:

$$\mathcal{D}(r) = P_o\left(N\left(b_r^*(0)\right) > 0\right),$$

where $b_r^*(0)$ is the punctuated neighborhood of radius r around the origin, and P_o denotes the palm probability distribution (i.e., conditioned on a point being at the origin). Letting $d(r) = \mathcal{D}'(r)$ be the associated probability density, one obtains $Y_L \sim d$. Because I assumed Y_L is the closer of the two resources, the distance distribution to Y_R is not directly found from $\mathcal{D}$. Instead, I use a hazard rate approach to find it. For notational simplicity, let the probability density functions for Y_L and Y_R be h_L and h_R, respectively. Then, the overall expected time to resource encounter is given by:

$$E(T) = \int_0^\infty \int_0^\infty h_L(y_L)\, h_R(y_R)\, E(T; y_L, y_R)\; dy_L\, dy_R$$

To emphasize that this is a function of the parameter τ, this can be written as:

$$\bar{t}(\tau) = \int_0^\infty \int_0^\infty h_L(y_L)\, h_R(y_R)\, E(T; y_L, y_R)\; dy_L\, dy_R.$$

Minimizing with respect to τ amounts to solving:

$$\int_0^\infty \int_0^\infty h_L(y_L)\, h_R(y_R)\, \frac{\partial}{\partial \tau}\left(E(T; y_L, y_R)\right)\; dy_L\, dy_R = 0.$$

In order to determine the optimal giving-up time, it is necessary to combine the

analysis from the fixed resource case with information about the resource distribution. If resources are distributed uniformly at low density, then the cases where $y_L \approx y_R$ will dominate, which corresponds to a situation that favors a pure ballistic strategy. If resources are distributed in clusters, there is a relatively high probability that $y_L \ll y_R$, or vis versa, and composite search is favored (the lavender regions in figure 1.8).

1.2.2 GUT forager: two-dimensional case

In the two-dimensional case, the resources are disks of radius ε, where ε is the perceptual radius of the forager. This reflects and underlying symmetry which will frequently be exploited in this chapter: the combination of point resources and a forager with perceptual radius ε is equivalent to a point forager searching for targets of radius ε. Assume that the forager begins its trajectory at the origin, having just consumed a resource. Initially, it's trajectory is given by the stochastic differential equation:

$$d\mathbf{X}(t) = \sqrt{2D}\, d\mathbf{W}(t), \quad \mathbf{X}(0) = (0,0)^T$$

Here $\mathbf{X}(t) = (X_1(t), X_2(t))^T$ and $\mathbf{W}(t) = (W_1(t),\, W_2(t))^T$ are both vectors of random variables. If time τ elapses without a resource encounter, the forager enters ballistic motion, and its trajectory is given by:

$$\mathbf{X}(t) = (t-\tau)\,(cos\,(\theta)\,, sin\,(\theta))^T + \mathbf{X}(\tau)$$

Here θ is a random variable, with uniform distribution on the interval $[0, 2\pi]$. One way to compute the mean-first passage time for the forager's diffusive phase would be to directly consider the Fokker-Planck equation, with boundary conditions proscribed

by the resource disks in $\mathbb{R}^2$. This approach is useful for computing first passage times of a specific realization of a point process, but is otherwise cumbersome. An easier approach involves radial averaging.

To use this technique, consider the probability of a forager encountering a resource between a radial distance of r and $r + dr$. This turns out to be related to the mean free path, given by $l(r) = (h(r)\,2\delta)^{-1}$. Here 2δ is the approximate cross-sectional area of a resource. Let $Q(r)$ be the probability of a particle traveling in a straight line from the origin and surviving until it reaches r. By examining the behavior of the particle in a thin annulus between r and $r + dr$ we can obtain a differential equation for $Q(r)$, as

$$Q(r + dr) - Q(r) = -Q(r)\,h(r)\,2\delta\,dr$$

So, $\frac{dQ}{dr} = -\frac{Q(r)}{l(r)}$. This needs to be converted to an encounter rate; i.e., so that the dependent variable is time. By using the expression for mean radial displacement, $r = 2\sqrt{Dt}$, one can write the average instantaneous radial velocity as $\frac{dr}{dt} = \sqrt{\frac{D}{t}} = \frac{2D}{r}$. Therefore,

$$\frac{dQ}{dt} = -\frac{2D}{r\,l(r)}Q(r)$$

With this expression, and the radially symmetric form of the Laplacian, one can find the partial differential equation for the probability distribution of a a forager's location in intensive search mode:

$$\frac{\partial u}{\partial t} = \frac{D}{r}\frac{\partial}{\partial r}\left(r\frac{\partial u}{\partial r}\right) - \frac{2D}{r\,l(r)}u(r,t)$$

$$\frac{\partial u}{\partial r}(0,t) = 0, \quad u(r,0) = \delta(r)$$

Solving this equation involves separation of variables. Suppose that $u(r,t) =$

$R(r)T(t)$. Then the partial differential equation becomes:

$$\frac{T'(t)}{T(t)} = \frac{D}{rR(r)}\left(R'(r) + r\,R''(r)\right) - \frac{2D}{r\,l(r)}$$

The left-hand side of this equation is a function of t, while the right-hand side is a function of r, hence they both must be equal to a constant, $-\lambda^2$. Then $T(t) = e^{-\lambda^2 t}$. The differential equation for R becomes:

$$rR''(r) + R'(r) + \left(\frac{\lambda^2}{D}r - \frac{2}{l(r)}\right)R(r) = 0$$

Solving this eigenvalue problem with the boundary conditions $\frac{dR}{dr}(0) = 0$, $lim_{r\to\infty}R(r) = 0$ yields an eigenfunction expansion for $u(r,t)$. Once this has been obtained, the mean survival time can be determined as:

$$\begin{aligned}
E(T;l) &= \int_0^\infty t\,f(t)\,dt = \int_0^\tau t\,f(t)\,dt + \left(\tau + \int_0^\infty l(r)\,u(r,\tau)\,dr\right)P_{in}(\tau) \\
&= \tau\,F(\tau) - \int_0^\tau F(t)\,dt + \left(\tau + \int_0^\infty l(r)\,u(r,\tau)\,dr\right)P_{in}(\tau) \\
&= \tau\,(1 - P_{in}(\tau)) - \int_0^\tau (1 - P_{in}(t))\,dt + \left(\tau + \int_0^\infty l(r)\,u(r,\tau)\,dr\right)P_{in}(\tau) \\
&= \int_0^\tau P_{in}(t)\,dt + P_{in}(\tau)\int_0^\infty l(r)\,u(r,\tau)\,dr
\end{aligned}$$

The notation $E(T;l)$ emphasizes the dependence of the expected survival time on the function $l(r)$.

1.3 Model Description and Analysis: Optimal zone forager

Now consider the case of a forager that has the ability to determine which regions of an environment are worthy of intensive search and which regions are not. We will call this forager an *optimal zone forager*. Like the optimal GUT forager, the optimal zone forager's strategy is based on switching between intensive and extensive search mode. Unlike the GUT forager, the optimal zone forager uses its location on the landscape to determine its search mode. The optimal zone metaphorically colors a map of the landscape black and white; black areas are the ones that it will search using Brownian motion, white areas are ones it will search using ballistic motion. Such a forager has *a priori* knowledge of where all of the resources on a landscape are, but it cannot use that knowledge to move directly from one resource to the next. Instead, the optimal forager can only use that information to determine zones for intensive search.

The optimal zone forager represents the ideal strategy for a searcher that switches between Brownian and ballistic search mode. In other words, optimal zone foraging is the behavior expected of an omniscient forager, provided that its search strategy is confined to non-oriented, bimodal stochastic search. It answers the question "where *should* a forager search intensively?", and thus provides a useful benchmark with which to judge empirically observed foraging behaviors.

Let Ω be a landscape. The optimal zone forager will determine a subset of the landscape, $\Omega_I \subseteq \Omega$, to search intensively. The complement of this area, $\Omega_E = \Omega \backslash \Omega_I$, is the part of the landscape that the forager will search extensively. These regions are determined by the particular realization of the point process that generates the resources. Consider a specific realization of the resource point process. Let $E_I(x_0)$ (respectively, $E_e(x_0)$), be the expected time for a forager at position x_0 engaged in Brownian motion

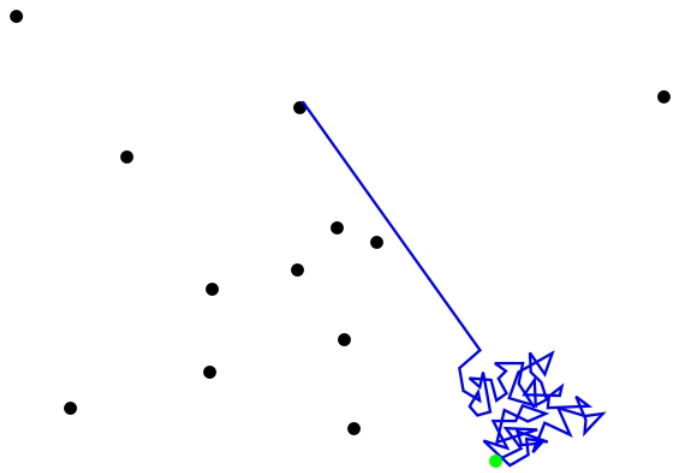

Figure 1.9: Schematic diagram of a composite forager (green) moving in two-dimensional space, searching for resources (black). The forager's trajectory (blue) starts in intensive mode, then shifts to extensive mode.

(respectively, ballistic motion) to encounter a resource. $\Omega_I = \{x \in \Omega | E_I(x) < E_e(x)\}$ and $\Omega_E = \{x \in \Omega | E_I(x) > E_e(x)\}$. Figure 1.9 shows a schematic diagram of the foraging process.

1.3.1 Optimal zone forager: one-dimensional case

First, consider the basic case of determining optimal zones for intensive and extensive search in one dimension. In this case, resources are distributed on $\mathbb{R}$, and it suffices to consider the resources immediately adjacent to the forager's initial location. Suppose that resources are located at the origin and L, and the forager has initial location $0 < x_0 < L$. Then $E_I(x_0) = \frac{1}{2D} x_0 (L - x_0)$ and $E_e(x_0) = \frac{L}{2}$. If $L < 4D$, then $(0, L) \subset \Omega_I$. If $L > 4D$, then $\left(0, \frac{L-\sqrt{L^2-4LD}}{2}\right) \bigcup \left(\frac{L+\sqrt{L^2-4LD}}{2}, L\right) \subset \Omega_I$

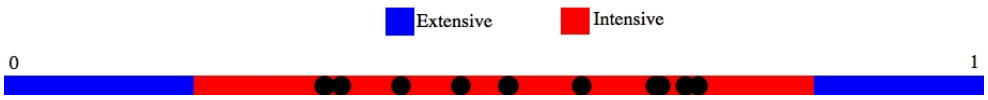

Figure 1.10: Optimal zones for a one-dimensional composite forager with $D = 1$. Black circles are resources. Red indicates regions that should be searched intensively, blue indicates regions that should be searched extensively.

and $\left(\frac{L-\sqrt{L^2-4LD}}{2}, \frac{L+\sqrt{L^2-4LD}}{2}\right) \subset \Omega_E$.

Given the spatial coordinates of resources on an landscape, one can directly determine Ω_I and Ω_E. An example is illustrated in figure 1.10. Ten resources are distributed on the interval $[0, 1]$. The endpoints of the interval are reflecting, and the resources are absorbing. In the figure, resources are shown with as disks with a finite radius, but in the model, they are points. Using the scheme above, the regions of intensive and extensive search are identified and color-coded.

1.3.2 Optimal zone forager: two-dimensional case

The case of a two-dimensional landscape is more complicated. In the one-dimensional case, the resources on each side of the forager provide natural boundaries for the mean first passage problem. In two dimensions, any simulated landscape will contain a finite number of resources. If the landscape has infinite area, then mean first passage times will diverge. To avoid this, I represent the landscape as a disk of radius ρ with reflecting boundaries. The landscape within the reflecting disk is assumed to be representative of the entire landscape. I will retain the notation Ω to denote the landscape. The resources are smaller disks, denoted by T_i (for "target") centered at positions $\{\mathbf{r}_i\}_{i=1}^N$ of radius $\epsilon << \rho$. Let $\Omega^* = \Omega \backslash \bigcup T_i$. The boundary of the resource disks, $\partial T = \bigcup_{i=1}^N \partial T_i$, is absorbing. The exterior boundary of the domain is denoted by $\partial\Omega$. $A = \pi$ is the area of Ω. As in the one-dimensional case, the goal is to the

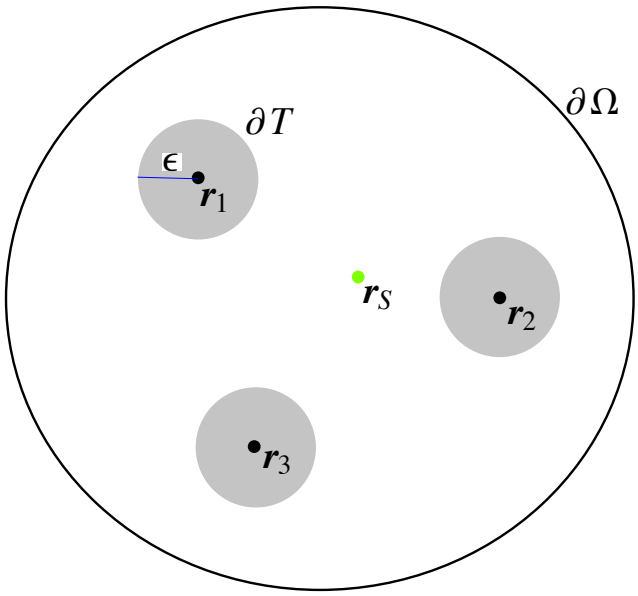

Figure 1.11: Schematic diagram of the variables used in the model of the two-dimensional optimal zone forager.

expected mean first passage time for intensive and extensive search. Given an initial condition $\mathbf{r}_S \in \Omega$, we will determine $E_I(\mathbf{r}_S)$ and $E_e(\mathbf{r}_S)$. The notation is chosen to follow the work of [23]; $\mathbf{r}$ is used because the domain is a disk, S is short for "starting". The relative sizes of $E_I(\mathbf{r}_S)$ and $E_e(\mathbf{r}_S)$ will determine whether the forager should engage in intensive or extensive search at that position. Figure 1.11 shows a schematic diagram of the domain.

The probability density of the location of the forager, $u(\mathbf{r}, t; \mathbf{r}_S)$ satisfies the Kolmogorov forward equation:

$$\Delta_{\mathbf{r}} u(\mathbf{r}, t; \mathbf{r}_S) = \frac{1}{D} \frac{\partial u}{\partial t}(\mathbf{r}, t; \mathbf{r}_S), \quad \mathbf{r} \in \Omega^*, \, t > 0$$

$$\partial_n u(\mathbf{r}, t; \mathbf{r}_S) = 0, \quad \mathbf{r} \in \partial\Omega, \, t > 0$$

$$u\left(\mathbf{r},t;\mathbf{r}_S\right)=0,\quad \mathbf{r}\in\partial T,\, t>0$$

$$u\left(\mathbf{r},0;\mathbf{r}_S\right)=\delta\left(\mathbf{r}-\mathbf{r}_S\right),\quad \mathbf{r}\in\Omega^*$$

Using the adjoint of this differential operator, we can write the Kolmogorov backward equation, which expresses the probability of the forager being at $\mathbf{r}_S$ at time 0 given it is at $\mathbf{r}$ at time t.

$$\Delta_{\mathbf{r}_S}v\left(\mathbf{r}_S,t;\mathbf{r}\right)=\frac{1}{D}\frac{\partial v}{\partial t}\left(\mathbf{r}_S,t;\mathbf{r}\right)\quad \mathbf{r}_S\in\Omega^*,\, t>0$$

$$\partial_n v\left(\mathbf{r}_S,t;\mathbf{r}\right)=0,\quad \mathbf{r}_S\in\partial\Omega,\, t>0$$

$$v\left(\mathbf{r}_S,t;\mathbf{r}\right)=0,\quad \mathbf{r}_S\in\partial T,\, t>0$$

$$v\left(\mathbf{r}_S,0;\mathbf{r}\right)=\delta\left(\mathbf{r}-\mathbf{r}_S\right),\quad \mathbf{r}\in\Omega^*$$

This equation allows for the derivation of an equation for the mean first passage time [60]. Let $p_{in}\left(\mathbf{r}_S,t\right)$ be the probability that a forager starting at $\mathbf{r}_S$ remains in Ω^* at time t. Then:

$$p_{in}\left(\mathbf{r}_S,t\right)=\int_{\Omega^*}v\left(\mathbf{r}_S,t;\mathbf{r}\right)d\mathbf{r}.$$

Integrating both sides of the Kolmogorov backward equation over Ω^* with respect to $\mathbf{r}$ yields:

$$\Delta p_{in}\left(\mathbf{r}_S, t\right) = \frac{1}{D}\frac{\partial p_{in}}{\partial t}\left(\mathbf{r}_S, t\right) \quad \mathbf{r}_S \in \Omega^*,\, t > 0$$

$$\partial_n p_{in}\left(\mathbf{r}_S, t\right) = 0, \quad \mathbf{r}_S \in \partial\Omega,\, t > 0$$

$$p_{in}\left(\mathbf{r}_S, t\right) = 0, \quad \mathbf{r}_S \in \partial T,\, t > 0$$

$$p_{in}\left(\mathbf{r}_S, 0\right) = 1, \quad \mathbf{r}_S \in \Omega^*$$

Let $F\left(t; \mathbf{r}_S\right)$ be the probability distribution for the mean first passage time of a forager that starts at position $\mathbf{r}_S$, and let $f\left(t; \mathbf{r}_S\right) = \frac{\partial F}{\partial t}\left(t; \mathbf{r}_S\right)$ be the associated probability density. Then $F\left(t; \mathbf{r}_S\right) = 1 - p_{in}\left(t; \mathbf{r}_S\right)$ and $f\left(t; \mathbf{r}_S\right) = \frac{\partial p}{\partial t}\left(t; \mathbf{r}_S\right)$.

Using integration by parts, the mean first passage time, $E\left(\mathbf{r}_S\right)$, satisfies:

$$E\left(\mathbf{r}_S\right) = \int_0^\infty t\, f\left(t; \mathbf{r}_S\right) dt = -\int_0^\infty t\frac{\partial p_{in}}{\partial t}\left(t, \mathbf{r}_s\right) dt = \int_0^\infty p_{in}\left(t; \mathbf{r}_S\right) dt.$$

The problem of mean first passage time for a diffusing particle in a two-dimensional domain with relatively small disk-shaped targets has been examined by Chevalier et al. [23]. I will use their approach and much of their notation in the following to analyze the mean first passage time for intensive search mode. One should read their paper for a fuller description of the solution method, but I will summarize it here.

The E_I notation will temporarily be dropped, because this section focuses on the intensive mean first passage time. Integrating both sides of the PDE for p_{in} with respect to t from 0 to ∞ yields:

$$\Delta E\left(\mathbf{r}_S\right) = -\frac{1}{D} \quad \mathbf{r}_S \in \Omega^*$$

$$\partial_n E\left(\mathbf{r}_S\right) = 0, \quad \mathbf{r}_S \in \partial\Omega$$

$$E\left(\mathbf{r}_S\right) = 0, \quad \mathbf{r}_S \in \partial T.$$

The Green's function, $G\left(\mathbf{r};\mathbf{r}_S\right)$, satisfies:

$$-\Delta_{\mathbf{r}} G\left(\mathbf{r};\mathbf{r}_S\right) = \delta\left(\mathbf{r}-\mathbf{r}_S\right), \quad \mathbf{r} \in \Omega^*$$

$$\partial_n G\left(\mathbf{r};\mathbf{r}_S\right) = 0 \quad \mathbf{r} \in \partial\Omega$$

$$G\left(\mathbf{r};\mathbf{r}_S\right) = 0 \quad \mathbf{r} \in \partial T.$$

The Green's function has Neuman boundary conditions on Ω and the mean first passage time has Dirichlet boundary conditions on ∂T, so

$$\int_{\partial\Omega^*} \partial_n G\left(\mathbf{r};\mathbf{r}_S\right) E\left(\mathbf{r}_S\right) d\mathbf{r} = \int_{\partial T} \partial_n G\left(\mathbf{r};\mathbf{r}_S\right) E\left(\mathbf{r}\right) d\mathbf{r} + \int_{\partial\Omega} \partial_n G\left(\mathbf{r};\mathbf{r}_S\right) E\left(\mathbf{r}\right) d\mathbf{r} = 0.$$

Similarly,

$$\int_{\partial\Omega^*} \partial_n E\left(\mathbf{r}\right) G\left(\mathbf{r};\mathbf{r}_S\right) d\mathbf{r} = 0.$$

By Green's formula,

$$\int_{\Omega^*} E(\mathbf{r})\,\Delta G(\mathbf{r};\mathbf{r}_S) - G(\mathbf{r};\mathbf{r}_S)\,\Delta E(\mathbf{r})\,d\mathbf{r} = \int_{\partial\Omega^*} \partial_n G(\mathbf{r};\mathbf{r}_S)\,E(\mathbf{r}) - \partial_n E(\mathbf{r})\,G(\mathbf{r};\mathbf{r}_S)\,d\mathbf{r} = 0.$$

Therefore,

$$E(\mathbf{r}_S) = -\int_{\Omega^*} E(\mathbf{r})\,\delta(\mathbf{r}-\mathbf{r}_S)\,d\mathbf{r} = -\int_{\Omega^*} E(\mathbf{r})\,\Delta G(\mathbf{r};\mathbf{r}_S)\,d\mathbf{r} = -\int_{\Omega^*} G(\mathbf{r};\mathbf{r}_S)\,\Delta E(\mathbf{r})\,d\mathbf{r}.$$

And hence,

$$E(\mathbf{r}_S) = \frac{1}{D}\int_{\Omega^*} G(\mathbf{r};\mathbf{r}_S)\,d\mathbf{r}.$$

Determining the Green's function for the domain Ω^* is difficult. Chevalier et al. begin by describing the simplest case, in which there is only one resource, and absorbing target at $\mathbf{r}_T$. It is possible to write the Green's function in terms of a pseudo-Green's function, $H(\mathbf{r};\mathbf{r}')$:

$$G(\mathbf{r};\mathbf{r}_S) = p_0(\mathbf{r}_S) + H(\mathbf{r};\mathbf{r}_S) - H(\mathbf{r};\mathbf{r}_T) + g_\epsilon.$$

Here $p_0(\mathbf{r}_S)$ is a correcting function, selected to make $G(\mathbf{r};\mathbf{r}_S) = 0$ for all $\mathbf{r} \in \partial T$. g_ϵ is an error term, and is $O(\epsilon)$.

The pseudo-Green's function $H(\mathbf{r};\mathbf{r}_S)$ is defined by:

$$-\Delta H_{\mathbf{r}}(\mathbf{r};\mathbf{r}') = \delta(\mathbf{r}-\mathbf{r}') - \frac{1}{A}, \quad \mathbf{r} \in \Omega$$

$$\partial_n H(\mathbf{r};\mathbf{r}') = 0 \quad \mathbf{r} \in \partial\Omega$$

$$H(\mathbf{r};\mathbf{r}') = H(\mathbf{r}';\mathbf{r})$$

$$\int_{\Omega} H(\mathbf{r}';\mathbf{r})\, d\mathbf{r}' = 0.$$

The pseudo-Green's function can be decomposed into two parts:

$$H(\mathbf{r};\mathbf{r}_T) = G_0(\mathbf{r};\mathbf{r}_T) + \chi(\mathbf{r};\mathbf{r}_T),$$

where $G_0(\mathbf{r};\mathbf{r}_S)$ is the infinite-space Green's function, and $\chi(\mathbf{r};\mathbf{r}_S)$ is the regular part of H as $\mathbf{r} \to \mathbf{r}_S$. These functions satisfy the following:

$$-\Delta G_0(\mathbf{r};\mathbf{r}_T) = \delta(\mathbf{r}-\mathbf{r}_T), \quad \mathbf{r} \in \mathbb{R}^2$$

$$\partial_n G_0(\mathbf{r};\mathbf{r}_T) = 0 \quad \mathbf{r} \to \infty$$

$$G_0(\mathbf{r};\mathbf{r}_T) = 0 \quad \mathbf{r} \to \infty.$$

$$-\Delta\chi(\mathbf{r};\mathbf{r}_T) = -\frac{1}{A}, \quad \mathbf{r} \in \Omega$$

$$\partial_n\chi(\mathbf{r};\mathbf{r}_T) = -\partial_n G_0(\mathbf{r};\mathbf{r}_T) \quad \mathbf{r} \in \partial\Omega$$

$$\chi(\mathbf{r};\mathbf{r}_T) = -G_0(\mathbf{r};\mathbf{r}_T) \quad \mathbf{r} \in \partial T$$

In order to satisfy the boundary condition on ∂T, define the function $p_0(\mathbf{r}_S)$ by:

$$p_0(\mathbf{r}_S) = G_0(\epsilon) + \chi(\mathbf{r}_T; \mathbf{r}_T) - H(\mathbf{r}_T; \mathbf{r}_S).$$

Using the Green's function, one sees that

$$E(\mathbf{r}_S) = \frac{A}{D}\left(G_0(\epsilon) + \chi(\mathbf{r}_T; \mathbf{r}_T) - H(\mathbf{r}_T; \mathbf{r}_S)\right) + \mathcal{O}\left(\epsilon^2 G_0(\epsilon)\right).$$

Following Chevalier et al., one can use the same approach for the case of two targets, $\mathbf{r}_1$ and $\mathbf{r}_2$. In this case, one must determine the splitting probabilities, $P_1(\mathbf{r})$ and $P_2(\mathbf{r})$, which determine the probability of ending at target 1 and target 2, respectively. The splitting probabilities satisfy the PDE's:

$$\Delta P_i(\mathbf{r}) = 0 \quad \mathbf{r} \in \Omega^*$$

$$\partial_n P_i(\mathbf{r}) = 0 \quad \mathbf{r} \in \partial\Omega$$

$$P_i(\mathbf{r}) = 1 \quad \mathbf{r} \in \partial T_i$$

$$P_i(\mathbf{r}) = 0 \quad \mathbf{r} \in \partial T_j,\ j \neq i.$$

The splitting probabilities can be related to the Green's function via:

$$P_i(\mathbf{r}_S) = -\int_{\partial T_i} G(\mathbf{r}; \mathbf{r}_S)\, d\mathbf{r}.$$

Guided by the one target case, one can obtain:

$$G(\mathbf{r};\mathbf{r}_S) = p(\mathbf{r}_S) + H(\mathbf{r};\mathbf{r}_S) - P_1(\mathbf{r}_S)\,H(\mathbf{r};\mathbf{r}_1) - P_2(\mathbf{r}_S)\,H(\mathbf{r};\mathbf{r}_2) + g_\epsilon.$$

In the following, for a given initial condition $\mathbf{r}_S$ let $H_{ij} = H(\mathbf{r}_i;\mathbf{r}_j)$, $p_0 = p_0(\mathbf{r}_S)$, $P_i = P_i(\mathbf{r}_S)$. Then successively setting $\mathbf{r} = \mathbf{r}_1$ and $\mathbf{r} = \mathbf{r}_2$ as $\epsilon \to 0$ yields:

$$p_0 + H_{1S} - P_1 H_{11} - P_2 H_{12}$$

$$p_0 + H_{2S} - P_1 H_{21} - P_2 H_{22}.$$

Together with $P_1 + P_2 = 1$, these equations allow one to solve for P_1, P_2, and p_0, and hence for the Green's function. These quantities determine $G(\mathbf{r};\mathbf{r}_S)$, and hence $E(\mathbf{r}_S)$.

This method can be extended to any finite number of targets $\mathbf{r}_1,\ \mathbf{r}_2,\ \ldots,\ \mathbf{r}_N$. In this case, the Green's function is:

$$G(\mathbf{r};\mathbf{r}_S) = p_0(\mathbf{r}_S) + H(\mathbf{r};\mathbf{r}_S) - \sum_{i=1}^{N} P(\mathbf{r}_i)\,H(\mathbf{r};\mathbf{r}_i) + g_\epsilon.$$

This leads to a set of $N+1$ equations:

$$P_i H_{ii} + \sum_{j\neq i} P_j H_{ji} - p_0 = H_{iS}$$

$$\sum_{i=1}^{N} P_i = 1.$$

After solving for p_0 and $\{P_i\}_{i=1}^{N}$, one can calculate the mean first passage time as:

$$E\left(\mathbf{r}_S\right) = \frac{A}{D}\left(\sum_{k=1}^{N} H_{kk}^{-1}\right)^{-1}\left(\sum_{k=1}^{N} P_k + \sum_{j\neq k} P_j H_{jk} H_{kk}^{-1} - H_{kS}H_{kk}\right).$$

The geometry of this problem yields the following:

$$G_0\left(|\mathbf{r}-\mathbf{r}_S|\right) = -\frac{1}{2\pi}\ln\left(|\mathbf{r}-\mathbf{r}_S|\right)$$

$$\chi\left(\mathbf{r};\mathbf{r}_S\right) = \frac{1}{2\pi}\left(-\ln\left(\frac{|r_S\mathbf{r}-\mathbf{r}_S|}{r_S^2}\right) + \frac{1}{2}\left(r^2+r_S^2\right) - \frac{3}{4}\right),$$

where $r = |\mathbf{r}|$ and $r_S = |\mathbf{r}_S|$.

The method just described, from Chevalier et al., allowed me to determine the approximate mean first passage time for a forager in intensive mode, $E_I\left(\mathbf{r}_S\right)$.

Next, the mean-first passage time under ballistic motion must be determined for each location, $E_e\left(\mathbf{r}_S\right)$. Assume that the forager in extensive mode selects a direction from a uniform distribution on $[0, 2\pi]$. There are two possible outcomes: either the forager's trajectory will intersect one of the targets (each of radius ϵ), or it will reach the domain boundary $\partial\Omega$. If the forager reaches the boundary before encountering a resource, its trajectory is reflected in a randomly selected direction.

An alternative modeling approach is to assume that ballistic trajectories reflect deterministically, like a light ray, with the angle of incidence equal to the angle of reflection. This presents a problem, though. The reflected trajectories will continue forever, without reaching certain regions called "caustics". If all of the resources were located within the caustics, this would produce an infinite time to resource encounter. Therefore, I use a model with random reorientations at reflecting boundaries.

For a given starting position $\mathbf{r}_S$ and a randomly selected flight orientation ϕ, one can calculate whether that ray $\mathbf{r}_S + t\left(\cos\left(\phi\right), \sin\left(\phi\right)\right)$ intersects $\bigcup_{i=1}^{N} B_\epsilon\left(\mathbf{r}_i\right)$ or $\partial\Omega$

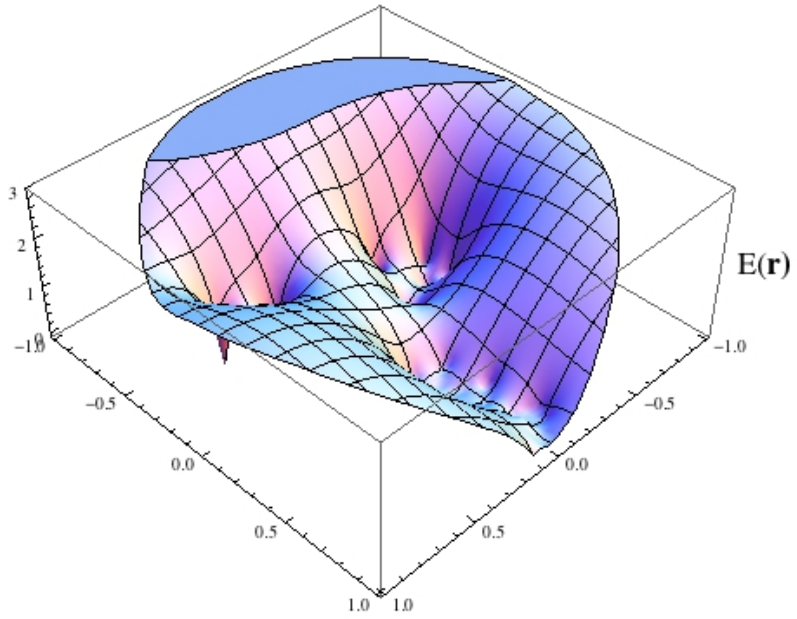

Figure 1.12: Mean first passage times for Brownian motion, $D = 0.1$. Targets have radius $\epsilon = 0.01$.

first. In the former case, the time of first intersection is the first passage time; in the latter case, the mean free path $h = \frac{A}{2N\epsilon}$ is added. Adding the mean free path is an approximate way of dealing with all of the "post-reflection" trajectory. The first passage times are averaged uniformly over $\phi \in [0, 2\pi]$. This yields $E_e(\mathbf{r}_S)$, the mean first passage time for extensive motion.

Figure 1.12 plots $E_I(\mathbf{r}_S)$ for a specific configuration of resources. Figure 1.13 plots $E_e(\mathbf{r}_S)$ for the same configuration of resources. By comparing these, one obtains a plot of the regions that warrant intensive search; this is plotted in figure 1.14.

1.4 Discussion

Researchers have long been interested in identifying optimal random search strategies. These strategies are of particular interest in foraging theory. The optimal strategies predicted by models can be used as benchmarks against which to measure real-world

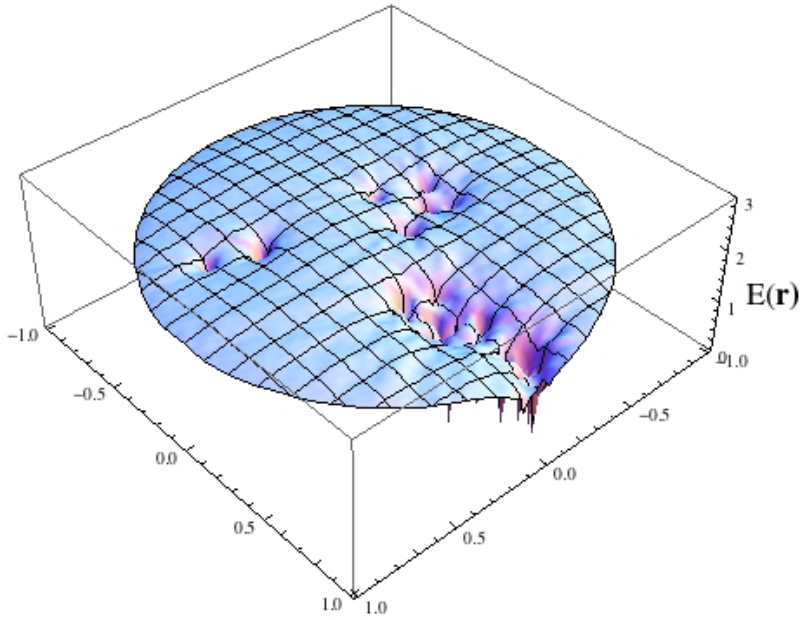

Figure 1.13: Mean first passage times for ballistic motion. Targets have radius $\epsilon = 0.01$.

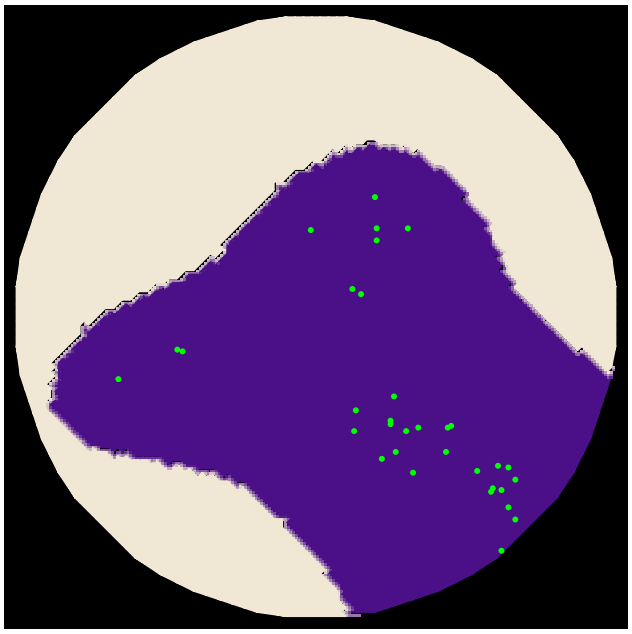

Figure 1.14: Optimal zones for intensive search (purple) and extensive search (cream). $D = 0.1$, $\epsilon = 0.01$. Resources are green.

foragers against. Deviations from these predictions indicate the presence of external factors, such as predator avoidance or competition with conspecifics. Over a decade ago, Viswanathan [116] argued that Lévy walks constituted an optimal search strategy, and hence should be ubiquitous in nature. Since then, a huge amount of research has been devoted to the theoretical efficiency of Lévy walks, and to their empirical observation in nature [7]. Many researchers [96, 101, 95, 98, 89, 36, 91] have argued that composite searches are theoretically more efficient than Lévy walks and provide a more accurate fit to observed data. In this chapter, I have sought to be extend previous mathematical analysis of composite search strategies.

The models introduced in this chapter make predictions about optimal composite search behavior based on explicit consideration of the distribution of resources on the landscape. Different strategies are expected to be favored on different types of landscapes, and the models in this chapter take this into account. The analyses performed in this chapter can accommodate a broad range of resource distributions.

The key difference between the GUT and optimal zone models is the criteria used for switching between intensive and extensive search modes. The GUT model, which adds to previous work on composite search, assumes that foragers use elapsed time since last resource encounter as the mode-switching criterion. There is no *a priori* reason that an optimal composite search should be based on GUT. A more efficient foraging strategy is to identify areas that are worthy of intensive search. The optimal zone forager does this, and provides a benchmark for the ideal behavior of a composite random searcher. Indeed, the GUT forager can be viewed as a heuristic approximation of the optimal zone forager. The GUT forager uses time between resource encounters to try to estimate when it is in an optimal zone. Giving-up-time is a useful rule-of-thumb for approximating the ideal behavior of the optimal zone forager.

The one-dimensional GUT model generates predictions for specific configurations of resources. This can be used together with the distribution of inter-resource distances to make predictions for many different types of resource distributions (in any number of spatial dimensions). Alternatively, the two-dimensional GUT forager model can produce predictions for many types of resource distributions using radial averaging. The optimal zone model makes predictions based on specific realizations of resource locations; it does not require knowledge of the underlying distribution that generates the resource locations.

The optimal zone forager can be interpreted as a spatially-explicit analog of the the Marginal Value Theorem. The Marginal Value Theorem is spatially implicit. It represents resources as discrete, well-defined patches. Resource harvesting within patches is a deterministic, continuous process. In many situations, resources are actually arbitrarily distributed points in space, and are not restricted to patches. These resources are stochastically encountered in discrete events. The optimal zone model provides a description of ideal composite search in such situations. Like the marginal value theorem, the optimal zone model determines how a forager should make decisions about switching between behavioral two modes. In the MVT case, those modes are within-patch harvesting and between patch travel, while in the optimal zone model those modes are intensive and extensive search. Also like the MVT, and unlike GUT-based composite search models, the optimal zone model gives the behavior of an "ideal forager" that has complete information about the landscape; it does not rely on rules-of-thumb to make decisions.

The models presented here will be useful for several reasons. The GUT model allows researchers to easily identify landscapes that are suited to composite search (as opposed to purely ballistic search). It will allow researchers to test the hypothesis that foragers use elapsed time to assess resource density. The optimal zone model

provides a Marginal Value Theorem-like benchmark with which to compare observed animal movement patterns. Overlaying the optimal zones predicted by the model for specific landscapes with empirically observed search paths will help determine how closely foragers adhere to maximally efficient behavior.

The models make several major assumptions that might limit their utility. The composite search foragers are assumed to engage in bimodal Brownian/ballistic search. Both of these search modes are non-oriented. While this may be appropriate for very simple organisms, [71, 51], it is unlikely to be an accurate description of animals that use more complicated sensory systems. The assumption that foragers have only two distinct movement modes is clearly an oversimplification. A promising future direction of work would be generalizing the analysis in this chapter to allow for directional biases in movement (due to sensory abilities or environmental conditions) and a continuum of search intensity levels (for example, the adaptive Lévy walks discussed by Reynolds 2010) [98]. The optimal zone model assumes that the zones obey a basic superposition principle, and that optimal radius around each resource is constant as resources are depleted. Both of these assumptions should be analyzed in more detail.

Future work on these models should include comparing the theoretical predictions with observed animal search paths. Good candidate organisms for such empirical observations are pelagic birds, parasitoids and other insects, and plankton. The assumptions about composite search made by these models may seem like oversimplifications of the complexities of real-world foraging behavior; however, simple models like the Marginal Value Theorem and Lévy walks have proved to be extremely useful in understanding important general concepts. Composite random search models will likely be just as useful, and it is hoped that the analysis presented here will contribute to understanding what constitutes an optimal composite search.

Chapter 2

Composite random search strategies based on non-proximate sensory cues

2.1 Introduction

For many organisms, the ability to efficiently find food resources is a key determinant of fitness [12]. It is advantageous for foraging animals to focus search effort on resource rich areas and minimize energy spent searching resource poor areas [117]. This search tactic has been termed composite search [89], area-restricted search [120], area-concentrated search [13], or intermittent search [16]. A forager using a composite search strategy alternates between intensive and extensive search modes. In intensive mode, a forager thoroughly searches resource rich areas by making short moves and reorienting frequently; in extensive mode, it moves directly across resource poor areas by making long, straight-line moves with few interruptions.

Composite search behavior is widespread, observed in taxa as diverse as slime moulds [68], beetles [39], honeybees [114], fish [53], birds [84], ungulates [114], turtles [114], and weasels [49]. Given the ubiquity of composite search, an important

question arises: how should a forager determine when to switch from intensive to extensive mode, and vice versa? Questions about optimal foraging have traditionally been addressed with patch models that envision intensive search taking place within patches and extensive search as movement between patches [22, 85]. These models are not directly applicable to cases where resources do not occur in well-defined patches, and instead take on more general spatial distributions [5]. Optimal foraging on such landscapes is more properly addressed using random search theory [117, 61, 95]. In random search models, resources are represented as points, and animal movement is modeled with stochastic processes. Unlike patch models, random search models are spatially explicit; resource locations in these models can be specified according to any spatial point pattern and are not limited to the case of clearly defined patches.

Recently, many studies have compared the efficiencies of different random search movement patterns [62, 63, 101], and composite searches have been a particular focus [98, 89, 97]. The criteria that foragers use to switch between modes have received far less attention. Most analyses of optimal composite search presume that foragers use a "giving-up time" (GUT) as their mode-switching criterion [98, 89, 97]. A forager using this criterion switches from extensive to intensive mode upon encountering a resource. It then stays in intensive mode until a fixed amount of time (the GUT) has elapsed without a subsequent resource encounter. GUT models accurately describe some foraging situations, such as ladybird beetle larvae (*Coccinella septempunctata*) feeding on aphids [21] and houseflies (*Musca domestica*) feeding on sucrose drops [11].

Rather than keeping track of time, many animals use sensory cues to determine when to switch between intensive and extensive mode. Parasitoids like *Nermeritis canecens* [118], *Venturia canescens* [11], and *Cardiochiles nigriceps* [109] use chemical cues to determine when to search intensively for hosts. When deciding when to leave a foraging site, wolf spiders rely more heavily on visual and vibratory cues

than elapsed time since their last prey encounter [87]. Procellariiform seabirds use chemicals like dimethyl sulfide to identify where to engage in intensive search [82]. Further examples of animals that use sensory cues to determine search mode include ciliates like *Paramecium* and *Tetrahymena* [72, 70], bacteria, like *Escherichia coli* and *Salmonella typhimurium* [1, 80, 35], cod larvae [34], and fruit flies [29].

In many situations, sensory cues are not precise enough to allow a forager to immediately locate and travel to resources; instead, the forager uses the cues to determine whether an area is profitable enough to warrant intensive search. For this reason, we refer to these mode-switching cues as non-proximate. When a forager's search brings it very close to a resource, it can use proximate cues to directly move to the resource and consume it. In random search models, proximate cues are only available within a small distance, called the proximate radius, from a resource. Proximate cues lead a forager to deterministically move to the resource, while non-proximate cues determine the type of stochastic movement pattern the forager executes at a larger scale. Proximate and non-proximate cues may represent different sensory modalities (e.g., non-proximate olfactory cues and proximate visual cues) or different levels of precision for a single sensory modality (e.g., non-proximate olfactory cues at the landscape scale and more precise olfactory gradient following at closer range). For many microorganisms, like bacteria and plankton, the proximate cue is simply coming into physical contact with a resource. Non-proximate cues are particularly important when limited sensory capabilities, very dilute cues, or turbulent and unpredictable signal profiles prevent foragers from directly orienting toward a resource [50].

Most theoretical work on composite random search strategies has focused on GUT as the only mode-switching criterion. The role of non-proximate sensory cues as potential mode-switching criteria has been largely ignored (but see [50]). In this study, we introduce a modeling framework that describes two classes of composite

search strategies: those with mode transitions triggered by resource encounters and elapsed time (the GUT criterion), and those with mode transitions triggered by non-proximate sensory cues. This modeling framework includes the added flexibility of incorporating a full spectrum of random movement patterns for both intensive and extensive mode. We used large simulations to compare the efficiencies of different search strategies. Searching efficiency depends in part on the spatial distribution of resources [26], so we compared search strategies on a variety of landscape types, characterized by different levels of resource aggregation and density. Further, we examined the performance of the search strategies in response to changes in resource aggregation to test the robustness of the search strategies to environmental change. We found that the search strategy based on non-proximate sensory cues outperformed the search strategy based on resource encounters across all landscape types, and was more robust to changes in resource aggregation.

2.2 Modeling Framework

2.2.1 Model overview

In our modeling framework, resources are represented as points distributed across a landscape, and a forager is represented as a moving point with a small fixed proximate radius. When a resource falls within the forager's proximate radius, the forager moves in a straight line to the resource and consumes it; otherwise, it implements a random search strategy. Random search strategies consist of a set of probabilistic movement rules. Although the resulting movement patterns are stochastic, the probability distributions that generate the movement provide a structure for the search. Random search strategies are often used in foraging models because they agree with

the movement patterns observed in many foraging animals, and because few animals possess the capability to execute a purely systematic search [117].

2.2.2 Movement patterns

Lévy walks are stochastic processes that provide a versatile tool for modeling animal movement [10, 95]. A Lévy walk with parameter μ is a random walk with step lengths l drawn from a Pareto distribution, $p(l) \sim l^{-\mu}$, $1 < \mu \leq 3$. Different values of μ produce different types of random walks. As $\mu \to 1$, the resulting random walk approaches ballistic (i.e., straight-line) motion. For random walks with step lengths drawn from a Pareto distribution with $\mu \geq 3$, the generalized central limit theorem shows that the resulting random walk converges to Brownian motion at sufficiently large temporal and spatial scales (for details, see 2.6). Thus, Lévy walks can be seen as spanning a spectrum of movement behavior, ranging from ballistic motion ($\mu = 1$) on one extreme to Brownian-like motion ($\mu = 3$) on the other.

Our model deals with both non-composite and composite foragers. Non-composite foragers move by Lévy walks with parameter μ. Composite foragers switch between extensive and intensive search modes. In extensive search mode, foragers move according to a Lévy walk with parameter μ_{ext}. In intensive search mode, foragers move according to a Lévy walk with parameter μ_{int}. Previously, composite searches have been modeled with Brownian motion in the intensive mode and ballistic motion in the extensive mode [89]. This was later generalized to consider a full range of Lévy walks in extensive mode [97]. Our model represents a further generalization, and is the first work that allows a full range of Lévy walks for both intensive and extensive search modes.

2.2.3 Mode-switching criteria

Our model considers two type of composite foragers: GUT foragers, which use resource encounters as their search mode criterion, and sensory foragers, which use non-proximate sensory cues as their search mode criterion. A GUT forager switches from extensive to intensive search when it encounters a resource. After encountering a resource, the forager reverts to extensive search as soon as a specified time (the GUT) elapses without a subsequent resource encounter.

For the sensory forager, we created a generalized non-proximate sensory field. We denote the intensity of non-proximate sensory cues generated by a resource i detected at a location x by $f_i(x)$. The shape of the function $f_i(x)$ will depend on the particular sensory mechanisms involved; here, in order to make the model as general as possible, we assume that the strength of non-proximate sensory cues generated by a resource follows a Gaussian distribution with variance σ^2 centered at that resource. This is particularly appropriate if, for example, the sensory cues are chemical signals that travel via diffusion. The total non-proximate sensory field is obtained by superimposing the fields produced by each resource, $f(x) = \sum_i f_i(x)$. The non-proximate sensory forager monitors this field at the end of every step in its random walk. If the value of the field is below a specified threshold, the forager engages in extensive search; if it is above the threshold, it engages in intensive search (Fig. 2.1).

2.3 Model Simulation

2.3.1 Simulation objectives

Using the modeling framework above and Netlogo [121], we simulated three classes of foraging strategies: non-composite, GUT, and non-proximate sensory. Within

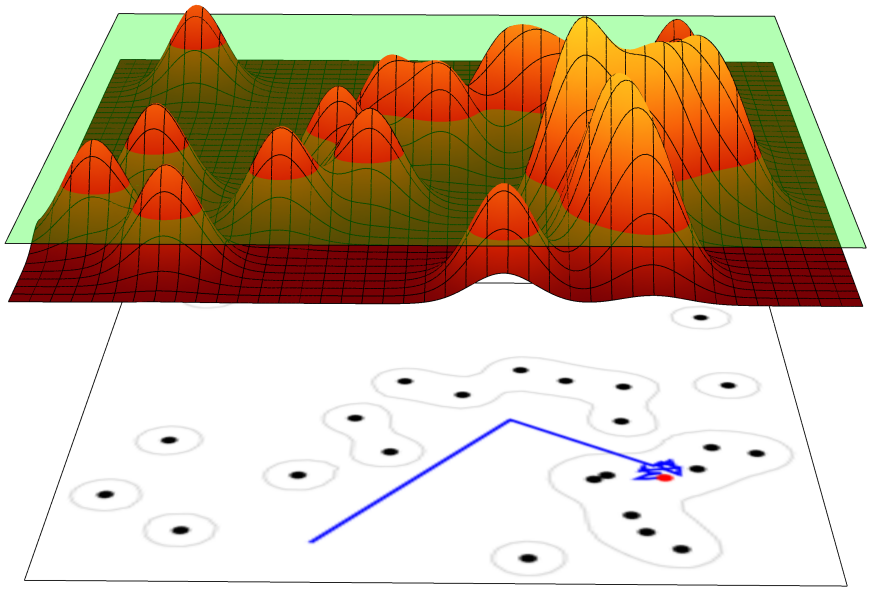

Figure 2.1: A schematic representation of the behavior of a non-proximate sensory forager. Resources are black dots on the two-dimensional landscape (bottom). The radius of a dot is the forager's proximate radius. A non-proximate sensory field (red surface) is generated by the resources. A non-proximate sensory forager has a fixed threshold (green plane) that it uses as a mode-switching criterion. When a forager reaches the end of a step-length, it assess the sensory field; if the field is above the threshold value (circled areas on landscape), the forager engages in intensive search. The forager's movement is represented by the blue line. In this case, it eventually consumes a resource (red disk).

each of these strategy classes, we sought to identify the movement parameters and mode-switching threshold that maximized search efficiency (defined as the number of resources consumed divided by the total distance moved). For the non-composite foragers, this amounted to optimizing the movement parameter μ. For GUT foragers, we optimized μ_{int}, μ_{ext}, and the GUT. For non-proximate sensory foragers, we optimized μ_{int}, μ_{ext}, and the level of the sensory field that would trigger switches in search mode (i.e., sensory field threshold, SFT). Using an optimization algorithm (see 2.7.1), we found the optimal parameter combination for each class of forager on each type of landscape, and compared the efficiencies of these optimal foragers. Then, we

examined the sensitivity of search efficiency to each of the optimized parameters (see 2.7.2). We also explored how a forager optimized to one type of landscape would fare in another; we quantified this ability with a measure called robustness (see 2.7.3). The sensitivity and robustness analyses were conducted with R [92].

2.3.2 Landscape characteristics

The landscape was simulated as square, 111 units in length and width. The units in NetLogo simply offer a spatial scale; coordinates are floating point numbers, and are not restricted to discrete values. Resources were distributed across the landscape according to a Neyman-Scott process (see 2.7.4). We selected this point process because it allowed us to adjust both the intensity and aggregation of the process. The distribution of the number of points in sample sets closely resembles a negative binomial distribution [123], but there is no stationary spatial point process that directly generates a negative binomial distribution of points in its sample sets [31]. The resource distributions were specified by two parameters: the radius of the clusters of resources and the total initial number of resources. We used 100, 400, 700, and 1000 as our initial resource levels, and cluster radii of 4, 8, 16, 32, and 64.

2.3.3 Forger characteristics

Foragers in our simulations traveled with a uniform speed of 0.25 units per time step and had a proximate radius of 0.5 units. When a forager consumed a resource, it stayed at that point for one unit of time. Consumed resources were not replaced; hence our simulations represent destructive foraging (resource depletion). If a forager encountered a resource during a step of a random walk, that step was truncated. The non-proximate sensory field was composed of Gaussian distributions with variance

one.

2.4 Results

2.4.1 Optimal parameters

The optimal search parameters of the non-proximate sensory foragers displayed a different pattern than those of the GUT foragers. For all degrees of resource aggregation, the best non-proximate sensory foraging strategies involved Brownian motion in intensive mode ($\mu_{\text{int}} = 3$). The optimal non-proximate sensory foragers used an extensive mode that depended on the landscape (although these extensive modes were always ballistic or close to ballistic). Thus, optimal non-proximate sensory foragers used intensive and extensive movement parameters that are consistent with conventional composite search (although the criteria they use for mode-switching distinguishes them from previous composite search models). The optimal parameter for non-composite search generally ranged from $\mu = 1.0$ on landscapes with low resource aggregation to $\mu = 1.8$ on landscapes with high resource aggregation (Table 2.1). Although optimizing the parameter for non-composite Lévy walks is a well-studied problem, the case of destructive foraging on patchily distributed resources is not; such situations were once assumed to be equivalent to non-destructive foraging on uniform landscapes, but this is not true [98]. Our non-composite results are largely in agreement with previous results about destructive searches on landscapes generated by cellular automata [98].

The optimal search parameters for composite foragers showed several interesting patterns. Conventional composite search strategies, which use ballistic motion in extensive search and Brownian motion in intensive search [89], provide a useful baseline

Table 2.1: Parameter combinations for three different search strategies producing the highest mean searching efficiency for different resource densities and cluster radii. Resource aggregation decreases with increasing cluster radius.

Resource Density	Cluster Radius	NCS[1]	GUT Strategy			NPS Strategy[2]		
		μ	μ_{ext}	μ_{int}	GUT	μ_{ext}	μ_{int}	SFT[3]
100	4	1.6	1.0	3.0	250	1.2	3.0	0.0005
100	8	1.4	1.0	3.0	400	1.4	3.0	0.0005
100	16	1.2	1.0	2.6	250	1.6	3.0	0.0005
100	32	1.4	1.0	1.8	150	1.4	3.0	0.0005
100	64	1.2	1.0	1.4	100	1.6	3.0	0.0005
400	4	1.6	1.0	3.0	150	1.2	3.0	0.0005
400	8	1.6	1.0	3.0	150	1.2	3.0	0.0020
400	16	1.4	1.0	2.6	150	1.0	3.0	0.0010
400	32	1.2	1.0	2.0	100	1.0	3.0	0.0010
400	64	1.2	1.0	1.6	50	1.2	3.0	0.0040
700	4	1.6	1.0	3.0	100	1.2	3.0	0.0020
700	8	1.4	1.0	3.0	100	1.0	3.0	0.0010
700	16	1.4	1.0	2.6	50	1.2	3.0	0.0160
700	32	1.2	1.0	2.0	50	1.0	3.0	0.0320
700	64	1.0	1.0	1.0	—	1.0	3.0	0.0320
1000	4	1.8	1.0	3.0	100	1.0	3.0	0.0005
1000	8	1.6	1.0	3.0	100	1.0	3.0	0.0005
1000	16	1.4	1.0	2.4	50	1.0	3.0	0.0320
1000	32	1.4	1.0	2.0	50	1.0	3.0	0.0640
1000	64	1.0	1.0	1.0	—	1.0	2.8	0.0640

[1]Non-composite search strategy
[2]Non-proximate sensory search strategy
[3]Sensory field threshold

for comparison. For all degrees of resource aggregation, the best GUT foraging strategies involved ballistic motion in extensive mode ($\mu_{\text{ext}} = 1$) (Table 2.1). The optimal intensive mode for GUT foragers depended on the degree of resource aggregation. On landscapes with a high degree of resource aggregation, optimal GUT foragers used Brownian motion in intensive mode ($\mu_{\text{int}} = 3$). Thus, the optimal GUT foragers for landscapes with a high degree of resource aggregation behaved as a conventional composite searcher. The optimal GUT foragers for other landscapes used the conventional extensive strategy but deviated from the conventional intensive strategy ($\mu_{\text{int}} < 3$).

2.4.2 Search strategy comparisons

After identifying optimal parameters for non-composite, GUT, and non-proximate sensory foragers, we compared the search efficiencies of these foraging strategies. The composite search strategies outperformed the non-composite search strategy when resources were highly aggregated, and the relative advantage of composite search increased with the degree of resource aggregation (Fig. 2.2). Composite search also produced lower variability in search efficiency than non-composite search when resources were highly aggregated (Fig. 2.3). For all search strategies, both search efficiency (Fig. 2.2) and variability in search efficiency (Fig. 2.3) increased with degree of resource aggregation.

The non-proximate sensory strategy performed better than the GUT strategy across the full spectrum of resource aggregation (Fig. 2.2). At first glance, this result may seem obvious; having sensory capabilities is clearly better than not having them at all. Recall, however, that the non-proximate sensory forager is not simply an enhanced GUT forager. The GUT forager has the ability to keep track of time since the last resource encounter, an ability that the non-proximate sensory forager lacks.

The non-proximate sensory forager's performance advantage over the GUT forager can be attributed to two main causes. First, the sensory forager has more opportunities to switch search mode. The GUT forager only switches mode upon encountering resources or when the time threshold expires. The sensory forager examines the sensory field at every resource encounter and at the end of every step of its random walk; this happens very frequently when move lengths are short (i.e., when μ is close to 3.0). When the sensory forager engages in intensive mode, it is not making a large time commitment, because it has frequent opportunities to revert to extensive mode. When the GUT forager engages in intensive search, it is stuck in that mode until

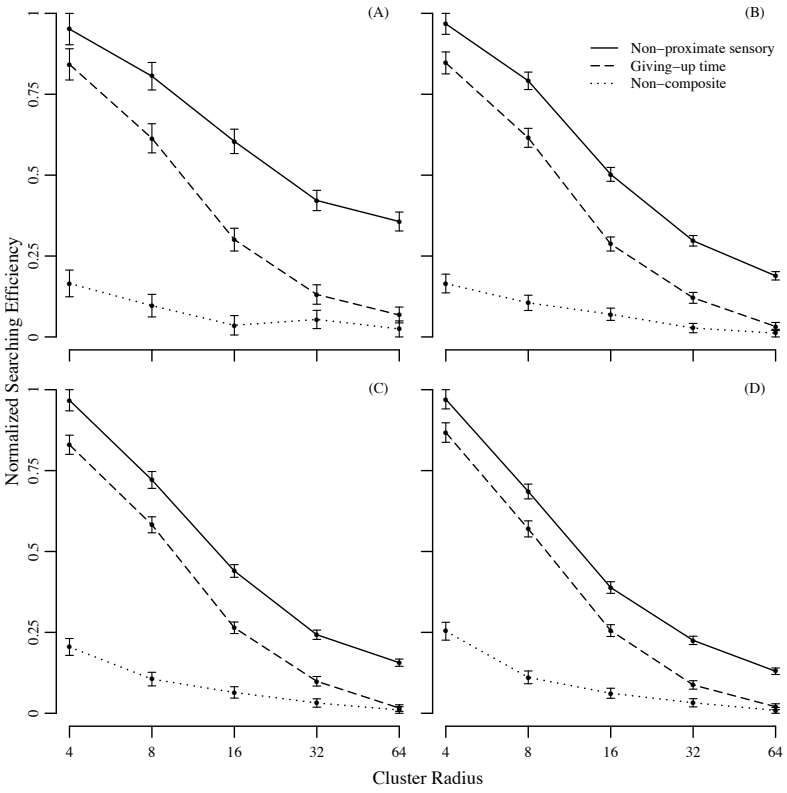

Figure 2.2: Normalized searching efficiency for three search strategies across 5 levels of resource aggregation and 4 levels of resource density: (A) 100, (B) 400, (C) 700, (D) 1000. Searching efficiency was normalized for comparison across resource densities. Resource aggregation decreases with increasing cluster radius. Error bars represent 95% confidence intervals. The x-axis is presented on the $\log_2$ scale.

the time threshold elapses. Second, the GUT forager's search strategy relies on the spatial autocorrelation of resources. When a GUT forager encounters a resource, it enters intensive search, under the assumption that other resources are nearby. In contrast, the sensory forager can be triggered into intensive search by local deviations in the sensory field, which is beneficial regardless of the spatial autocorrelation of the resources. This effect is evident in figure 2.2, where the advantage of sensory search over GUT search increases slightly as landscapes become more dispersed.

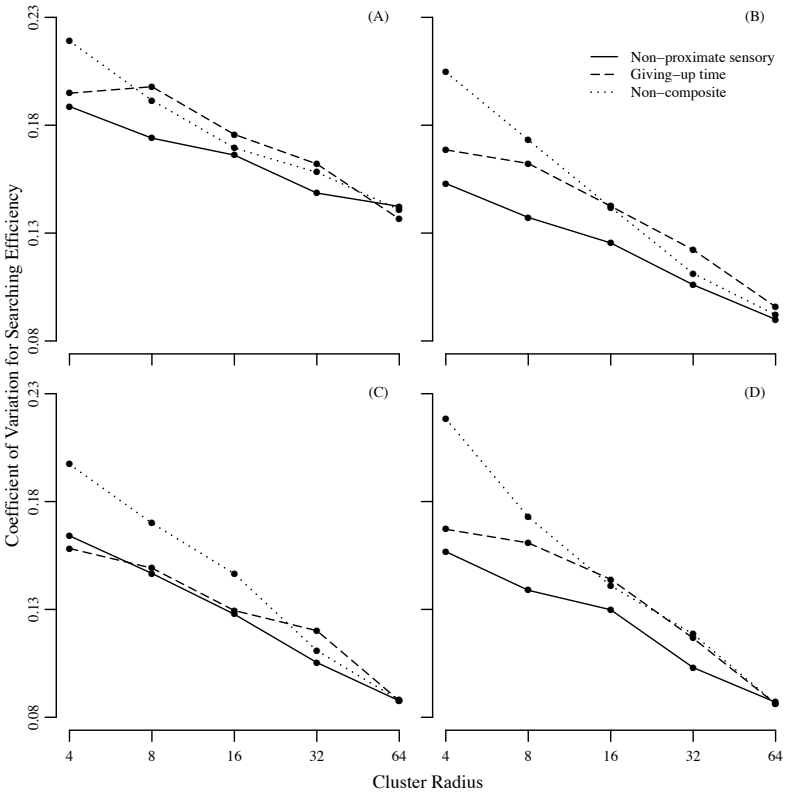

Figure 2.3: Coefficient of variation in searching efficiency for three search strategies across 5 levels of resource aggregation and 4 levels of resource density: (A) 100, (B) 400, (C) 700, (D) 1000. Resource aggregation decreases with increasing cluster radius. The x-axis is presented on the $\log_2$ scale.

2.4.3 Sensitivity

For both composite search classes, searching efficiency was most sensitive to movement behavior in extensive mode, μ_{ext} (Fig. 2.4). The difference in searching efficiency between the optimal μ_{ext} and the worst μ_{ext} was up to 70%. In contrast, the difference in searching efficiency between the optimal μ_{int} and the worst μ_{ext} was no more than 45%.

Setting the threshold parameter (the time threshold for GUT foragers, the sensory field threshold for non-proximate sensory foragers) below the optimal value caused greater decreases in efficiency than when these parameters were set above the optimal

value. When the time threshold is set too low, the GUT forager spends too much time in extensive mode; in the extreme, setting the time threshold to zero leads to a reduction in efficiency of nearly 40%. When the sensory field threshold is set too low, the non-proximate sensory forager spends too much time in intensive search; in the extreme, setting this threshold to zero leads to a reduction in efficiency of over 60% (figure 2.4).

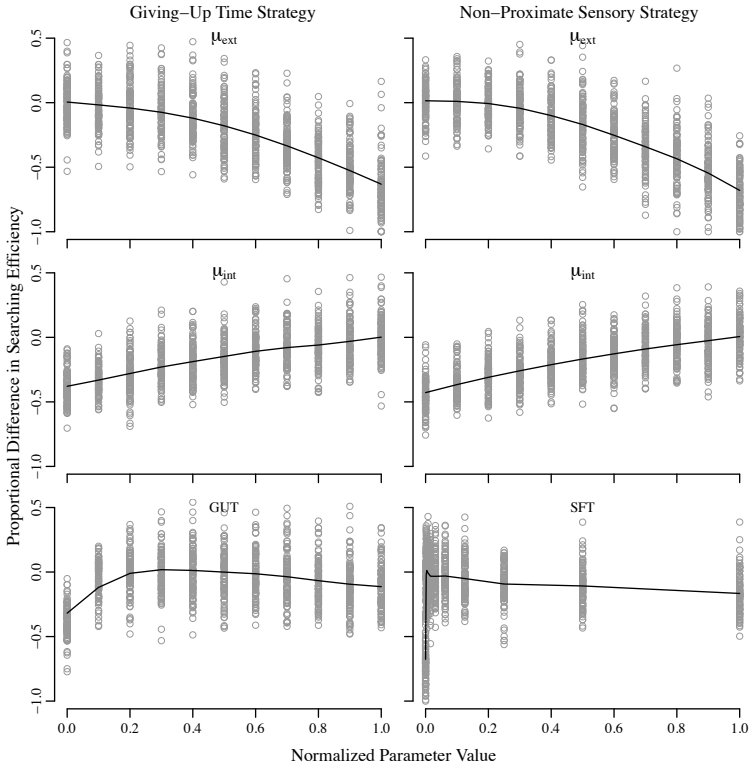

Figure 2.4: Representative example of sensitivity analysis for the three parameters associated with giving-up time and non-proximate sensory search strategies (resource density = 400; cluster radius = 4). Points represent proportional difference in searching efficiency for a single run relative to the mean searching efficiency produced by the optimal parameter combination. Parameter values were normalized for comparison. μ_{int} is the intensive movement parameter, μ_{ext} is the extensive movement parameter, GUT is the giving-up time, and SFT is the sensory field threshold. Lines represent smoothing splines fitted to the relationship. Sensitivity analysis based on 100 runs of the model for each parameter value. See Appendix B.2 for additional details.

2.4.4 Robustness

Our robustness analysis (explained in detail in 2.7.3) allowed us to determine how a forager optimized for a particular level of resource aggregation would fare in landscapes with different levels of resource aggregation. The non-proximate sensory strategy was less affected by changes in resource aggregation than the GUT strategy, particularly for foragers that were optimized for dispersed resources (black lines in Fig. 2.5). The optimal GUT strategy for harvesting dispersed resources approximated non-composite search behavior (i.e., the values for μ_{ext} and μ_{ext} converged) (Table 2.1). Placing these foragers in landscapes with more aggregated resources drastically reduced their searching efficiency (black dashed lines in Fig. 2.5). In contrast, GUT foragers optimized for clumped resources were relatively robust to decreasing degrees of resource aggregation (grey dashed lines in Fig. 2.5). The non-proximate sensory strategy was relatively robust to deviations from the resource distribution pattern to which a forager was optimized (solid lines in Fig. 2.5).

2.5 Discussion

Composite search strategies, which consist of extensive and intensive search modes, help foragers focus search effort on resource rich regions and devote less effort to resource poor regions. The central objective of this study was to compare the efficiency of two possible criteria for switching search modes: giving-up time (GUT) and non-proximate sensory cues. To our knowledge, GUT is the only mode-switching mechanism previously used in composite search models [63, 97, 89], and our model with mode-switching based on non-proximate sensory cues is novel. As discussed in the introduction, composite searches based on non-proximate cues are a general tactic used by a wide variety of organisms, and hence this model has broad applications.

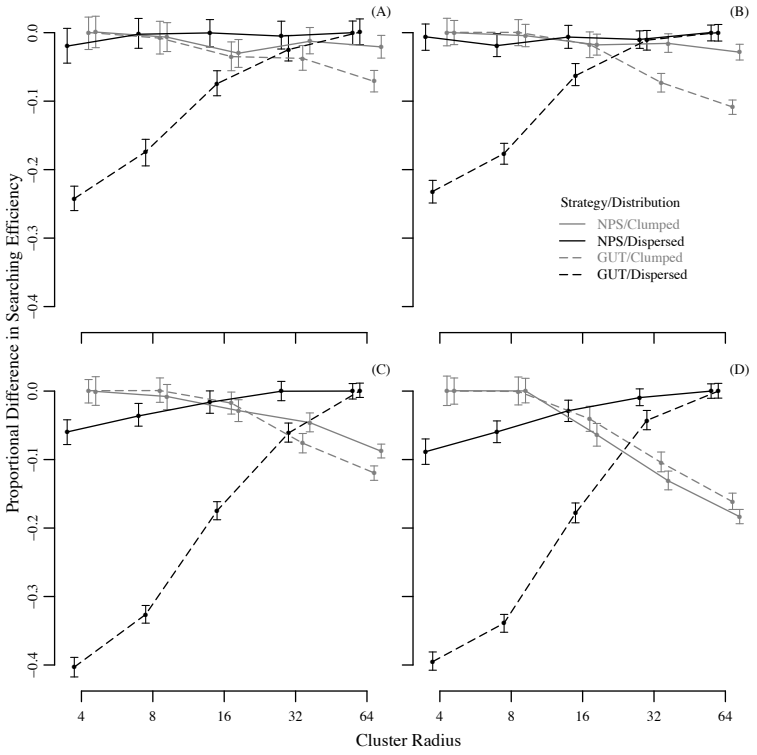

Figure 2.5: Robustness of non-proximate sensory (NPS) and giving-up time (GUT) search strategies across 5 levels of resource aggregation and 4 levels of resource density: (A) 100, (B) 400, (C) 700, (D) 1000. The performance of foragers that evolved in landscapes with clumped (grey lines) or dispersed (black lines) resources was tested in landscapes with different degrees of resource aggregation. Robustness was calculated as the proportional difference in mean searching efficiency between a forager that is new to a landscape type and a forager that evolved in that landscape type. Points represent the mean proportional difference in searching efficiency, D_{R}, and error bars represent the 2.5% and 97.5% quantiles of the bootstrapped data set. See Appendix B.3 for additional details. Resource aggregation decreases with increasing cluster radius. Points are offset from x-coordinates for clarity of presentation. The x-axis is presented on the $\log_2$ scale.

Our simulations revealed that non-proximate sensory foragers outperformed GUT foragers across a full spectrum of resource distributions, ranging from highly aggregated to highly dispersed. In addition, non-proximate sensory foragers were more robust to changes in resource distribution, implying that they would be better able to cope with environmental change. These results indicate that it is better to inform

search behavior with a non-directional sensory cue than with resource encounters and elapsed time. Together with empirical evidence indicating that sensory cues are more important than recent resource encounters in determining foraging mode [87], our simulations suggest that the existing GUT composite search paradigm should be considered as only a subset of a broader class of composite search strategies.

In an attempt to keep our model as general as possible, we have neglected several important ecological factors. First, we did not consider the costs involved in the evolution or development of the cognitive and sensory abilities foragers would need to detect non-proximate cues versus the cost to keep track of time. Second, we only considered non-proximate sensory fields that were Gaussian; the exact shape of these fields will depend on the specific environment and cues under examination. For example, chemical cues are often transported via prevailing winds [100]. Third, our simulation was done in two dimensions; for many species, especially marine organisms, a three-dimensional model would be more appropriate. Finally, we did not take into account factors like cooperative foraging, interspecific competition, or predation risk. The balance between food acquisition and predation risk is a particularly important determinant of a forager's fitness [19]. Following [98], we could incorporate proxies for predation risk in our model, such as forcing GUT searchers to use giving-up-times that are shorter than optimal, or by making resource detection within the proximal radius imperfect (under the assumption that vigilance against predators detracts from a forager's ability to consistently detect resources). However, in some situations [115], more convoluted movement exposes a forager to less predation risk, not more. One solution would be to directly and spatially explicitly include predators in the model. For our non-proximate sensory foragers, the sensory field generated by resources could be combined with an inhibitory field generated by predators, so that intensive search is encouraged by proximity to resources, but discouraged by proximity to predators.

The aim of this study, though, is to understand baseline foraging behavior before considering how it interacts with predation risk.

The modeling framework outlined in this study has the potential to help bridge the gap between two traditionally disparate fields of study: random search theory and classic patch use theory. The former focuses on animal movement patterns, the latter on patch use decisions [8]. Recent work [10] has sought to establish a "stochastic optimal foraging theory" to unify these approaches; our model could contribute to that effort. One of the foundational results of classic foraging theory is Charnov's Marginal Value Theorem (MVT), which dictates that an optimal forager should deplete patches so that the intake rate in each patch is equal to the expected intake rate averaged over the rest of the environment [22]. The predictions of the MVT provide a useful benchmark to measure real-world foragers against. Unfortunately, the MVT is not easily translated to the realm of random search theory, where resources have arbitrary spatial distributions (hence patches are not well-defined) and resource encounters are typically discrete events (hence instantaneous intake rate is not well-defined).

On landscapes where resources are distributed as points, the best possible forager would solve a famous optimization problem known as the traveling salesman problem. The traveling salesman problem essentially asks: given a set of points, what is the shortest possible route that visits each point exactly once? Many books are devoted to solution algorithms for this challenging problem [3, 64], and it is unlikely that animals solve this problem to arrive at the optimal strategy. Therefore, the question of how to best describe optimal foraging on spatially distributed point resources remains. If the MVT could successfully be translated into the context of random search, then we would have a useful null-model for such landscapes.

Plank and James [89] proposed an analogue between between patch-use models and composite random search models: within patch harvesting corresponds to inten-

sive search, while between-patch travel corresponds to extensive search. They further suggested that optimal GUT composite searchers represent the random search version of MVT optimal foragers. There are important differences between the optimal behavior predicted by these two models, though. MVT optimal foragers make decisions based on the current local and global resource levels. They are omniscient, and hence have no need to use past experience or memory. This contrasts with GUT optimal foragers, whose behavior is highly dependent on stochastic resource encounters. The non-proximate sensory optimal foragers introduced in this chapter might provide a better analogue to MVT optimal foragers. Like MVT optimal foragers, non-proximate sensory optimal foragers make instantaneous assessments of local and global resource conditions to determine when to switch behavioral modes. Just as MVT optimal foragers provide a useful null-model for foraging on landscapes with resource patches, non-proximate sensory optimal foragers could provide a useful null-model for foraging on landscapes with resources distributed as arbitrary point patterns. The non-proximate sensory forager model predicts areas that warrant intensive search; by overlaying this with observed animal movement trajectories, one could determine how close those animals come to optimal behavior.

2.6 Appendix: Lévy walks with $\mu = 3$

In this section, we examine the properties of Lévy walks with $\mu = 3$. Many studies about random search strategies, including this one, use Lévy walks with parameters $\mu \in (1, 3]$ to represent a spectrum of movement types, ranging from ballistic motion on one extreme to Brownian motion on the other [97, 101, 62]. It is thus important to verify that the $\mu = 3$ case can indeed be characterized as Brownian. The categorization of Lévy walks with $\mu = 3$ has been treated with ambiguity in the ecological

literature. [62, 96, 89] and [95] all label Lévy walks with $\mu = 3$ as Brownian motion. [98, 108, 10] and [63] state that power-law walks with $\mu > 3$ are Brownian, and either classify the $\mu = 3$ case as superdiffusive or do not mention it at all. We seek to provide clarification here.

The categorization of a stochastic process depends on how its mean-square displacement, $\langle x^2 \rangle$, scales with time. For Brownian motion, $\langle x^2 \rangle \sim t$, while for superdiffusion, $\langle x^2 \rangle \sim t^\alpha$, $\alpha > 1$. As we explain below, Lévy walks with $\mu = 3$ scale as $\langle x^2 \rangle \sim \ln(t)\, t$, a marginal case between Brownian motion and superdiffusion. Ecology papers rarely remark on this $\langle x^2 \rangle \sim \ln(t)\, t$ scaling behavior, and, to our knowledge, never provide a mathematical explanation. In this section, we provide a concise derivation for ecological readers. Our approach follows the continuous time random walk framework presented in [124], where a similar scaling relationship was derived for random walks on a spatial lattice. We examine the one-dimensional case for simplicity, but the same arguments carry over to higher dimensions.

Let $\phi(x,t)$ be the probability density function for a random walk to be located at position x at time t. The jump probability density function, $h(x,t)$, determines the probability of transitioning from one position to another. The probability that a walker makes a jump of distance between x and $x + \Delta x$ in the time between t and $t + \Delta t$ is $\int_x^{x+\Delta x} \int_t^{t+\Delta t} h(y,\tau)\, d\tau\, dy$. For a Lévy walk with $\mu = 3$, constant velocity v, and proximate radius l_0, the jump probability density function is

$$h(x,t) = \frac{1}{2} p(t)\, \delta(|x| - vt)$$

$$p(t) = \begin{cases} 2\, l_0^2\, t^{-3} & t \geq l_0 \\ 0 & t < l_0 \end{cases}.$$

The choice of velocity and proximate radius do not affect the scaling relationship, so

we choose $v = l_0 = 1$. The delta function couples the length of a step with the time it takes to execute it, so taking a step of length $|x|$ requires time $t = |x|$. Therefore, the probability density for the step times, $p(t)$, determines both the distance and duration of steps. The factor of $\frac{1}{2}$ arises because the walker can take a step to either the left or right.

Consider the probability that a walker arrives at position x at time t at the exact end of a step-length. The associated probability density function, $\omega(x,t)$, satisfies the equation

$$\omega(x,t) = \delta(t)\ \delta(x) + \int_{-\infty}^{\infty}\int_{0}^{t} \omega(y,\tau)\, h(x-y, t-\tau)\, d\tau\, dy. \tag{2.1}$$

The first term on the right hand side arises because the walker starts at the origin. The second term sums all contributions from steps that start at position y and time τ and end at position x at time t. This is not quite an equation for the probability density $\phi(x,t)$; for that, we must consider that a walker can pass a given position during a step. The probability that a walker passes position x at time t in a single step from the origin is given by the density function

$$g(x,t) = \frac{1}{2}\delta(|x| - t)\int_{t}^{\infty} p(\tau)\, d\tau = \frac{1}{2}\delta(|x| - t)\, t^{-2}.$$

With this, we can obtain an equation for $\phi(x,t)$:

$$\phi(x,t) = \int_{-\infty}^{\infty}\int_{0}^{t} g(y,\tau)\, \omega(x-y, t-\tau)\, d\tau\, dy. \tag{2.2}$$

This accounts for all possible ways of finishing the previous step at exactly position $x - y$ at time $t - \tau$, then passing position x at time t during the next step. We next take both Fourier and Laplace transforms of (2.1) and (2.2). A capital letter

for a function name and a switch in the argument from t to s will indicate a Laplace transform; a carat over the function and a switch in the argument from x to k will indicate a Fourier transform. Using convolution properties, we find $\hat{\Omega}(k,s) = \frac{1}{1-\hat{H}(k,s)}$ and $\hat{\Phi}(k,s) = \hat{G}(k,s)\,\hat{\Omega}(k,s)$, so

$$\hat{\Phi}(k,s) = \frac{\hat{G}(k,s)}{1-\hat{H}(k,s)}. \tag{2.3}$$

The Fourier-Laplace transformed function $\hat{\Phi}(k,s)$ is particularly useful, because the following relationship yields the Laplace transform of the mean-square displacement:

$$\langle \hat{x^2} \rangle = \int_0^\infty x^2 \Phi(x,s)\, e^{-ikx} dx = -\frac{\partial^2 \hat{\Phi}}{\partial k^2}(0,s)\ . \tag{2.4}$$

To find $\hat{\Phi}(k,s)$, we need to calculate the Fourier-Laplace transforms of $h(x,t)$ and $g(x,t)$. For the former,

$$\begin{aligned} \hat{H}(k,s) &= \int_1^\infty \int_{-\infty}^\infty \delta(|x|-t)\, t^{-3} e^{-st} e^{-ikx} dx\, dt \\ &= \int_1^\infty t^{-3} e^{-t(s+ik)} dt + \int_1^\infty t^{-3} e^{-t(s-ik)} dt\,. \end{aligned}$$

Let $z = s+ik$, $\lambda(z) = \int_1^\infty t^{-3} e^{-tz} dt$, and observe that $\hat{H}(k,s) = \lambda(s+ik) + \lambda(s-ik)$. To calculate $\lambda(z)$, we perform integration by parts twice and obtain

$$\lambda(z) = \frac{1}{2}\left(e^{-z} - z e^{-z} - z^2 Ei(-z)\right),$$

where $Ei(z)$ is the exponential integral function, which can be written as $Ei(-z) = \gamma + \ln(z) - \sum_{k=1}^\infty \frac{(-1)^{k+1} z^k}{k\, k!}$. Performing a small z expansion for $\lambda(z)$ yields

$$\lambda(z) = \frac{1}{2}\left(1 - 2z - z^2 \ln(z)\right) + O\left(|z|^2\right).$$

A similar approach can be used to calculate $\hat{G}(k,s)$. Letting $z = s + ik$ and $\psi(z) = \frac{1}{2}\int_1^\infty t^{-2}e^{-tz}dt$, we have $\hat{G}(k,s) = \psi(s+ik) + \psi(s-ik)$. To calculate $\psi(z)$, note that $\psi(z) = \frac{1}{z}\left(\frac{e^{-z}}{2} - \lambda(z)\right)$, so

$$\psi(z) = \frac{1}{2}\left(e^{-z} + z\,Ei(-z)\right),$$

and the small z expansion is

$$\psi(z) = \frac{1}{2}\left(1 + (\gamma - 1)z + z\ln(z)\right) + O\left(|z|^2\right).$$

The small z expansions for $\lambda(z)$ and $\psi(z)$ give small k and s expansions for $\hat{H}(k,s)$ and $\hat{G}(k,s)$, respectively, and, by (2.3), for $\hat{\Phi}(k,s)$. Using (2.4), we obtain, for small s,

$$\hat{\langle x^2\rangle} \simeq -\frac{1 + 3s(\gamma-1) + 2\ln(s) + 2s\gamma\ln(s) + 2s(\ln(s))^2}{s^2(2 + s\ln(s))^2}.$$

The Tauberian theorems [38] relate the asymptotic behavior of a function as $t \to \infty$ to the behavior of its Lapalce transform as $s \to 0$. In this case, for large t,

$$\langle x^2\rangle \simeq \frac{t\,\ln(t)}{2} - \frac{1}{4}t + \frac{1}{4}\left(3 - 3\gamma - \ln(t) + 2\gamma\,\ln(t)\right),$$

Keeping only the largest term and ignoring constants,

$$\langle x^2\rangle \simeq t\,\ln(t).$$

Therefore, even though simulation studies like this one loosely refer to Lévy walks with $\mu = 3$ as Brownian, they actually represent marginal behavior between the diffusive and superdiffusive regimes.

It's important to note the difference between Lévy flights, in which a walker takes

instantaneous jumps, and Lévy walks, in which a walker moves continuously with finite velocity along each step [63]. For the former case, central limit theorems can be used to categorize how mean-square displacement scales with the number of steps. For power-law step-length distributions with $\mu > 3$, the standard central limit theorem implies convergence to Brownian motion; for $\mu = 3$, Gnedenko and Kolmogorov's generalized central limit theorem implies that the random walk's distribution is in the (confusingly named) non-normal domain of attraction of the normal distribution [43]. The continuous time random walk approach used above allows for the analysis of actual Lévy walks instead of their Lévy flight cousins.

2.7 Appendix: Model details

2.7.1 Parameter Optimiziation

We used a grid-based search to explore the searching efficiency associated with large regions of the parameter space of our simulation model. A non-composite forager is characterized by a single parameter μ. We ran non-composite simulations using parameter values $\mu = 1.0, 1.2, 1.4, ..., 3.0$ on each landscape type (specified by initial resource distribution and resource aggregation). For the composite foragers, we examined 4 initial resource densities, 5 cluster radii, 2 search strategies (GUT and non-proximate sensory), and 11 values for each of the 3 search parameters (μ_{ext}, μ_{int}, switching threshold). In the first sweep of the parameter space, we conducted 100 runs for each parameter combination for a total of 5,324,000 runs (4 densities * 5 radii * 2 strategies * 11^3 = 1331 search parameter combinations * 100 runs). Each run of the model consisted of 20,000 discrete time steps. The full grid-based search produced a rough fitness surface based on the searching efficiency of each parameter

combination. The fitness surface allowed us to exclude regions of the parameter space that led to poor searching efficiency, thereby focusing our computational resources on increasing replication in regions of the parameter space that were likely to contain the optimal parameter combination. We used an iterative process (described below) to narrow the regions of the parameter space selected for increased replication. The iterative process did not produce a finer-scale resolution of the parameter space but rather increased the replication for subsets of the parameter combinations used in the full grid-based search. Within each landscape type, we used the mean searching efficiency from the full grid-based search to select the top 13 of the 1331 (1%) possible parameter combinations. For each parameter, we used the range of values found within the top 1% to reduce the parameter space. For example, suppose the top 1% parameter combinations included μ_{ext} values that ranged from 1.0-1.4, μ_{int} values from 2.6-3.0, and GUT values from 100-200. Then we would have increased replication for the 27 parameter combinations (μ_{ext}, μ_{int}, GUT) that represented parameter values within those ranges: μ_{ext} = 1.0, 1.2, 1.4; μ_{int} = 2.6, 2.8, 3.0; GUT = 100, 150, 200. For some landscape types, this approach did not reduce the parameter space substantially. Thus, we conducted 200 runs for each parameter combination in the reduced parameter space and again calculated the top 1% of the parameter combinations to further reduce the parameter space. This process was repeated until the optimal parameter combination was comprised of at least 500 runs because preliminary exploration of the model indicated that 500 runs produced good estimates of mean searching efficiency.

2.7.2 Sensitivity

We examined the sensitivity of searching efficiency to each search parameter by varying one search parameter while holding the other two parameters at their optimal values. μ_{ext} and μ_{int} ranged from 1 to 3, GUT ranged from 0 to 500, and the sensory field threshold ranged from 0 to 0.256 (Table 2.2). The μ parameters have a naturally bounded range, but the threshold parameters have arbitrary upper bounds, which were selected based on preliminary explorations of parameter space. We normalized the parameter values to fall between 0 and 1 to facilitate comparisons across the different ranges of the parameters. We calculated the proportional difference in searching efficiency as $D_{\text{S}} = (y - \bar{y}_{\text{o}})/\bar{y}_{\text{o}}$, where y was the searching efficiency for a single run and $\bar{y}_{\text{o}}$ was the mean searching efficiency for the optimal parameter combination. We fitted smoothing splines to the relationship between D_{S} and the normalized value of each parameter for each landscape type. The shape of the smoothing splines provided an indication of the sensitivity of searching efficiency to changes in each parameter. In two cases (see Table 2.1), the optimal μ_{ext} and μ_{int} were the same, which made the best giving-up time parameter irrelevant. Thus, those landscape types were excluded from the sensitivity analysis.

2.7.3 Robustness

To assess the robustness of the optimal strategies to changes in resource aggregation, we examined how a search strategy that maximized the searching efficiency for one landscape type performed in landscape types with different degrees of resource aggregation. Specifically, we calculated robustness as $D_R = (\bar{y}_{i,j} - \bar{y}_{i,i})/\bar{y}_{i,i}$, where $\bar{y}_{i,j}$ was the mean searching efficiency in landscapes of type i for a forager that was optimized for a landscape of type j. In this formula, landscape types are indexed by cluster

Table 2.2: Parameter values used in the simulation model

Parameter	Value
Resources	
Initial number of resources	100, 400, 700, 1000
Number of clusters[1]	15
Radius of resource cluster[2]	4, 8, 16, 32, 64
Forager	
Speed (distance/time step)	0.25
Detection radius	0.5
Lévy exponent (μ)	
Extensive search mode	1.0, 1.2, 1.4, 1.6, ..., 3.0
Intensive search mode	1.0, 1.2, 1.4, 1.6, ..., 3.0
Mode-switching criteria[3]	
Giving-up time	0, 50, 100, 150, 200, ..., 500
Sensory field threshold	0, 0.0005, 0.001, 0.002, ..., 0.128, 0.256

[1]Poisson random variable with an expected value of 15
[2]Resource aggregation decreases with increasing cluster radius
[3]Forager employs only one mode-switching criteria in a run of the simulation

radius. We examined how foragers optimized for very clumped and very disperse landscapes ($j = 4$ and $j = 64$, respectively) performed on a full range of landscape types ($i = 4, 8, 16, 32, 64$). This analysis was done on four different levels of resource density (100, 400, 700, 1000). Then we resampled the data with replacement (i.e., bootstrap method) 500 times for each landscape type and calculated the mean and 2.5% and 97.5% quantiles of the distribution of robustness values.

2.7.4 Resource distribution

Resources were distributed across landscapes according to Neyman-Scott processes [57]. The algorithm involved randomly drawing the number of resource aggregations, or clusters, from a Poisson distribution with an expected value of 15 (Table 2.2). The center of each cluster was randomly assigned to a point in the landscape (i.e., parent point). Then resources were sequentially assigned to a random parent and randomly placed within a specified radius (i.e., cluster radius) of the parent point until all re-

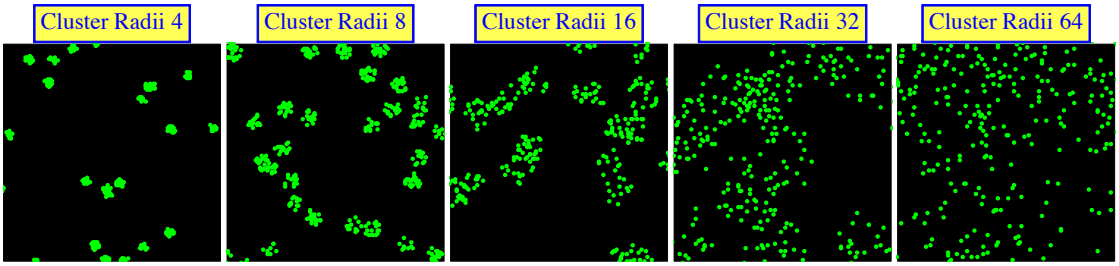

Figure 2.6: Sample landscapes for different cluster radii. 700 resources per landscape.

sources were distributed among the parents. Thus, for each run of the simulation, the algorithm randomly determined the number of clusters and the number of resources per cluster, but the initial total resource density and the cluster radius were fixed. By changing a single parameter (i.e., cluster radius), we were able to vary the degree of aggregation of resources, which ranged from tightly clumped (cluster radius = 4) to dispersed (cluster radius= 64). Representative landscapes are shown in figure 2.6

2.7.5 Boundary conditions

Landscape boundary conditions play an important role in individual-based models [17]. Most simulations use one of three types of boundary conditions: reflecting, periodic, or absorbing. Reflecting boundaries are appropriate for modeling animals that live in a restricted environment, like animals on an island, but are otherwise unrealistic [17]. Reflecting boundary conditions can also be interpreted as having a new forager enter the landscape at the exact place where the previous forager left it. This biases the initial conditions for the new forager and creates edge effects.

Periodic boundary conditions can be interpreted in three different ways. First, the landscape is literally a torus; this tends not to occur in nature. Second, the landscape is infinite, but repeating; this is problematic when resource consumption is destructive, and a forager's actions at one point on a landscape affect an infinite number

of other points. Third, a new forager enters the landscape at a point determined by where the original forager left it; like with reflecting boundary conditions, this has the potential to create edge effects. Our modeling framework presents a few additional problems associated with periodic boundary conditions. The resource distributions and the sensory field are generated under the assumptions that the topology of the landscape is a plane; periodic boundary conditions would mean that resources on opposite ends of the landscape are close to each other, leading to logical inconsistencies.

In our model we implemented a modified version of absorbing boundary conditions. The major challenge with absorbing boundary conditions is that a forager could leave the landscape by chance almost immediately after entering it. The performance of such a forager would not provide much information about the efficiency of the strategy it employed. Therefore, we chose to force each forager to spend 20,000 discrete time steps foraging on the landscape. If the forager was absorbed by a boundary, it was randomly dropped back into the landscape to resume foraging. This can be interpreted as a forager leaving the landscape, then returning later to resume foraging. We chose 20,000 time steps, because this was a sufficient time for foragers to appreciably deplete landscapes. Finally, we included a small resource-free buffer zone at the edge of the landscape. The entire landscape was a square 111 units long and 111 units wide, but only the 101 unit long, 101 unit wide square in the center contained resources. Resource-free buffer zones occupied 5 unit thick strips at the top, bottom, left, and right edges of the landscape. This ensured that all resources could be approached from every direction, and that no resources were protected by edge effects.

Chapter 3

A new framework for analyzing pollinator foraging behavior

3.1 Introduction

Pollinator foraging behavior is a topic of great interest in evolutionary biology [105], ecology [122], and animal behavior [41]. Researchers in all of these disciplines have made significant advances toward understanding pollinator behavior. Nonetheless, important questions remain about how to disentangle the factors that determine which flowers a pollinator visits. These factors can include preferences for specific flower colors [90], sizes [104], odors [103], shape [79], or species [119]. Other factors include previous individual experience [112], socially shared information [48], predation risk [94], the composition of the surrounding community of plants [52], and the spatial configuration of plants [28].

The role of the spatial configuration of plants can be particularly difficult to separate from other factors. If a pollinator moves from flower A to flower B, is it because of flower B's traits, or simply because of its convenient location? Researchers have at-

tempted to circumvent this problem using experimental arrays of flowers [58, 28, 81], and these studies have yielded important insights about pollinator preferences. While the regularity of an experimental array might seem to remove spatial configuration as a confounding factor, it does not; the sequence of flowers that a pollinator visits is always contingent upon the precise spatial configuration of flowers. An experimental array is only one specific configuration that pollinators could potentially experience. It is impossible to make arrays for every possible spatial configuration of flowers. Given that researchers can only observe pollinator behavior on a finite number of spatial configurations, how should these configurations be selected? An obvious answer is to chose those configurations that are already available in the natural world: that is, to use field observations rather than experimental arrays. This leaves the problem of how to disentangle spatial configuration from other factors that influence pollinator foraging. We propose a maximum likelihood framework for analyzing field observations of pollinator foraging. This framework allows researchers to quantify factors like pollinator preference, independent of the confounding effects of spatial configuration. Furthermore, it uses observations of pollinator behavior in environments that have not been subject to experimental modifications. This simplifies the assessment of pollinator behavior, and avoids introducing confounding artificial influences into the pollinator's environment.

In section 3.2, we define several important concepts in pollinator behavior. In section 3.3, we describe one of the key motivations for understanding pollinator foraging: hybridization and speciation of flowering plants. In section 3.4, we describe how spatial configuration of flowers offers special challenges for understanding foraging behavior, and we discuss previous attempts to address this problem. In section 3.5, we describe our maximum likelihood framework. In section 3.6, we describe a study system involving sweat bees in Western Nebraska, and we use this system to

demonstrate the usefulness of our maximum likelihood framework. In section 3.7, we describe the results from the study system and we discuss this framework more generally.

3.2 Preference, Constancy, and Bias

Constancy and *preference* are two behavioral patterns exhibited by pollinators that have important consequences for the reproduction of flowering plants. Constancy refers to the tendency of a pollinator to visit flowers of the same species (or morph) in sequence [119]. If a pollinator with high constancy visits a flower of species A, it will be predisposed to make its next visit to another flower of that species. The term preference has been used with some ambiguity in the literature [119]; here, we will use the term *bias* to avoid confusion. Bias refers to the tendency of a pollinator to visit a particular species (or morph). Bias can result from an innate, evolved affinity to a certain type of flower. It can also result from the individual experience of a pollinator, if, for example, the pollinator learns to associate a high food reward with a flower type. Importantly, bias is distinct from constancy. Bias and constancy can together make a pollinator visit one species (or morph) of a flower more than another, but due to different mechanisms. The combined effects of these tendencies is sometimes labeled preference.

An example will illustrate these behavioral patterns. Suppose that a pollinator visits a field that contains two species of flower, species A and species B. A pollinator with high constancy but no bias might exhibit a sequence of visits like AAAAAAAAABBBBBBBB. This pollinator has a tendency to stay with the same species that it just visited, but it does not visit one species more than the other. A pollinator with a bias for species A but no constancy might exhibit a sequence of vis-

its like AAABAABABAAABAAA. This pollinator visits species A more frequently than species B, yet also switches between species. A pollinator with a visit sequence like AAAAAAAAABAAAAA exhibits a preference for species A, but it is unclear whether the preference is due to constancy or bias.

In this chapter, we will primarily be concerned with identifying constancy and bias, and not uncovering the phenomena that give rise to these behaviors. The causes of constancy and bias are rooted in the foraging strategy employed by the pollinators. We briefly review some of these strategies here. Pollinators exploring new terrain often use a stochastic search pattern called a Lévy walk [95]. Lévy walks are also used when previously discovered food resources disappear, and pollinators must find new ones [102]. Depending on the species involved, pollinators can use visual or olfactory cues to detect flowers, and to discriminate between flowers types [24, 103]. Social pollinators share information with each other, both within the hive [48], and by applying scent marks to depleted flowers [42].

Memory plays a key role in determining which flowers a pollinator visits. Pollinators have both short-term memory (which persists for seconds to minutes) and long-term memory (which persists for days) [25]. Some pollinator species are able to store many flower locations in their long-term memory, and use this information to visit a predictable sequence of flowers, called a trapline, in each foraging bout [112, 73]. Bumblebees, butterflies, hummingbirds, and bat have all been observed to engage in trapline foraging [2]. Prior to establishing a trapline, pollinators must rely on search mechanisms. It is also important for pollinators to modify traplines as resources change (due to changes in available flowers) and as new resources are discovered [73].

Short-term memory plays an important role for pollinators that are exploring a new area or modifying existing traplines. There are several hypotheses about how

short-term memory limitations can give rise to constancy [25]. As pollinators move from flower to flower, they store a search image that describes the appearance of the flowers that they are looking for. Keeping a single search image in short-term memory is easier than keeping multiple images; hence, short-term memory limitations could make pollinators focus on one flower type at a time. A similar phenomenon involve the handling procedures for obtaining food for flowers. As with search images, a pollinator may only be able to hold the motor skill procedure for one flower type in its short-term memory at a time. When a pollinator foragers on a new flower type, this experience may "overstrike" its previous experience, establishing a new search image and handling routine in its short-term memory [58].

3.3 Consequences for hybridization and speciation

One of the major motivations for studying pollinator foraging behavior is to understand the consequences for gene flow between flowering plants. These consequences are nicely summarized by Hersch and Roy [52], and we will recapitulate them here. Both bias and constancy play important roles in assortative mating between plants [52]. Pollinator bias toward a particular species will enhance that species' overall fitness. Bias for a particular morph within a species reduces gene flow between morphs, and in extreme cases, may ultimately lead to speciation. Species level constancy maintains genetic barriers and prevents the formation of hybrids. Morph level constancy reduces gene flow within a species, and can ultimately lead to speciation. Inconstancy by pollinators at the species level can contribute to hybridization.

Many studies have examined the consequences of pollinator bias and constancy in speciation or hybridization. *Chamerion angustifolium* is a bee-pollinated species of fireweed that has two major ploidy types [55]. Polyploidy, the existence of more than

two sets of homologous chromosomes in the cells of an organism, is one of the few identified mechanisms that can lead to sympatric speciation [55]. *C. angustifolium* has two different ploidy types: a diploid (the cells of these plants have two homologous chromosomes), and an autotetraploid (the cells of these plants have four homologous chromosomes. Although these two ploidy types occupy largely different geographic regions, there are some zones where they come in contact. In these contact zones, pollinator behavior offers one potential mechanism for preventing hybridization. The study of pollinator behavior in this system is described in [55, 66, 56].

Pollinator bias and/or constancy may be an important factor in maintaining reproductive isolation between sympatric, closely-related plant species that share the same pollinators. This possibility was investigated in the neotropical herbs *Costus pulverulentus* and *C. scaber* [65], but it was found that other mechanisms of reproductive isolation played larger roles. The effects of pollinator behavior on reproductive isolation of *Rhinanthus minor* and *Rhinanthus angustifolius* was shown to be complex, and depended on the relative abundances of the two plants [81].

Quantitative trait locus analysis (QTL) provides a method of determining which floral genes impact pollinator behavior. QTL analysis was used to investigate how specific genes of sympatric, closely related Louisiana Irises, *Iris fulva* and *I. brevicaulis,* lead to floral traits that favor pollination by different species [75]. Similar work was conducted on sympatric, closely related monkeyflower species *Mimulus cardinalis* and *Mimulus lewisii* [104].

3.4 Spatial configuration of flowers

The simplest way to evaluate pollinator bias and constancy involves observing pollinator flights within a specified area. To measure bias, the number of pollinator visits

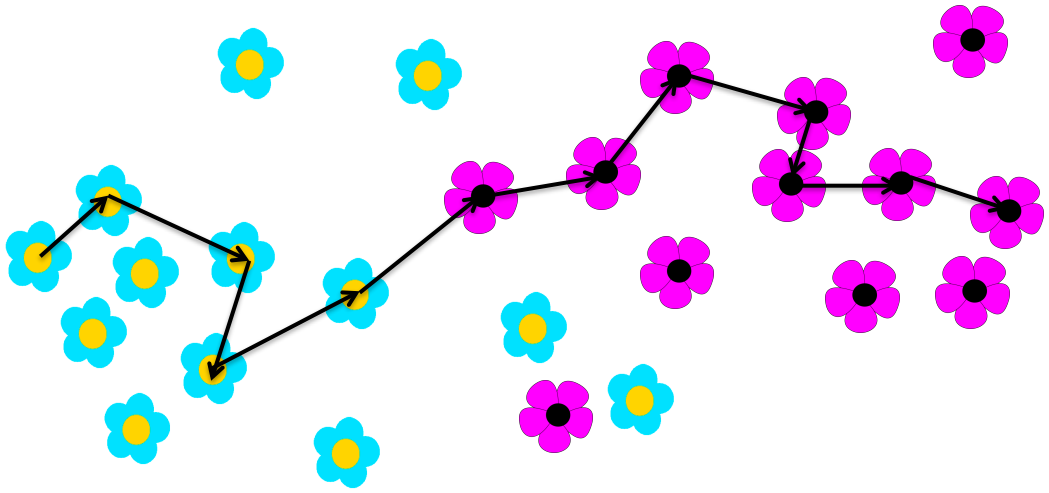

Figure 3.1: A hypothetical trajectory of a bee foraging on two species of flower. It is ambiguous whether the bee displays constancy, or whether this constancy is simply induced by the spatial arrangement of the flowers.

to each flower species is recorded, and then compared to the expected number of visits, given the number of flowers of each species in the plot. To measure constancy, the number of flower transitions within and between species is recorded, and then compared to the expected values of these quantities, given the number of flowers of each species within the plot. Bateman's constancy index [119] provides an easy metric that incorporates this information.

A key problem with such simple approaches to evaluating bias and constancy is that they neglect the spatial arrangement of flowers. Pollinator movements are often dictated by the distances between flowers. If a pollinator is foraging in a clump of a particular plant species, it is likely that its visit pattern will show sequences of visits to plants of the same species. This will occur even if the pollinator has no intrinsic propensity to be constant for that plant species; it is only an effect of the clumped distribution of flowers. Figure 3.1 shows an example of this situation. This problem of spatial arrangement in bias and constancy studies has been widely recognized [52, 55, 65, 66, 81, 56, 25, 111].

One approach to solving this problem is to monitor pollinator movement on experimental arrays of flowers. Examples of this type of study can be found in [90, 52, 58, 81]. Experimental arrays allow researchers to manipulate the number of plants of each species and the distances between each plant. Unfortunately, this does not eliminate the problem of spatial arrangement of flowers; it only changes the spatial arrangement. Consider, for example, a pollinator that naturally displays constancy. If it forages on a grid of alternating flower types, the nearest neighboring flowers will always be of a different species than the one it just visited. Thus, it is possible that the pollinator will not display constancy, even though that is its natural tendency.

If plant species are randomly assigned to positions within the array, problems still remain. It is unlikely that the grid arrangement provides accurately represents the pattern of flowers a pollinator would experience in a nature. There is no "neutral" landscape on which to test foraging behavior. All pollinator behavior is contingent on the spatial arrangement of flowers, and introducing an artificial arrangement does not fix this problem. Given that a "neutral" landscape is unobtainable, the most logical choice is to use a natural landscape. The key with using observations on a natural landscape is determining how to disentangle the effects of spatial distribution of flowers when making inferences about bias and constancy from visit data. We will describe several previous approaches, before suggesting an alternative method.

Husband and Schemske [56] identified the problem of spatial configuration, and used a randomization technique to analyze pollinator movement data. They observed pollinators in natural plots (i.e., not arrays). The flower locations from the plot were used in simulations of pollinator visits. Simulated flights were generated by selecting flight lengths from the empirical distribution of observed flight lengths. Once a flight length is selected, the pollinator moved to a flower that was within that flight

distance. This randomization procedure was used to simulate many pollinator flights, and the results were analyzed to determine if they agreed with constancy measured in the original data. A truncation effect may produce artifacts in this randomization procedure. That is, if a long flight is selected from the move-length distribution, all flowers within that distance will be eligible, and hence the realized flight could be shorter than the selected flight. Over many flights, this means that the realized move-length distribution will be very different than the observed move-length distribution. An alternative randomization technique, in which the flower that had the distance was closest to the selected flight length is chosen, may introduce artifacts because of the discrete nature of observed flight lengths.

A model of pollinator-mediated plant disease transmission was created by Ferrari et al. [40]. In this model, pollinator movement was modeled as a diffusive process, and hence probability of pollinator flights between plants was assumed to depend on distance via Bessel functions. The number of flowers per plant and the time spent foraging on each plant helped were also incorporated into the model of disease transmission. Disease outbreaks were simulated on different arrays of virtual plants. This study highlighted the effects of the spatial configuration of plants on pollinator movement, and motivated further work by Yang et al [122].

Yang et al [122] used observations on an experimental array of flowers to parameterize a movement model. The model included distance-dependence (assumed to behave as an exponential distribution) and bias as possible factors influencing pollinator visits. Once the parameters for the movement model had been identified from the array observations, the model was used to simulate pollinator movement. The movement model then provided them with the flexibility to simulate movement data for spatial arrangements beyond those the array observations.

To our knowledge, [56] is the only existing effort to assess pollinator bias and/or

constancy from observations on naturally occurring plants that accounts for spatial configuration. Our goal in this work is to provide a different approach to account for spatial configuration of plants in the assessment of bias and constancy on naturally occurring plants. This approach is built on a maximum likelihood framework. Unlike [56], it does not rely on simulation. Our framework avoids potential artifacts produced by simulation, and provides researchers with an easy-to-implement method to assess pollinator bias and/or constancy in natural environments.

3.5 Maximum Likelihood Framework

Consider a plot that contains flowers at locations $\{x_i\}_{i=1}^N$. The flowers are divided into two species; call them G and S (this notation is motivated by the actual species names of the flowers in our demonstration study). We will abuse notation slightly, and also use G and S to be the set of indices of $\{x_i\}$ corresponding to those species. The probability that a pollinator moves from one flower to another could potentially depend on the distance between flowers. The relationship between distance and visit probability is not known a priori, but there are several probability distributions that are good candidates for distance kernel functions. For example, an exponential distribution with parameter θ is a good candidate for the way that visit probability decays with distance. Let

$$D = \{d_{i,j}\}_{i,j=1}^N = \{\|x_i - x_j\|\}_{i,j=1}^N$$

be the matrix of inter-flower distances. For a given kernel f with parameter(s) θ, let $f(x, \theta)$ be the relative probability of visiting a flower a distance x from the current flower. Note that the term "relative probability" is used, because the actual probability of visiting those flowers will depend on the number of and distances to all the other

available flowers. Define a matrix of these relative probabilities by $D^* = \left\{d^*_{i,j}\right\}_{i,j=1}^{N}$, where $d^*_{i,j} = \begin{cases} f\left(d_{i,j}, \theta\right) & i \neq j \\ 0 & i = j \end{cases}$.

Let b be the bias parameter, which specifies the odds of a pollinator to visit a species G flower versus a species S flower, all other things being equal. If $b = 1$, the pollinator is equally likely to visit the two flowers. If $b = 2$, it is twice as likely to visit the a species G flower. If $b = \frac{1}{2}$, it is twice as likely to visit the a species S flower. Let c be the constancy parameter, which specifies the odds of a pollinator visiting a flower of the same species it last visited versus the other species, all other things being equal. If $c = 1$, the pollinator is equally likely to visit the two flowers. If $c = 2$, it is twice as likely to visit the flower of the species it just came from.

Define a bias matrix $B = \{b_{i,j}\}_{i,j=1}^{N}$ where

$$b_{i,j} = \begin{cases} b & i \neq j,\ j \in G \\ 1 & i \neq j,\ j \in S \\ 0 & i = j \end{cases}.$$

Define a constancy matrix $C = \{c_{i,j}\}_{i,j=1}^{N}$ where

$$c_{i,j} = \begin{cases} c & i \neq j,\ i, j \in G \text{ or } i, j \in S \\ 1 & i \neq j,\ i \in G \text{ and } j \in S \text{ or } i \in S \text{ and } j \in G. \\ 0 & i = j \end{cases}$$

Define a weight matrix $W = \{w_{i,j}\}_{i,j=1}^{N}$ by $w_{i,j} = b_{i,j} c_{i,j} d^*_{i,j}$. In order to convert these weights into visit probabilities, each column must be normalized. Define $P =$

$\{p_{i,j}\}_{i,j=1}^{N}$, where $p_{i,j} = \frac{w_{i,j}}{\sum_{j=1}^{N} w_{i,j}}$. Note that the probability transition is determined by the set (f, θ, b, c), where f is a family of functions (for example, the exponential family), and θ the vector of parameters (often a single parameter) that specifies the exact distance kernel function.

Suppose that j plots are observed. In each plot, several pollinators are followed from flower to flower. Each pollinator is caught and killed once it leaves the plot. A flight from one flower to another is called a *transition.* In the following, we assume that all of the pollinators of a given species exhibit the same basic foraging characteristics, and hence the transitions observed in a given plot can be pooled across individuals. This assumption is difficult to verify, as the number of transitions observed per pollinator is frequently small (< 10). The most obvious way this assumption could fail is if different individual pollinators have different learned preferences. Even if this is the case, by observing at least several pollinators of a particular species, it is possible to discern general foraging characteristics from pooled data. The fact that individuals are killed upon exiting the plot ensures that the idiosyncratic behavior of a single individual will not have undue influence on the results.

For plot number k, let $P^{(k)}$ be the associated probability matrix. Let $T^{(k)} = \left\{t_1^{(k)}, t_2^{(k)}, \ldots, t_{m_k}^{(k)}\right\}$ be the list of observed transitions in plot k, where each $t_i^{(k)}$ is an ordered pair of integers that specifies a pollinators flight from one flower to another (initial flower, terminal flower). Writing $p\,(i, j, k) = p_{i,j}^{(k)}$, the log likelihood function for the observed flights in plot k is:

$$L_k\left(f, \theta, b, c|T^{(k)}\right) = -\sum_{i=1}^{m_k} \ln\left(p\left(t_i^{(k)}, k\right)\right).$$

Finally, the total log likelihood function is:

$$L\left(f,\,\theta,\,b,\,c|T\right) := \sum_{k=1}^{j} L_k\left(f,\,\theta,\,b,\,c|T^{(k)}\right).$$

The distribution functions that we considered were: beta prime, Dagum, Erlang, exponential, Lindley, and Sigh Maddala. AIC identified that the exponential distribution fit best, and this was consistent regardless of the inclusion of other parameters like bias or constancy.

Directional persistence is another factor that could potentially influence flower visits. Directional persistence means that a pollinator that moves from flower A to flower B is most likely to select its next flower C so that C is close to the ray extending from A through B. Adding directional persistence into the maximum likelihood framework introduced complications to the previously described maximum likelihood framework, because the probability of visits is affected by the previous flower visited (not just the current flower the pollinator is on). To accomplish this, we defined a tensor of persistence weights, $\{z_{i,j,k}\}_{i,j,k=1}^{N}$, where $z_{i,j,k}$ is the relative probability of transitioning from flower j to flower k given the last transition was from flower i to flower k. This weight was determined using a Von-Mises probability distribution.

$$z_{i,j,k} = \begin{cases} g\left(x_k;\, \frac{x_j - x_i}{\|x_j - x_i\|}, \kappa\right) & k \neq j \\ 0 & k = j \end{cases}.$$

Here $g\left(x;,\mu,\kappa\right) = \frac{e^{\kappa\cos(x-\mu)}}{2\pi I_0(\kappa)}$; μ is the location parameter and κ is the dispersion parameter. These weights were incorporated into the total weights as above.

The factors that we have thus far considered are: distance, bias, constancy, and directional persistence. This list could easily be expanded to include environmental factors, preference for certain morphological traits, or any number of other phenomena that could potentially influence foraging behavior. The distance factor is characterized

Figure 3.2: Prairie near Cedar Point Biological Station. Ogallala, Nebraska.

by both a distribution family (for example, exponential), and a parameter set (in the example of an exponential distribution, the single parameter is the expected value). The other factors depend on one of more parameters (for example, the bias constant). We can identify the best distance distribution and the best parameters by maximizing the likelihood give the observed transitions. Once this is done, we can compare a model that has all of the factors with simpler models that just contain subsets of those factors. This is accomplished using the Akaikie Information Criterion (AIC).

3.6 Study system and field methods

To illustrate the utility of the maximum likelihood framework (described below) for assessing pollinator bias and constancy, we examined the behavior of *Agapostemon*, a metallic green sweat bee, in Western Nebraska. The study site was at Cedar Point Biological station on Lake McCauneghy near Ogallala, NE (figure 3.2). Two species of flower, *Thelesperma filifolium* (Greenthread; Asteraceae family) and *Tradescantia occidentals* (Spiderwort; Commelinaceae family) are common in the area, and are pollinated by *Agapostemon*.

To begin data collection, team members waited to spot a pollinator. Once a pollinator was spotted, tracking began with its first flower visit. A team member observed this first flower visitation from a distance. As the pollinator moved on, a second team member waited to identify its next flower visitation. This observation continued, with team members observing which flowers were visited from a distance. Once the pollinator moved a safe distance away (at least 5 meters), the team member that observed a specific flower visitation would mark that flower with a flag. The flags were placed at the base of the flowers, well below the inflorescences. The flags were numbered, and colored to represent whether the pollinator spent time foraging on an inflorescence, or whether it rejected the inflorescence (arriving at the inflorescence, but immediately departing without foraging on it). The tracking process continued until a pollinator had either visited 8 different flowers, or until it tried to leave the local area. At this time, team members netted the pollinator, killed it, and preserved it for identification. The information about the bee's visits was recorded, and the flags were removed.

The visits of the first pollinator defined a plot for further pollinator tracking. The two flowers that were furthest apart in the initial pollinator's visit sequence were designated as flower X and flower Y; the distance between them was designated as L. A line of length $2L$ through points X and Y was created, extending a distance of $\frac{L}{3}$ on either side of the flowers. A square plot was created, with the midpoint between X and Y at the center. All of the flowers in the plot were labeled with numbered flags at their bases, well below the inflorescences. The distance from each flower to X and Y was recorded, so that a mapped version of the plot could be reconstructed later via triangulation. These distances were measured using a laser distance finder. A compass was used to determine the orientation of the plot.

Having established a plot with spatially mapped flowers, tracking of further pol-

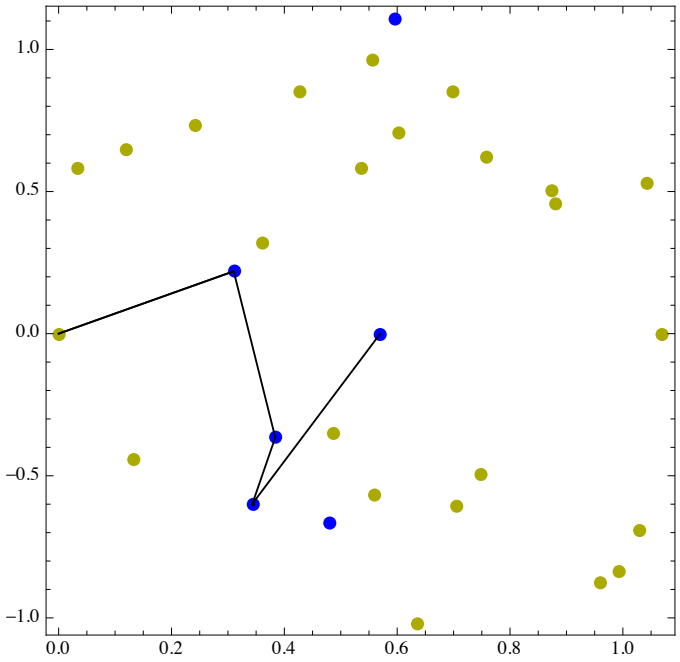

Figure 3.3: Selected pollinator trajectory. Blue dots are spiderwort, yellow dots are greenthread. Dimensions of the plot are in meters, with the first focal flower at the origin.

linator visits was faster. Six different plots were constructed this way, and a total of 39 pollinators were tracked. Of these, 34 ended up being identified as *Agapostemon.* The trajectory of one of the observed pollinators is illustrated in figure 3.3. A chart of flower transitions observed in a particular plot is shown in figure 3.4.

3.7 Results and Discussion

Our analysis showed that a model that incorporates distance and constancy was the best, according to the Akaike Information Criterion. The AIC score is based on the log likelihood of each model (with suitably optimized parameters), with a penalty for including extra parameters. The AIC score is a good way to compare models, because it balances goodness of fit against the number of parameters. According to

Plot number: 1

Number of Flowers in Plot:

y	24
b	6

Pollinator visitation info

Pollinator #1	y	y	y	b	y	y	y		
Pollinator #2	b	b	y	y	y				
Pollinator #4	y	y	y	y					
Pollinator #9	y	y	y	b	y				
Pollinator #19	y	y	b	y	b	y	y	y	
Pollinator #21	y	y	y	b	y				
Pollinator #24	y	b	y						
Pollinator #26	y	y	b	y	b	y	y	y	y
Pollinator #28	b	y	y	y					
Pollinator #30	y	y	y	y					
Pollinator #31	y	y	y	y	y				
Pollinator #32	b	y	y	y	y	y	y		
Pollinator #34	b	y	b	y	y	y			
Pollinator #36	y	y	y	y	y	y	y	y	y
Pollinator #39	y	y	y	y					

Total visits

y	b
71	14

Transition info

Pollinator #1	{y, y}	{y, y}	{y, b}	{b, y}	{y, y}	{y, y}		
Pollinator #2	{b, b}	{b, y}	{y, y}	{y, y}				
Pollinator #4	{y, y}	{y, y}	{y, y}					
Pollinator #9	{y, y}	{y, y}	{y, b}	{b, y}				
Pollinator #19	{y, y}	{y, b}	{b, y}	{y, b}	{b, y}	{y, y}	{y, y}	
Pollinator #21	{y, y}	{y, y}	{y, b}	{b, y}				
Pollinator #24	{y, b}	{b, y}						
Pollinator #26	{y, y}	{y, b}	{b, y}	{y, b}	{b, y}	{y, y}	{y, y}	{y, y}
Pollinator #28	{b, y}	{y, y}	{y, y}					
Pollinator #30	{y, y}	{y, y}	{y, y}					
Pollinator #31	{y, y}	{y, y}	{y, y}	{y, y}				
Pollinator #32	{b, y}	{y, y}	{y, y}	{y, y}	{y, y}	{y, y}		
Pollinator #34	{b, y}	{y, b}	{b, y}	{y, y}	{y, y}			
Pollinator #36	{y, y}	{y, y}	{y, y}	{y, y}	{y, y}	{y, y}	{y, y}	{y, y}
Pollinator #39	{y, y}	{y, y}	{y, y}					

Transition Totals

{y, y}	47
{y, b}	9
{b, y}	13
{b, b}	1

Figure 3.4: Example of transition data for a plot. y=Greenthread, b=Spiderwort

Figure 3.5: Model rankings based on Akaike information criterion.

model	# parameters	-LogLik	AIC	Delta AIC
Distance, Constancy	2	429.877	863.754	0.
Distance, Bias, Constancy	3	429.737	865.474	1.72
Distance, Constancy, Dir. Per	3	429.877	865.754	2.
Distance, Bias, Constancy, Dir. Per.	4	429.737	867.474	3.72
Distance, Bias	2	434.974	873.948	10.194
Distance	1	435.979	873.958	10.204
Distance, Bias, Dir. Per.	3	434.974	875.948	12.194
Distance,Dir. Per.	2	435.979	875.958	12.204
Constancy	1	519.819	1041.64	177.884
Bias, Constancy	2	519.297	1042.59	178.84
Constancy, Dir. Per.	2	519.819	1043.64	179.884
Bias, Constancy, Dir. Per.	3	519.297	1044.59	180.84
Nothing	0	523.763	1047.53	183.772
Bias	1	523.58	1049.16	185.406
Dir. Per.	1	523.763	1049.53	185.772
Bias, Dir. Per.	2	523.58	1051.16	187.406

[20], a good rule of thumb is that an ΔAIC (the deviation in AIC from the best model) less than two implies a model still has substantial support, an ΔAIC between 3 and 7 means considerably less support, and an ΔAIC greater than 10 means the model is very unlikely. It is interesting to note that neither bias nor directional persistence was a part of the best model. This implies that *Agapostemon* shows no bias to forage on Greenthread over Spiderwort or vice versa, and it does not have a tendency to maintain its heading from its previous interflowed flight. If pollinators show constancy but not bias, it means that they do not *a priori* favor one flower species over the other, but they tend to stick to one species during a foraging bout. This is the case for *Agapostemon*. The model rankings based on AIC are shown in figure 3.5.

The maximum likelihood analysis that we performed does not identify the precise mechanisms that lead to flower discrimination. For example, we are not sure what cues that *Agapostemon* uses to select flowers. We can make some rough inferences, though. The distance kernel identified from our data analysis was exponential, which is consistent with "ballistic", (i.e., nearly straight-line) motion. A normal distribution distance kernel would have been expected from diffusive behavior. This implies that

a mathematical movement model for these pollinators should involve straight-line trajectories, not Brownian motion. This information has important consequences: the plant disease model in [40] modeled the probabilities of pollinator flights between plants to be consistent with Brownian motion. If pollinator transition probabilities decay less sharply with interflower distance, as with ballistic motion, then plant disease would spread more rapidly. Furthermore, gene flow would be more spatially extensive than it would be under Brownian motion.

The primary goal of this study was to demonstrate the utility of a new maximum likelihood framework for analyzing pollinator bias and constancy. The motivation for identifying these behavioral phenomena is largely due to the role that pollinator foraging plays in floral reproductive isolation. In this study system, the consequences for reproductive isolation are not that interesting; there is clearly no hybridizing occurring between these distinctly different flower species. This methodology could be implemented in many ecological situations, to evaluate the role of pollinator behavior in gene flow.

Our framework for assessing pollinator bias and constancy offers three major benefits: it accounts for the spatial configuration of plants, it uses observations of pollinators in natural settings (i.e., not on experimental arrays), and it does not rely on simulation. To our knowledge, no existing studies of pollinator bias and constancy possess these three features. The importance of the spatial configuration of plants in assessing bias and constancy has been widely appreciated [52, 55, 65, 66, 81, 56, 25, 111]. The benefits of the other two major advantages of our framework have yet to be quantified. Aside from the logistical complications in establishing artificial arrays, it is unknown how much artificial arrays make pollinators depart from the behavior that they exhibit in natural settings. It is also unknown what, if any, role artifacts play in randomization techniques. Future work should compare results obtained from

analyzing data using both our maximum likelihood framework and randomization techniques. If the results are in agreement, it would be an encouraging sign that both approaches are useful. We feel that, whether they use our framework or randomization, more researchers should use observations of pollinator behavior in natural (i.e., not experimentally modified) systems, and account for the spatial configuration of plants.

Chapter 4

Supplementary Material

In these supplementary materials, I provide details about modeling foraging on landscapes with clumped resource distributions. First, I give a brief overview of spatial point processes, following the approach of Daley and Vere-Jones [30]. Next, I focus on a popular distribution used in ecology: the negative binomial distribution. Following Diggle's observations [32], I discuss the negative binomials shortcomings in foraging models. Finally, I explain results of foraging simulations on landscapes generated by alternative point processes.

4.1 Spatial Point Processes

4.1.1 Defining Spatial Point Processes

Daley and Vere-Jones [30] authored a detailed, multivolume treatment of spatial point processes. I summarize some of the essential points here.

For simplicity, this section will consider spatial point processes on $\mathbb{R}^2$, although these ideas are easily generalized. Let $\mathcal{B}(\mathbb{R}^2)$ be the σ-algebra of Borel sets of $\mathbb{R}^2$. Let $\mathcal{N}$ be the set of all locally finite nonnegative integer measures on $\mathbb{R}^2$. If $N \in \mathcal{N}$ and

$Y \in \mathcal{B}(\mathbb{R}^2)$, then $N(Y)$ can be interpreted as the number of points in Y. For each $k = 0, 1, 2, \ldots$, and each $Y \in \mathcal{B}(\mathbb{R}^2)$, let $U(k, Y) = \{N \in \mathcal{N} : N(Y) = k\}$. That is, $U(k, Y)$ is the set of all locally finite integer measures that have a value of k on the set Y. Let $\mathcal{M}$ be the σ-algebra generated by all sets of the form $U(k, Y)$. Then $(\mathcal{N}, \mathcal{M})$ is a measurable space. For a fixed $Y \in \mathcal{B}(\mathbb{R}^2)$, the mapping $\rho_Y : \mathcal{N} \to \mathbb{N} \cup \{0\}$ defined by $\rho_Y(N) = N(Y)$ is a measure on $\mathcal{N}$. Note that the elements $N \in \mathcal{N}$ are themselves measures on $\mathbb{R}^2$.

Let $(\Omega, \mathcal{E}, P)$ be a probability space. Then a spatial point process is a measurable mapping N from $(\Omega, \mathcal{E}, P)$ to $(\mathcal{N}, \mathcal{M})$. Here N represents a mapping from a probability space to a measure space; this contrasts with the usage in the previous paragraph, where N was an element of the measure space. For each outcome $\omega \in \Omega$, the point process N assigns a measure $N_\omega \in \mathcal{N}$. That is, N is an assignment $\omega \to N_\omega$. $(\Omega, \mathcal{E}, P)$ is a probability space, so N is a random variable, each realization of which is a measure on $\mathbb{R}^2$. Thus one says that N is a random measure on $\mathbb{R}^2$.

This is a lot of notation, so here is a list:

- Ω is the sample space. Each $\omega \in \Omega$ corresponds to a realization of the point process.
- $\mathcal{E}$ is the σ-algebra of events, and P is the associated probability measure.
- $\mathcal{N}$ is a set of measures on $\mathbb{R}^2$. Each $N \in \mathcal{N}$ corresponds to a pattern of points (i.e., a nonnegative integer-valued measure) on $\mathbb{R}^2$.
- $\mathcal{M}$ is the σ-algebra on $\mathcal{N}$, defined so that the ρ_Y mappings above are measures.
- A measurable mapping N from $(\Omega, \mathcal{E}, P)$ to $(\mathcal{N}, \mathcal{M})$ is a spatial point process. Thus, a spatial point process associates a measure (which can be interpreted as a pattern of points) with each outcome in the sample space.

- N_ω is a realization of N associated with the event $\omega \in \Omega$. N_ω is a measure on $\mathbb{R}^2$.

4.1.2 Probability Generating Functionals

For a fixed $Y \in \mathcal{B}(\mathbb{R}^2)$, the distribution of the random variable $N(Y)$ is called a one-dimensional distribution of N. For $n \in \mathbb{N}$ and $Y_1, Y_2, \ldots, Y_n \in \mathcal{B}(\mathbb{R}^2)$, the joint distribution of $(N(Y_1), N(Y_2), N(Y_n))$ is called a finite-dimensional distribution of N. The finite-dimensional distributions of a spatial point process N (and, in particular, the one-dimensional distributions of N) are completely determined by something called the generating functional, which will be explained here.

If X is a discrete random variable that takes on values $\{x_1, x_2, \ldots, x_n\}$ with probabilities $P(X = x_i) = p_i$, then the probability generating function for X is

$$G_X(z) = E\left(z^X\right) = \sum_{k=1}^{\infty} p_k \, z^{x_k}.$$

Given the probability generating function, one can find the associated probability for each value from the relationship $p_k = \frac{G^k(0)}{k!}$.

If $X_1, X_2 \ldots, X_d$ are discrete random variables, then the joint probability generating function is

$$G_{X_1,\ldots,X_d}(z_1, z_2, \ldots z_d) = E\left(z_1^{X_1} z_2^{X_2} \cdots z_d^{X_d}\right).$$

One can further generalize this concept for spatial point processes. Let N be a spatial point process on $\mathbb{R}^2$, and let $\{y_1, y_2, \ldots, y_m\}$ represent a realization of this point process. Note that this uses the dual interpretations of a spatial point process: as a random measure and as a random set of points. Suppose that $A_1, A_2, \ldots, A_d$

are pairwise disjoint subsets of $\mathbb{R}^2$. Let $h : \mathbb{R}^2 \to C_\infty(-1,1)$ be defined by $h(x) = \sum_{k=1}^{d} z_k I_{A_k}(x)$, where I_{A_k} is the indicator function on A_k. Then

$$E\left(\prod_{k=1}^{m} h(y_k)\right) = E\left(\prod_{k=1}^{d} z_k^{N(A_k)}\right).$$

With this as motivation, define the probability generating functional $\mathcal{G} : \mathcal{U} \to C_\infty(-1,1)$, where $\mathcal{U}$ is the set of Borel measurable functions h satisfying $|h(x)| \leq 1$, as follows:

$$\mathcal{G}(h) = E\left(\prod_{k=1}^{m} h(y_k)\right),$$

where the expectation is taken over all realizations of the spatial point process N.

4.1.3 Negative Binomial Spatial Point Processes

A negative binomial process is a point process with one-dimensional distributions that follow a negative binomial distribution. That is, for each $Y \in \mathcal{B}(\mathbb{R}^2)$,

$$E\left(z^{N(Y)}\right) = (1 + \mu(Y)(1 - z))^{\alpha(Y)}.$$

For each $Y \in \mathcal{B}(\mathbb{R}^2)$, $\mu(Y)$ and $\alpha(Y)$ are the parameters for a negative binomial distribution. The challenge in building a negative binomial spatial point process is finding a way for the one-dimensional distributions to be put together in a logically consistent way (e.g., so that the process satisfies the definition of a point process outlined above).

There are two well-known ways to build a negative binomial spatial point process: 1) a compound Poisson process, and 2) a mixed poisson process.

1. Compound Poisson Process: This process is built by first generating a set of

locations with a Poisson process with intensity μ, then placing a random number of points at that location. The number of points at a selected location is drawn from a logarithmic distribution of the form $p_n = \frac{\rho^n}{n} \ln\left(\frac{1}{1-\rho}\right)$. The resulting probability generating functional is

$$\mathcal{G}(h) = \exp\left(\int_{\mathbb{R}^2} \frac{\ln\left(\left(1-\rho\, h(x)\right)/(1-\rho)\right)}{\ln(1-\rho)} \mu\, dx\right).$$

2. Mixed Poisson Process: This process is built by first selecting λ from a gamma distribution with shape parameter α and scale parameter β, and then using λ as the intensity parameter for a Poisson process. The resulting probability generating functional is

$$\mathcal{G}(h) = \left(1 + \int_{\mathbb{R}^2} (1-h(x))\, \lambda\, \mu\, dx\right)^{-\alpha}.$$

4.1.4 Desirable Properties

Diggle and Milne [32] argue that there are three properties that are desirable for spatial point processes: stationarity, orderliness, and ergodicity.

1. A point process is *stationary* if it is invariant under spatial translation. To be precise, for $u, v \in \mathbb{R}^2$ and $Y \in \mathcal{B}(\mathbb{R}^2)$, define $S_u v = u + v$ and $S_u Y = \{x + u : x \in Y\}$. This induces a transformation on $T_u : \mathcal{N} \to \mathcal{N}$ by $T_u N(Y) = N(S_u Y)$. Then $N \in \mathcal{N}$ is stationary if N and $T_u N$ have the same finite-dimensional distributions for all $u \in \mathbb{R}^2$. Stationarity is important, because it means that there are no special points on a landscape. Points can be aggregated or dispersed, but their position does not depend on any external landscape variable. Fortunately, both the compound Poisson process and the mixed Poisson

process are stationary.

2. A point process is *orderly* if two points cannot occupy the same location. To be precise, if $\lim_{|dx|\to 0} \Pr\{N(dx) > 1\} = 0$, then N is an orderly point process. This is a desirable feature, because most resources (whether they be seeds, prey, fruit, etc.) cannot occupy the same position at the same time. The mixed Poisson process is orderly; the compound Poisson process is not.

3. A point process is *ergodic* if the spatial averages over a large scale of a single realization are the same as the average over a small scale of many realizations. In mathematical terms, $\Pr\{\lim_{r\to\infty} r^{-1} N_\omega(B_r) = E(N)\} = 1$. Ergodicity is a desirable factor, because it allows a single realization to be used as "representative" of typical outcomes of the process. This is important in ecology; for example, consider the spatial locations of trees in a forest. It is only possible to observe a single realization of the process that generated the trees, but, if we assume ergodicity, then large scale patterns can be seen as indicative of the underlying process. The compound Poisson process is ergodic, but the mixed Poisson process is not. In fact, each realization of the mixed Poisson process is just a uniform Poisson process, and has no clumpiness at all. Simulating realizations of a mixed Poisson process thus misses the clumpiness that is usually considered the defining characteristic of negative binomial processes.

It turns out that there are no stationary, ergodic, orderly spatial point processes with negative binomial one-dimensional distributions [57]. There are some processes (like Matern and Neyman-Scott processes) that possess those three properties, and have roughly negative binomial one-dimensional distributions. Of course, if either the orderly or ergodic requirement is removed, then the compound or mixed Pois-

son processes (respectively) can be used to generate exactly negative binomial one-dimensional distributions.

4.2 Simulations

In the first set of simulations, clusters are distributed by a Poisson process with intensity $\lambda = -r \ln(1-p)$. The number of resources in each cluster is drawn from a logarithmic distribution with parameter p. The resulting one-dimensional distributions of the spatial process for resources follows a negative binomial distribution with parameters r and p. The expected value for the number of resources in region with unit area is $\frac{r\,p}{1-p}$. In all of the following simulations, $\frac{r\,p}{1-p} = 1$. Note that this spatial point process is stationary and ergodic, but not orderly. Figure 4.1 shows three different representative landscapes for different parameter combinations. The height of the points represents the number of resources located at that point.

In these simulations, a forager executes a random walks, and travels with unit speed. When it comes within 0.1 units of a cluster, it moves to the cluster and consumes all of the resources there. The landscape is $(-10, 10) \times (-10, 10)$, but periodic boundary conditions make it a torus. If the forager exits on one side it emerges on the other. Foraging is destructive (i.e., resources are not replenished after being consumed). A forager's initial position is selected randomly.

In its random walk, the forager selects a "segment length" and a direction. The segment length and direction specify a target for the forager to move towards. If the forager encounters a cluster while traversing a segment length, it truncates the segment, and selects a new segment length and direction. For our purposes, the direction is always chosen from a uniform distribution, so the resulting random walk is non-oriented. The probability distribution for the segment lengths determine the

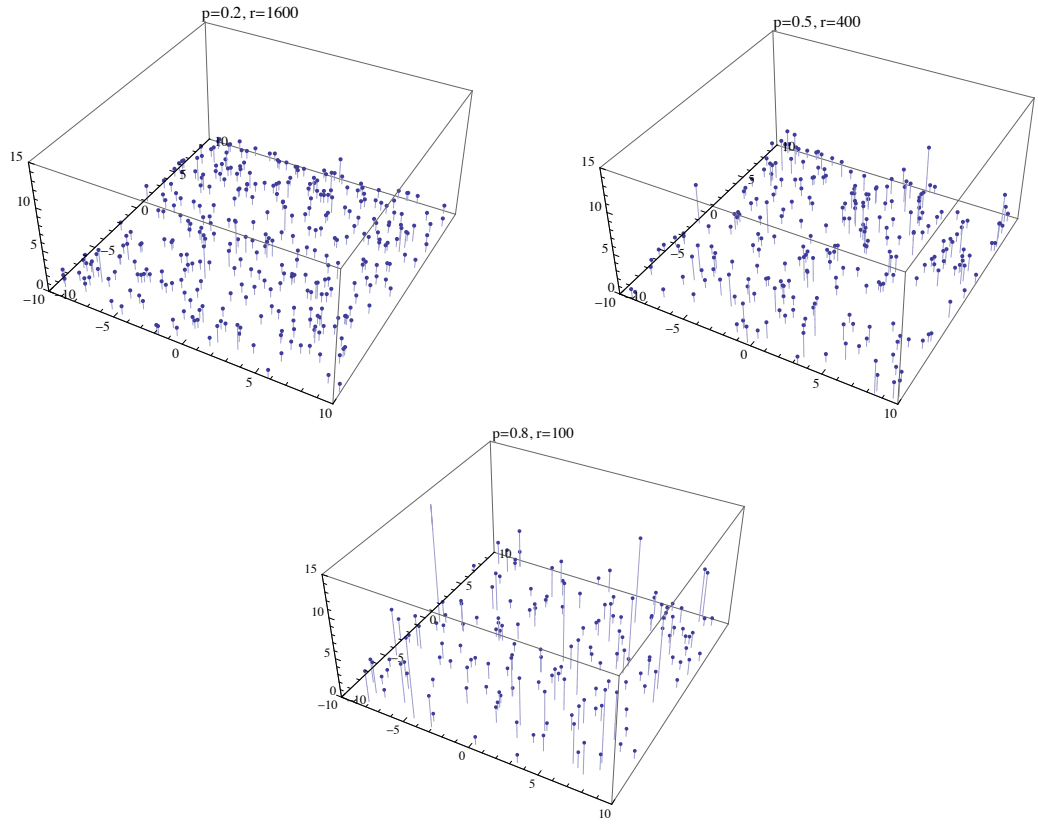

Figure 4.1: Realizations of negative binomial point processes for different parameter combinations. Vertical axis indicates the number of resources per location.

type of random walk. A Lévy walk results from using a power law distribution. Making all of the segment lengths very tiny results in (approximately) Brownian motion. Note that we are modeling the forager's trajectory as a continuous path, so each straight-line segment is simulated by many tiny steps.

In each simulation, a landscape is generated and a forager spends 1000 time units searching it. At the end of that time, its searching efficiency is calculated as resources consumed divided by time. This was repeated 300 times per parameter combination. Figure 4.2 shows the distribution of searching efficiencies across a range of aggregation levels, from dispersed (low p) to highly aggregated (high p), and for two types of random walks (Lévy and Brownian).

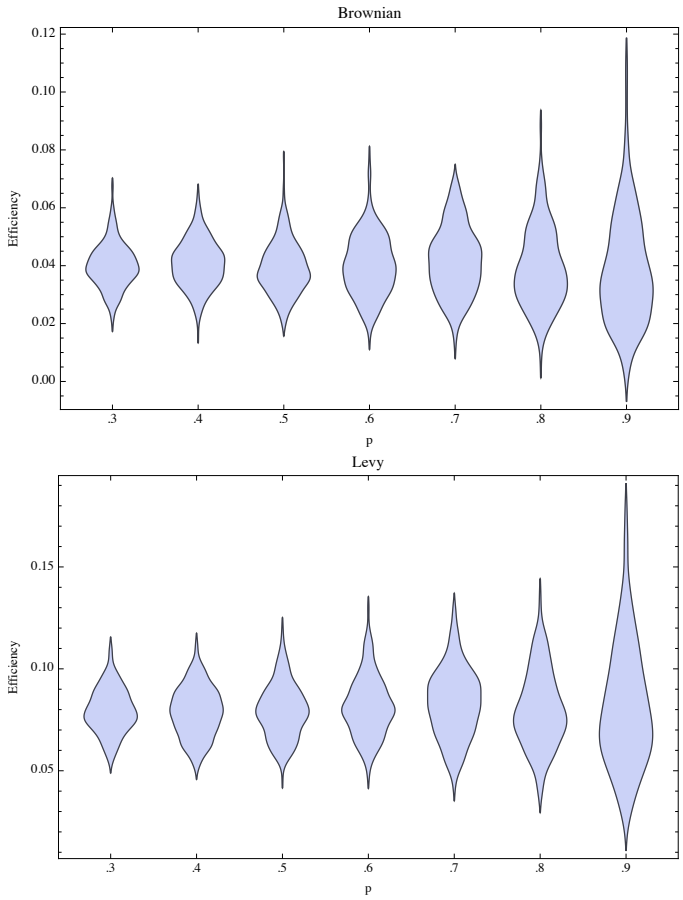

Figure 4.2: Simulated foraging efficiencies on (non-orderly) negative-binomial landscapes.

The point processes used to produce the landscapes above were not orderly, because multiple resources could occupy a single location. This situation is often not biologically realistic. An alternative approach is to use a stationary, ergodic, and orderly point process, such as a Neyman-Scott process. This type of process is generated by a set of Poisson distributed parent points, each of which produces a Poisson distributed cluster of daughter points. The one-dimensional distributions are not negative binomial, but they approximate negative binomial in the case of tight clusters. The important parameters are the intensity of the parent process, κ, and the intensity of the daughter process, α. The product of these intensities determines the expected

value of the total number of points; in the simulations below, we keep this product constant. Figure 4.3 shows three representative landscapes:

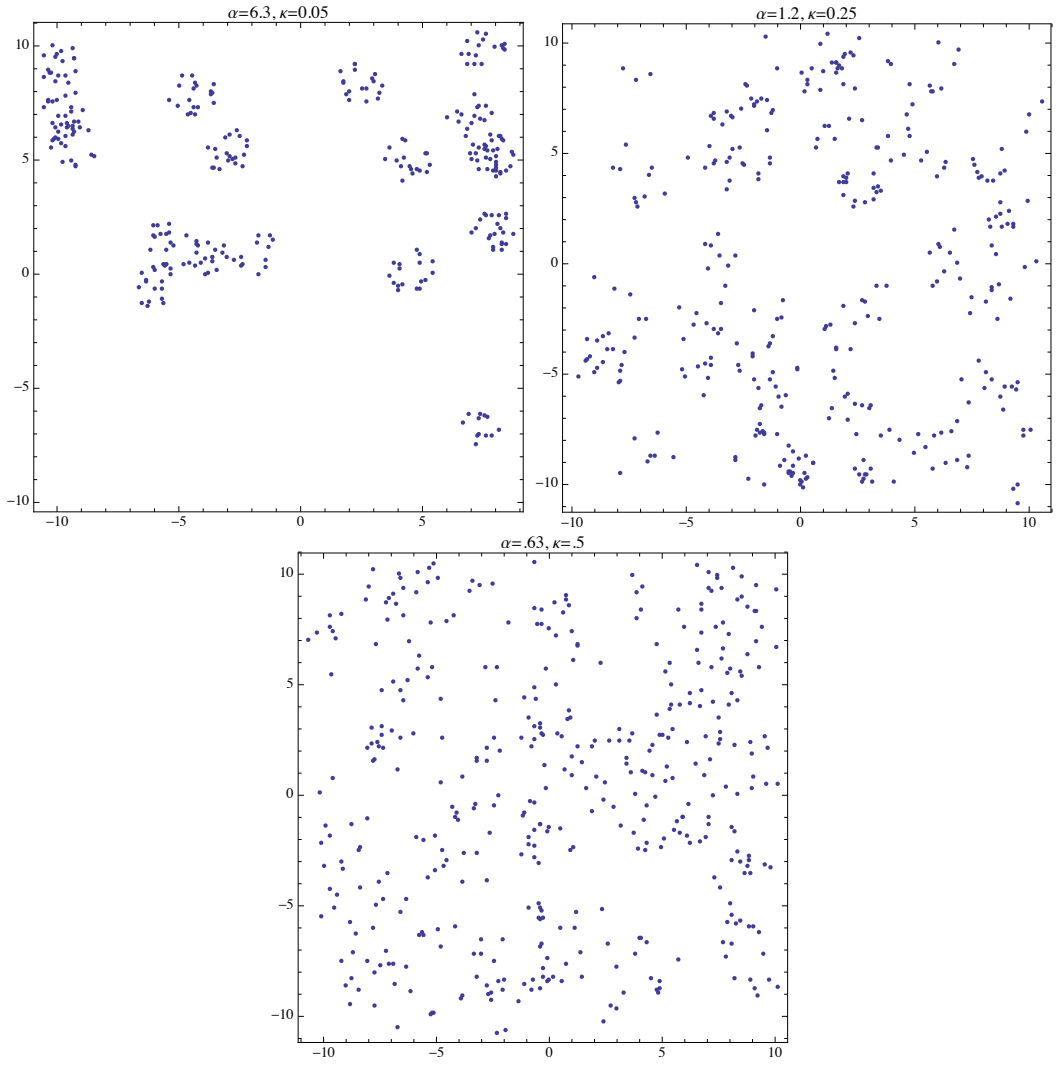

Figure 4.3: Realizations of Neyman-Scott point processes for different parameter combinations.

Figure 4.4 shows the distributions of searching efficiencies for different values of κ. Low values of κ correspond to highly aggregated landscapes; high values of κ correspond to dispersed landscapes. Only 100 runs were done for each parameter combination of these models.

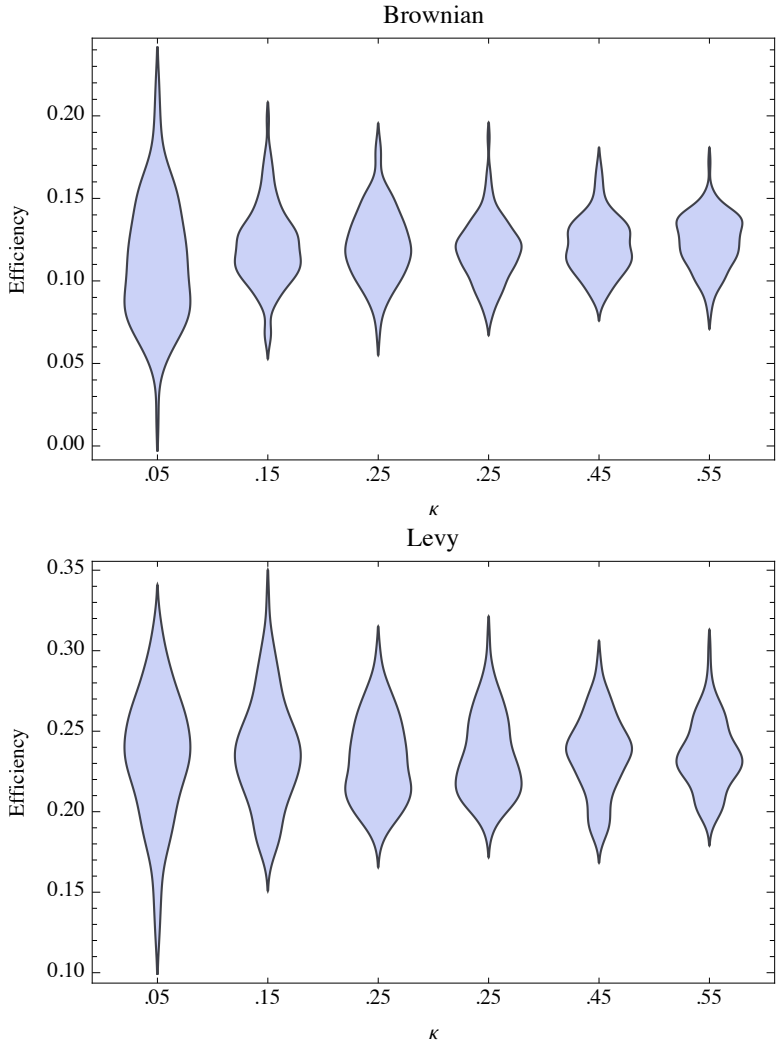

Figure 4.4: Simulated foraging efficiencies on Neyman-Scott landscapes.

Two general observations:

1) Lévy walks tend to be more efficient than Brownian motion, because there is a lower probability of revisiting the same terrain.

2) More clumped landscapes result in a higher variance in searching success.

Bibliography

[1] Adler, J. Chemotaxis in bacteria. *Annual review of biochemistry 44*, 1 (1975), 341–356.

[2] Amaya-Márquez, M. Floral constancy in bees: a revision of theories and a comparison with other pollinators. *Revista Colombiana de Entomología 35*, 2 (2009), 206–216.

[3] Applegate, D. L., Bixby, R. E., and Chvatal, V. *The Traveling Salesman Problem: A Computational Approach*. Princeton University Press, Princeton, NJ, 2007.

[4] Arditi, R., and Dacorogna, B. Optimal foraging in nonpatchy habitats. I. Bounded one-dimensional resource. *Mathematical Biosciences 76*, 2 (1985), 127–145.

[5] Arditi, R., and Dacorogna, B. Optimal foraging on arbitrary food distributions and the definition of habitat patches. *Am Nat 131*, 6 (1988), 837–846.

[6] Auger-Methe, M., St Clair, C., Lewis, M., and Derocher, A. Sampling rate and misidentification of Levy and non-Levy movement paths: comment. *Ecology* (2011).

[7] Bartumeus, F. Behavioral intermittence, Levy patterns, and randomness in animal movement. *Oikos 118*, 4 (2009), 488–494.

[8] Bartumeus, F., and Catalan, J. Optimal search behavior and classic foraging theory. *Journal of Physics a-Mathematical and Theoretical 42*, 43 (2009), 434002–434002.

[9] Bartumeus, F., Da Luz, M., Viswanathan, G., and Catalan, J. Animal search strategies: A quantitative random-walk analysis. *Ecology 86*, 11 (2005), 3078–3087.

[10] Bartumeus, F., Viswanathan, G. M., Raposo, E. P., and da Luz, M. G. E. Stochastic Optimal Foraging Theory. In *Dispersal, Individual Movement and Spatial Ecology, Lecture Notes in Mathematics*, M. Lewis, P. K. Maini, and S. Petrovskii, Eds. Springer-Verlag Berlin Heidelberg, 2013, pp. 3–32.

[11] Bell, W. J. Searching behavior patterns in insects. *Annual Review of Entomology 35*, 1 (1990), 447–467.

[12] Bell, W. J. *Searching Behaviour: The Behavioural Ecology of Finding Resources*. Chapman and Hall, New York, NY, USA, 1991.

[13] Benhamou, S. Efficiency of area-concentrated searching behavior in a continuous patchy environment. *J Theor Biol 159*, 1 (1992), 67–81.

[14] Benhamou, S. How many animals really do the Levy walk? *Ecology 88*, 8 (2007), 1962–1969.

[15] Benichou, O., Loverdo, C., and Moreau, M. A minimal model of intermittent search in dimension two. *Journal of Physics: ... 19*, 6 (2007), 065141.

[16] Benichou, O., Loverdo, C., Moreau, M., and Voituriez, R. Intermittent search strategies. *Review of Modern Physics 83*, 1 (2011), 81–130.

[17] Berec, L. Techniques of spatially explicit individual-based models: construction, simulation, and mean-field analysis. *Ecol Model 150* (2002), 55–81.

[18] Berezhkovskii, A., Makhnovskii, Y., and Bogachev, L. Brownian-particle trapping by clusters of traps. *Physical Review E 47*, 6 (1993).

[19] Brown, J. S., and Kotler, B. P. Hazardous duty pay and the foraging cost of predation. *Ecol Lett 7*, 10 (2004), 999–1014.

[20] Burnham, K. P., and Anderson, D. R. *Model Selection and Multi-Model Inference: A Practical Information-Theoretic Approach*. Springer, 2002.

[21] Carter, M. C., and Dixon, F. G. Habitat quality and the foraging behaviour of coccinellid larvae. *The Journal of Animal Ecology* (1982), 865–878.

[22] Charnov, E. Optimal foraging, the marginal value theorem. *Theoretical population biology* (1976).

[23] Chevalier, C., Benichou, O., Meyer, B., and Voituriez, R. First-passage quantities of Brownian motion in a bounded domain with multiple targets: a unified approach. *Journal of Physics a-Mathematical and Theoretical 44*, 2 (2010), 025002.

[24] Chittka, L., and Raine, N. E. Recognition of flowers by pollinators. *Current opinion in plant biology 9*, 4 (Aug. 2006), 428–435.

[25] Chittka, L., Thomson, J. D., and Waser, N. M. Flower constancy, insect psychology, and plant evolution. *Naturwissenschaften 86*, 8 (1999), 361–377.

[26] Cianelli, D., Uttieri, M., Strickler, J. R., and Zambianchi, E. Zooplankton encounters in patchy particle distributions. *Ecol Model 220*, 5 (2009), 596–604.

[27] Codling, E. A., Plank, M. J., and Benhamou, S. Random walk models in biology. *Journal of the Royal Society Interface 5*, 25 (2008), 813–834.

[28] Cresswell, J. E. Spatial heterogeneity, pollinator behaviour and pollinator-mediated gene flow: bumblebee movements in variously aggregated rows of oil-seed rape. *Oikos* (1997), 546–556.

[29] Dalby Ball, G., and Meats, A. Influence of the odour of fruit, yeast and cue lure on the flight activity of the Queensland fruit fly, Bactrocera tryoni, Froggatt Diptera: Tephritidae. *Australian Journal of Entomology 39*, 3 (2000), 195–200.

[30] Daley, D., and Vere-Jones, D. *An Introduction to the Theory of Point Processes: Volume II: General Theory and Structure.* An Introduction to the Theory of Point Processes. Springer, 2008.

[31] Diggle, P. J. *Statistical Analysis of Spatial Point Patterns.* Academic Press, London, UK, 2003.

[32] Diggle, P. J., and Milne, R. K. Negative binomial quadrat counts and point processes. *Scandinavian journal of statistics* (1983), 257–267.

[33] Donsker, M. Asymptotics for the Wiener sausage. *Communications on Pure and Applied Mathematics* (1975).

[34] Doving, K. B., Marstol, M., Andersen, J. R., and Knutsen, J. A. Experimental evidence of chemokinesis in newly hatched cod larvae (Gadus morhua L.). *Marine Biology 120*, 3 (1994), 351–358.

[35] Dusenbery, D. B. Spatial Sensing of Stimulus Gradients Can Be Superior to Temporal Sensing for Free-Swimming Bacteria. *Biophysical journal 74*, 5 (1998), 2272–2277.

[36] Edwards, A. M. Overturning conclusions of Levy flight movement patterns by fishing boats and foraging animals. *Ecology 92*, 6 (2011), 1247–1257.

[37] Edwards, A. M., Phillips, R. A., Watkins, N. W., Freeman, M. P., Murphy, E. J., Afanasyev, V., Buldyrev, S. V., da Luz, M. G. E., Raposo, E. P., Stanley, H. E., and Viswanathan, G. M. Revisiting Levy flight search patterns of wandering albatrosses, bumblebees and deer. *Nature 449*, 7165 (2007), 1044–1048.

[38] Feller, W. *An Introduction To Probability Theory and Its Applications*, vol. 2. Wiley, New York, 1971.

[39] Ferran, A., Ettifouri, M., Clement, P., and Bell, W. J. Sources of Variability in the Transition from Extensive to Intensive Search in Coccinellid Predators Homoptera: Coccinellidae. *Journal of Insect Behavior 7*, 5 (1994).

[40] Ferrari, M. J., Bjornstad, O. N., Partain, J. L., and Antonovics, J. A Gravity Model for the Spread of a Pollinator Borne Plant Pathogen. *The American Naturalist 168*, 3 (Sept. 2006), 294–303.

[41] Fontaine, C., Collin, C. L., and Dajoz, I. Generalist foraging of pollinators: diet expansion at high density. *Journal of Ecology 96*, 5 (June 2008), 1002–1010.

[42] Giurfa, M., and Núñez, J. A. Honeybees mark with scent and reject recently visited flowers. *Oecologia 89*, 1 (1992), 113–117.

[43] Gnedenko, B. V., and Kolmogorov, A. N. *Limit Distributions for Sums of Independent Random Variables*. Addison-Wesley, Reading, MA, 1954.

[44] Green, F. A simpler, more general method of finding the optimal foraging strategy for Bayesian birds. *Oikos 112*, 2 (2006), 274–284.

[45] Green, R. Bayesian birds: A simple example of Oaten's stochastic model of optimal foraging. *Theoretical population biology 18*, 2 (1980), 244–256.

[46] Green, R. Stopping rules for optimal foragers. *The American Naturalist* (1984).

[47] Green, R. Optimal foraging for patchily distributed prey: random search. *Techinical report* (1988).

[48] Grüter, C., Acosta, L. E., and Farina, W. M. Propagation of olfactory information within the honeybee hive. *Behavioral Ecology and Sociobiology 60*, 5 (June 2006), 707–715.

[49] Haskell, D. G. Experiments and a model examining learning in the area-restricted search behavior of ferrets (Mustela putorius furo). *Behavioral Ecology 8*, 4 (1997), 448–455.

[50] Hein, A. M., and McKinley, S. A. Sensing and decision-making in random search. *P Natl Acad Sci USA 109*, 30 (2012), 12070–12074.

[51] Hellung-Larsen, P., Leick, V., Tommerup, N., and Kronborg, D. Chemotaxis in tetrahymena. *European journal of protistology 25*, 3 (1990), 229–233.

[52] Hersch, E. I., and Roy, B. A. Context-Dependent Pollinator Behavior: An Explanation For Patterns Of Hybridization Among Three Species Of Indian Paintbrush. *Evolution 61*, 1 (Jan. 2007), 111–124.

[53] Hill, S. L., Burrows, M. T., and Hughes, R. N. The efficiency of adaptive search tactics for different prey distribution patterns: a simulation model based on the behaviour of juvenile plaice. *J Fish Biol 63* (2003), 117–130.

[54] Hills, T. T., and Adler, F. R. Time's crooked arrow: optimal foraging and rate-biased time perception. *Anim Behav 64*, 4 (2002), 589–597.

[55] Husband, B. C., and Sabara, H. A. Reproductive isolation between autotetraploids and their diploid progenitors in fireweed, Chamerion angustifolium (Onagraceae). *New Phytologist 161*, 3 (2003), 703–713.

[56] Husband, B. C., and Schemske, D. W. Ecological mechanisms of reproductive isolation between diploid and tetraploid Chamerion angustifolium. *Journal of Ecology 88*, 4 (2000), 689–701.

[57] Illian, J., Penttinen, A., Stoyan, H., and Stoyan, D. *Statistical Analysis and Modelling of Spatial Point Patterns*. John Wiley and Sons, Ltd., West Sussex, UK, 2008.

[58] Ishii, H. S. Analysis of bumblebee visitation sequences within single bouts: implication of the overstrike effect on short-term memory. *Behavioral Ecology and Sociobiology 57*, 6 (Jan. 2005), 599–610.

[59] Iwasa, Y., Higashi, M., and Yamamura, N. Prey distribution as a factor determining the choice of optimal foraging strategy. *American Naturalist* (1981), 710–723.

[60] Jacobs, K. *Stochastic Processes for Physicists*. Cambridge University Press, 2010.

[61] James, A., Pitchford, J. W., and Plank, M. J. Efficient or inaccurate? Analytical and numerical modelling of random search strategies. *Bull Math Biol 72*, 4 (2010), 896–913.

[62] James, A., Plank, M., and Brown, R. A. Optimizing the encounter rate in biological interactions: Ballistic versus Lévy versus Brownian strategies. *Phys Rev E 78*, 5 (2008), 051128.

[63] James, A., Plank, M. J., and Edwards, A. M. Assessing Levy walks as models of animal foraging. *Journal of the Royal Society Interface 8*, 62 (2011), 1233–1247.

[64] Johnson, D. S., and Papadimitriou, C. H. The traveling salesman problem: A guided tour of combinatorial optimization. In *Computational Complexity*, E. L. Lawler, J. K. Lenstra, A. H. G. Rinnooy Kan, and D. B. Shmoys, Eds. John Wiley and Sons, Ltd., Chichester, UK, 2009, pp. 37–87.

[65] Kay, K. M. Reproductive isolation between two closely related hummingbird pollinated neotropical gingers. *Evolution 60*, 3 (2006), 538–552.

[66] Kennedy, B. F., Sabara, H. A., Haydon, D., and Husband, B. C. Pollinator-mediated assortative mating in mixed ploidy populations of Chamerion angustifolium (Onagraceae). *Oecologia 150*, 3 (Sept. 2006), 398–408.

[67] Kurella, V. *Asymptotic Analysis of First Passage Processes*. PhD thesis, The University of British Columbia, Vancouver, 2011.

[68] Latty, T., and Beekman, M. Food quality affects search strategy in the cellular slime mould, Physarum polyycephalum. *Behavioral Ecology 20* (2009), 1160–1167.

[69] Le Gall, J.-F. Fluctuation results for the Wiener sausage. *The Annals of Probability* (1988), 991–1018.

[70] Leick, V., and Hellung Larsen, P. Chemosensory behaviour of *Tetrahymena*. *BioEssays 14*, 1 (1992), 61–66.

[71] Leick, V., and Larsen, P. H. Chemosensory Responses in Tetrahymena: The Involvement of Peptides and other Signal Substances. *Journal of Eukaryotic Microbiology 32*, 3 (1985), 550–553.

[72] Levandowsky, M., and Klafter, J. Feeding and swimming behavior in grazing microzooplankton. *Journal of Eukaryotic Microbiology* (1988).

[73] Lihoreau, M., Chittka, L., and Raine, N. E. Travel optimization by foraging bumblebees through readjustments of traplines after discovery of new feeding locations. *The American Naturalist 176*, 6 (2010), 744–757.

[74] Makhnovskii, Y., Berezhkovskii, A., and Yang, D. Trapping by clusters of traps. *Physical Review E 61*, 6 (2000).

[75] Martin, N. H., Sapir, Y., and Arnold, M. L. The Genetic Architecture Of Reproductive Isolation In Louisiana Irises: Pollination Syndromes And Pollinator Preferences. *Evolution 62*, 4 (Apr. 2008), 740–752.

[76] McKenzie, H. W., Lewis, M. A., and Merrill, E. H. First Passage Time Analysis of Animal Movement and Insights into the Functional Response. *Bulletin of Mathematical Biology 71*, 1 (2008), 107–129.

[77] McKenzie, H. W., Merrill, E. H., Spiteri, R. J., and Lewis, M. How linear features alter predator movement and the functional response. *Interface Focus 2*, 2 (2012), 205–216.

[78] McNair, J. A class of patch-use strategies. *American Zoologist* (1983).

[79] Møller, A. P., and Eriksson, M. Pollinator preference for symmetrical flowers and sexual selection in plants. *Oikos* (1995), 15–22.

[80] Moore, P., and Crimaldi, J. Odor landscapes and animal behavior: tracking odor plumes in different physical worlds. *Journal of Marine Systems 49*, 1-4 (2004), 55–64.

[81] Natalis, L. C., and Wesselingh, R. A. Parental Frequencies And Spatial Configuration Shape Bumblebee Behavior And Floral Isolation In Hybridizing Rhinanthus. *Evolution 67*, 6 (Jan. 2013), 1692–1705.

[82] Nevitt, G. Olfactory foraging by Antarctic procellariiform seabirds: life at high Reynolds numbers. *The Biological Bulletin 198*, 2 (2000), 245–253.

[83] Nishimura, K. Foraging in an uncertain environment: Patch exploitation. *Journal of Theoretical Biology* (1992).

[84] Nolet, B. A., and Mooij, W. M. Search paths of swans foraging on spatially autocorrelated tubers. *Journal of Animal Ecology 71*, 3 (2002), 451–462.

[85] Oaten, A. Optimal foraging in patches: A case for stochasticity. *Theoretical population biology 12*, 3 (1977), 263–285.

[86] Olsson, O., and Holmgren, N. M. The survival-rate-maximizing policy for Bayesian foragers: wait for good news. *Behavioral Ecology 9*, 4 (1998), 345–353.

[87] Persons, M., and Uetz, G. Foraging patch residence time decisions in wolf spiders: Is perceiving prey as important as eating prey? *Ecoscience. Sainte-Foy 4*, 1 (1997), 1–5.

[88] Plank, M. J., Auger-Methe, M., and Codling, E. A. Levy or Not? Analysing Positional Data from Animal Movement Paths. *Movement and Spatial Ecology* (2013).

[89] Plank, M. J., and James, A. Optimal foraging: Levy pattern or process? *Journal of the Royal Society Interface 5*, 26 (2008), 1077–1086.

[90] Pohl, N. B., Van Wyk, J., and Campbell, D. R. Butterflies show flower colour preferences but not constancy in foraging at four plant species. *Ecological Entomology 36*, 3 (Mar. 2011), 290–300.

[91] Preston, M. D., Pitchford, J. W., and Wood, A. J. Evolutionary optimality in stochastic search problems. *Journal of the Royal Society Interface 7*, 50 (2010), 1301–1310.

[92] R Development Core Team. *R: A Language and Environment for Statistical Computing*. R Foundation for Statistical Computing, Vienna, Austria, 2011.

[93] Raposo, E. P., Buldyrev, S. V., da Luz, M. G. E., Viswanathan, G. M., and Stanley, H. E. Optimizing the success of random searches. *Journal of Physics a-Mathematical and Theoretical 401*, 6756 (2009), 911–914.

[94] Reader, T., Higginson, A. D., Barnard, C. J., Gilbert, F. S., and The Behavioural Ecology Field Course. The effects of predation risk from crab spiders on bee foraging behavior. *Behavioral Ecology 17*, 6 (Sept. 2006), 933–939.

[95] Reynolds, A., and Rhodes, C. The Levy flight paradigm: random search patterns and mechanisms. *Ecology 90*, 4 (2009), 877–887.

[96] Reynolds, A. M. How many animals really do the Lévy walk? Comment. *Ecology 89*, 8 (2008), 2347–2351.

[97] Reynolds, A. M. Adaptive Lévy walks can outperform composite Brownian walks in non-destructive random searching scenarios. *Physica A 388*, 5 (2009), 561–564.

[98] Reynolds, A. M. Balancing the competing demands of harvesting and safety from predation: Levy walk searches outperform composite Brownian walk searches but only when foraging under the risk of predation. *Physica a-Statistical Mechanics and Its Applications 389*, 21 (2010), 4740–4746.

[99] Reynolds, A. M. Bridging the gulf between correlated random walks and Levy walks: autocorrelation as a source of Levy walk movement patterns. *Journal of the Royal Society Interface 7*, 53 (2010), 1753–1758.

[100] Reynolds, A. M. Olfactory search behaviour in the wandering albatross is predicted to give rise Lévy flight movement patterns. *Anim Behav 83*, 5 (2012), 1225–1229.

[101] Reynolds, A. M., and Bartumeus, F. Optimising the success of random destructive searches: Levy walks can outperform ballistic motions. *Journal of Theoretical Biology 260*, 1 (2009), 98–103.

[102] Reynolds, A. M., Smith, A., Reynolds, D., Carreck, N., and Osborne, J. Honeybees perform optimal scale-free searching flights when attempting to locate a food source. *Journal of Experimental Biology 210*, 21 (2007), 3763.

[103] Riffell, J. A., Alarcón, R., Abrell, L., Davidowitz, G., Bronstein, J. L., and Hildebrand, J. G. Behavioral consequences of innate preferences and olfactory learning in hawkmoth–flower interactions. *Proceedings of the National Academy of Sciences 105*, 9 (2008), 3404–3409.

[104] Schemske, D. W., and Bradshaw, H. D. Pollinator preference and the evolution of floral traits in monkeyflowers (Mimulus). *Proceedings of the National Academy of Sciences 96*, 21 (1999), 11910–11915.

[105] Schiestl, F. P., and Johnson, S. D. Pollinator-mediated evolution of floral signals. *Trends in Ecology & Evolution 28*, 5 (May 2013), 307–315.

[106] Sims, D. W., Humphries, N. E., Bradford, R. W., and Bruce, B. D. Levy flight and Brownian search patterns of a free-ranging predator reflect different prey field characteristics. *Journal of Animal Ecology* (2011).

[107] Singer, A., Schuss, Z., and Holcman, D. Narrow Escape, Part II: The Circular Disk. *Journal of Statistical Physics 122*, 3 (2006), 465–489.

[108] Smouse, P. E., Focardi, S., Moorcroft, P. R., Kie, J. G., Forester, J. D., and Morales, J. M. Stochastic modelling of animal movement. *Philosophical Transactions of the Royal Society B: Biological Sciences 365*, 1550 (2010), 2201–2211.

[109] Strand, M. R., and Vinson, S. B. Behavioral response of the parasitoid Cardiochiles nigriceps to a kairomone. *Entomologia experimentalis et applicata 31*, 2,3 (1982), 308–315.

[110] Tenhumberg, B., Keller, M. A., Possingham, H. P., and Tyre, A. J. Optimal patch leaving behaviour: a case study using the parasitoid Cotesia rubecula. *Journal of Animal Ecology 70*, 4 (2001), 683–691.

[111] Thomson, J. Field measures of flower constancy in bumblebees. *American Midland Naturalist* (1981).

[112] Thomson, J. D. Trapline foraging by bumblebees: I. Persistence of flight-path geometry. *Behavioral Ecology 7*, 2 (1996), 158–164.

[113] Turchin, P. *Quantitative analysis of movement : measuring and modeling population redistribution in animals and plants*. Sinauer, Sunderland, 1998.

[114] Tyson, R., Wilson, J., and Lane, W. Beyond diffusion: Modelling local and long-distance dispersal for organisms exhibiting intensive and extensive search modes. *Theoretical population biology* (2010).

[115] Visser, A. W., and Kiørboe, T. Plankton motility patterns and encounter rates. *Oecologia 148*, 3 (2006), 538–546.

[116] Viswanathan, G. M., Buldyrev, S. V., Havlin, S., Da Luz, M., Raposo, E. P., and Stanley, H. E. Optimizing the success of random searches. *Nature 401*, 6756 (1999), 911–914.

[117] Viswanathan, G. M., da Luz, M. G. E., Raposo, E. P., and Stanley, H. E. *The Physics of Foraging: An Introduction to Random Searches and Biological Encounters*. Cambridge University Press, Cambridge, UK, 2011.

[118] Waage, J. K. Foraging for patchily-distributed hosts by the parasitoid, Nemeritis canescens. *The Journal of Animal Ecology* (1979), 353–371.

[119] Waser, N. M. Flower constancy: definition, cause, and measurement. *American Naturalist* (1986), 593–603.

[120] Weimerskirch, H., Pinaud, D., Pawlowski, F., and Bost, C. A. Does Prey Capture Induce Area Restricted Search? A Fine Scale Study Using GPS in a Marine Predator, the Wandering Albatross. *The American Naturalist 170*, 5 (2007), 734–743.

[121] Wilensky, U. *Netlogo*. Center for Connected Learning and Computer-Based Modeling, Northwestern University, Evanston, IL USA, 1999.

[122] Yang, S., Ferrari, M. J., and Shea, K. Pollinator Behavior Mediates Negative Interactions between Two Congeneric Invasive Plant SpeciesAppend. *The American Naturalist 177*, 1 (Jan. 2011), 110–118.

[123] Zillio, T., and He, F. Modeling spatial aggregation of finite populations. *Ecology 91*, 12 (2010), 3698–3706.

[124] Zumofen, G., and Klafter, J. Scale-invariant motion in intermittent chaotic systems. *Physical Review E 47* (1993), 851–864.